Novel Molecular Mechanisms of Membrane Traffic in Yeast

by

Jorge Yamil Martínez-Márquez

A dissertation submitted in partial fulfillment
of the requirements for the degree of
Doctor of Philosophy
(Cell and Developmental Biology)
in the University of Michigan
2018

Doctoral Committee:

Professor Lois Weisman, Chair
Assistant Professor Mara C. Duncan
Assistant Professor Ann L. Miller
Professor Billy Tsai
Professor Kristen J. Verhey

Jorge Y. Martínez Márquez

majorge@umich.edu

ORCID iD: 0000-0003-1485-4800

Dedication

To my wife, Bárbara, the light of my life.

Thank you for all your love and support, and for all the *sweet* things that kept me going (yes, including the pastries full of sugar). It is funny and awesome that you, the baker, and me, the cellular biologist, can use the same organism for very different things. In this and many other, less dorky examples I can think of, you truly complete me.

To my mom, dad and brother.

Thank you for your support in this endeavor of which you don't know much, other than understanding that I would end up with a doctorate. Yes! I did it! I became a doctor!

To Luna, my living legacy, my daughter.

Luna, my days are brighter thanks to you.

Acknowledgments

First, I thank Mara C. Duncan for being the best mentor I could ask for. Thank you for all the hard work you put into making me the best researcher possible. I even – almost – enjoyed writing a lot.

Second, thank you to all the friends I made during my time as a student at the University of Michigan. Thank you to the closest friends I made here: Martha, Erika, Leilani and Joel. Having you all supporting me goes a very long way.

I also thank the members of my dissertation committee. I highly value all your support and encouragement. Surprisingly, I came out of my committee meetings more excited about my progress than going into those meetings.

I thank all the members from the Duncan lab members, past and present. I thank Chao-Wei, Jordan, Hannah, Fatima, Destiney, Robert and all past members for putting up with me. To the current members, Cristopher, Justin and Lucas, I hope I was a good mentor to all of you. I wish you all the best in your studies.

I also thank all the faculty from CDB, especially Benjamin Allen, Ajit Joglekar and Billy Tsai for keeping me in check through our everyday interactions. Thank you to the members of the Fingar, Tsai and Verhey labs for surviving my talks during joint lab meetings.

A big thank you to the Developing Future Biologists program at the University of Michigan. Thank you for making DFB. Thank you for having me as a part of DFB. I

learned much in the two years I was part of the group and wish the best for future iterations of the program.

Finally, I thank all members of CDB (students, postdocs, faculty, staff) for making our department a great environment to work in. To all the people who I interacted with over the years, thank you!

Preface

The work presented in this dissertation has all been possible thanks to the awesome power of genetics of the budding yeast (*Saccharomyces cerevisiae*, also known as baker's or brewer's yeast). Coming into the lab of Dr. Mara C. Duncan, I had a small amount of experience working with yeast. However, it was working in her lab where I really understood why people were unusually excited about being able to work with the humble yeast.

One of the advantages of working with yeast is its genetic tractability. For example, yeast strains with a tagged or deleted gene can be generated in a matter of days or weeks, depending on the reagents at hand. In comparison, other organisms (i.e. mouse) require many months to create a single edited gene. Coupled with an ever-increasing toolkit of techniques amenable for use in yeast, it is easy to understand why it is such a great model organism for research.

Finally, and maybe more importantly, many of the molecular processes and proteins in yeast have homologous counterparts in higher eukaryotes. Examples include the DNA replication machinery, kinase signaling cascades and, most important for my work, vesicular membrane trafficking machinery. Thus, the combination of ease of use and extrapolated significance of many of the molecular processes observed in yeast captivated me throughout the course of the research presented in this dissertation. I hope you enjoy it as much as I did.

Table of Contents

List of Tables

List of Figures

List of Appendices

Abstract

Proper membrane traffic is important to target cargo proteins to their designated locations in the cell and maintain homeostasis. Cargo protein traffic through the endomembrane system is a highly regulated process that depends, in part, on clathrin-coated vesicles. Clathrin-coated vesicles are used by the cell in endocytosis and post-Golgi traffic. Clathrin coat formation depends on the action of many proteins that help in the formation of clathrin vesicles. Some of these proteins include clathrin adaptors, proteins that select cargo to be packaged, vesicle terminating proteins, and other proteins that regulate each step of vesicle formation.

This thesis addresses two related topics. The first topic explores the role of membrane trafficking proteins in cell survival in stress conditions, such as nutrient starvation. To survive nutrient starvation, cells can use a process known as autophagy. Autophagy is a mechanism to recycle cellular components to their molecular components. Although it was thought to contribute to survival during glucose starvation, our investigation indicates that autophagy is not essential for survival in glucose starvation for the budding yeast, *Saccharomyces cerevisiae*. Instead, we found that during glucose starvation the clearance of cell surface proteins and their traffic to, and degradation at, the vacuole (the lysosome in yeast) promotes cell survival. Furthermore, we found that autophagy is inhibited in glucose starved cells. These results suggest that endocytosis and endosomal traffic, not autophagy, is the mechanism used by the cell to survive in glucose starvation.

The second topic covered by this thesis is the characterization of Art1/Ldb19, a member of the α-arrestins family. This topic started with the investigation of the clearance of cell surface proteins in glucose starved cells. This response was similar to the clearance of cell surface proteins caused by heat shock and cycloheximide treatment. These cell surface clearance events depend on the function of α-arrestins, a family of proteins involved in the ubiquitination of cargo proteins. Based on this similarity, we initiated an investigation of α-arrestins in glucose starvation-induced endocytosis. We found that the α-arrestin Art1/Ldb19 was required for efficient clearance of cell surface proteins in glucose starvation. Interestingly, Art1 localizes to internal structures that resemble trans-Golgi network (TGN) localization of clathrin adaptors at steady-state conditions. This localization could suggest an additional role for Art1, a known endocytic protein, in TGN traffic. The second part of this thesis explores the role of Art1 at the TGN. Using fluorescence microscopy approaches, we found that Art1 localizes to the late TGN and could potentially interact with the clathrin adaptor, AP-1. Additionally, we found genetic interactions of *ART1* with another clathrin adaptor, *GGA2*, and a hypomorphic allele of clathrin. Finally, we found that deletion of *ART1* suppresses secretion defects observed in cells that express a hypomorphic allele of clathrin.

In summary, the doctoral research presented here provides novel mechanisms of membrane trafficking, with particular relevance for α-arrestins-dependent TGN traffic. Specifically, we found a novel mechanism for cell survival during glucose starvation independent of autophagy. Additionally, our data supports emerging evidence that suggest a role for Art1 at the TGN, in addition to its established role in endocytosis.

Chapter 1: Introduction

Vesicular membrane traffic

One of the defining features of a eukaryotic cell is the presence of intracellular membranous organelles. The proper formation and function of many organelles requires vesicular membrane traffic. In vesicular membrane traffic, cell contents traffic between membranous compartments using vesicles or other membranous carriers. Vesicular membrane traffic enables the cell to move proteins between organelles. This protein traffic is essential for newly synthesized proteins to be targeted to the correct organelle. In addition, protein traffic is required to retrieve transmembrane proteins involved in protein traffic, such as cargo receptors. Defects in membrane traffic contribute to the development of diseases like cancer and diabetes (Foley et al., 2011; Sigismund et al., 2018).

The endomembrane system is a critical set of organelles that are important for secretion and endocytosis (Figure 1.1). The proteins within the endomembrane system originate at the endoplasmic reticulum (ER). The ER membrane contains the translocation apparatus, which is required to transport protein polypeptides through the lipid bilayer. This machinery is responsible for the translocation of both lumenal and transmembrane proteins that populate the endomembrane system. At the ER, cargo proteins are packaged into vesicles that are directed to and fuse with the Golgi. From

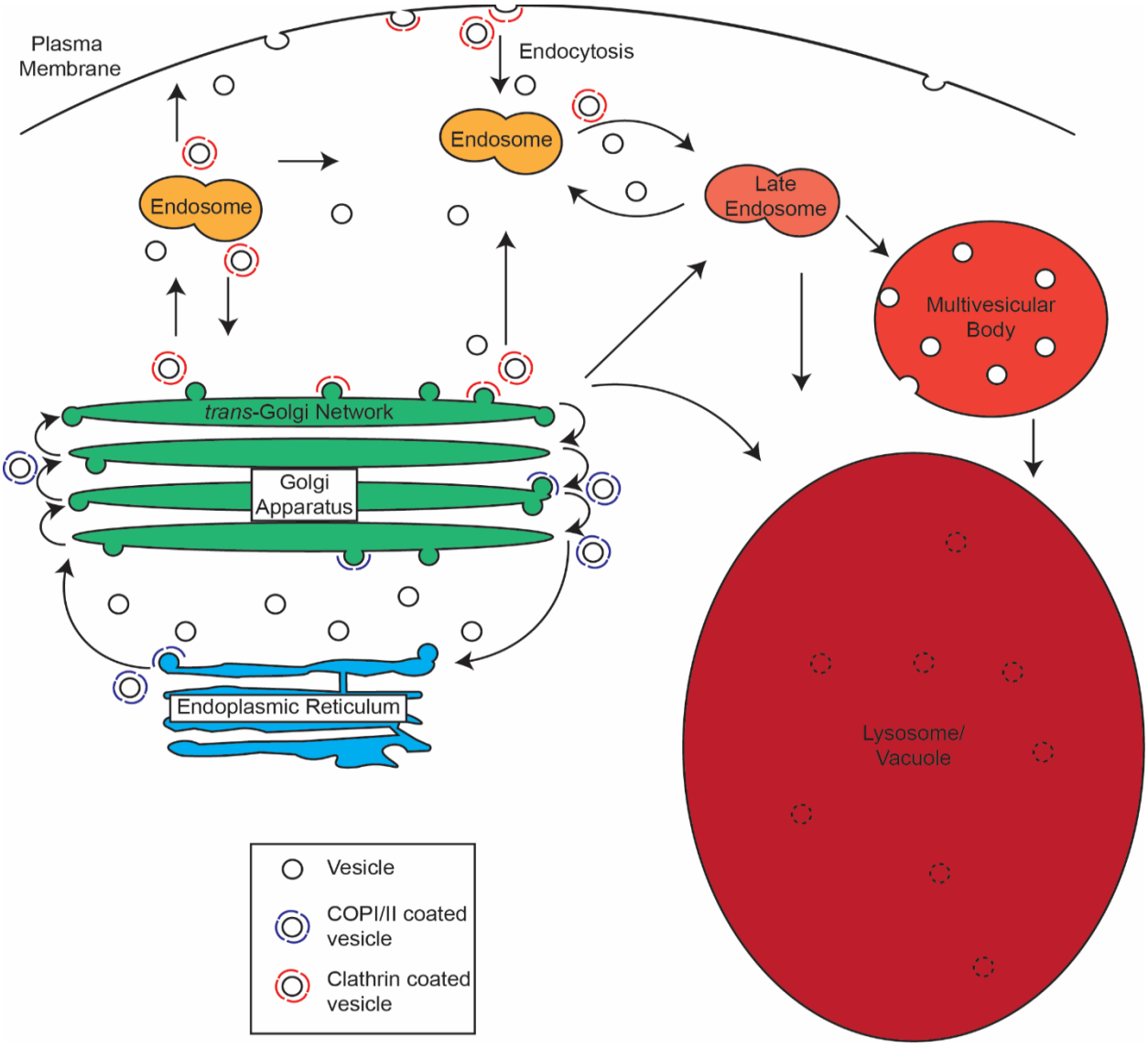

Figure 1.1 Overview of vesicular membrane traffic
Cargo proteins synthesized at the ER are trafficked to the Golgi apparatus by COPII vesicles. Anterograde and retrograde traffic through the Golgi stacks depend on COPII and COPI vesicles, respectively. Post-Golgi traffic from the *trans*-Golgi network (TGN) to other organelles depends on clathrin coat vesicles. Additionally, clathrin coat trafficking is also used in the process of endocytosis and traffic through endosomal compartments. Traffic of cargo proteins to the vacuole/lysosome results in their degradation.

other organelles are packaged into distinct transport carriers. At the same time, proteins required for ER to Golgi traffic must be recycled to the ER to allow for continued rounds of ER to Golgi traffic. Similar, recycling pathways are required between the endosome and Golgi, and plasma membrane and endosomes. The correct trafficking of cargo proteins from one organelle to the next therefore requires several different types of vesicles or carriers. These distinct vesicles or carriers are formed by different sets or subsets of proteins known as traffic effector proteins.

The formation of a vesicle generally occurs in three steps: initiation, elongation and scission (Figure 1.2). Many of these steps are carried out by cytosolic proteins. The first step is the initiation of the vesicle. In this step, early traffic effectors usually bind to cargo proteins and membrane on the cytosolic face of the donor organelle. In the second step, elongation, early traffic effectors recruit coat proteins. Coat proteins help shape the vesicle as more cargo is packaged into it. During the last step, scission, proteins are recruited to the base of the forming vesicle to help constrict the attachment between the vesicle and the donor organelle. After scission occurs, the coat disassembles, and the vesicle moves to its target membrane. This disassembly is required both to allow fusion of the vesicle with the target membrane and to replenish the cytosolic pool of effector proteins for their reuse for additional vesicle formation events.

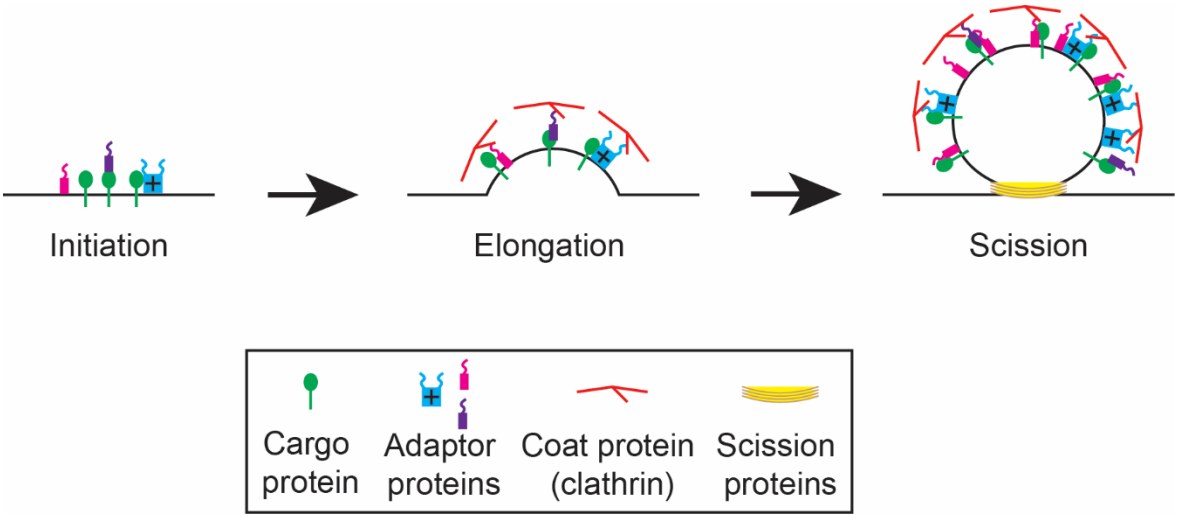

Figure 1.2. Steps of vesicle formation.
At the initiation step, clathrin adaptors are recruited to the site of vesicle formation by their interactions with cargo proteins and the membrane. During the elongation step, more clathrin adaptors are recruited to the site of vesicle formation. The clathrin adaptors then recruit clathrin, which helps shape the forming vesicle. Near the end stages of vesicle formation, scission proteins are recruited to the neck of the emerging vesicle to help detach the forming vesicle from the donor membrane.

Coat proteins involved in membrane traffic

The normal functioning of the endomembrane system requires several distinct coats (Faini et al., 2013; Feyder et al., 2015; Robinson, 2015). The COPI and COPII coats function at the ER and Golgi. The clathrin coat functions in post-Golgi traffic at the *trans*-Golgi network and endosomes, and endocytosis. This coat includes the clathrin coat and its adaptors. Clathrin recruitment to the plasma membrane for endocytosis depends in part on the AP-2 adaptor complex. However, recruitment of clathrin to the TGN and endosomal compartments depends on a different cast of adaptor proteins. These adaptor proteins include the AP-1 complex, GGA proteins and other adaptors that work at the TGN and endosomes. These TGN clathrin adaptors help the cell sort many proteins synthesized at the ER en route to various locations in the cell. The identification and characterization of proteins involved in the regulation of coats is an area of much research with implications in health (Guo et al., 2014).

Clathrin adaptors are recruited to the TGN

Proteins involved in clathrin-mediated traffic, such as the clathrin adaptors, are recruited to the site of vesicle formation in a sequential manner (Daboussi et al., 2012; Kaksonen et al., 2005). Clathrin adaptors are recruited at the late stages of the TGN, which is formed after a transitional maturation of Golgi cisternae (Kim et al., 2016; Losev et al., 2006; McDonold and Fromme, 2014). The clathrin adaptors follow a set of recruitment waves for each adaptor (Daboussi et al., 2012; Hung et al., 2012). The clathrin adaptor Gga2 is recruited first to the TGN, followed by the recruitment of clathrin

adaptors Ent5 and AP-1 (Daboussi et al., 2012; Hung et al., 2012). The sequential recruitment of clathrin adaptors potentially occurs, in part, through their interactions with proteins and other molecules. One such protein involved in the recruitment of clathrin adaptors is the Arf1-GTPase (Arf). However, this is not true for all clathrin adaptors, as Gga2 is recruited to membranes independent of Arf activity (Aoh et al., 2013; Daboussi et al., 2012). Clathrin adaptors are also recruited to cargo proteins (Höning et al., 1997; Nielsen et al., 2001; Puertollano et al., 2001; Zhu et al., 2001). Furthermore, clathrin adaptors can bind to other adaptors (Hung et al., 2012; O'Donnell et al., 2010; Whitfield et al., 2016). The interactions between adaptors creates a protein interaction network that results in a more efficient coat formation. Moreover, clathrin adaptors can also bind proteins that regulate cargo vesicle traffic. For example, in yeast, AP-1 has been shown to interact with the α-arrestins Aly1 and Aly2, which regulate the traffic itinerary of cargo proteins. (O'Donnell et al., 2010). Thus, the interactions of clathrin adaptors with each other, cargo and regulatory proteins ensure correct and efficient traffic at the TGN.

Membrane traffic in response to stress and nutrient changes

One of the major functions of the endomembrane system is the formation of the lysosome. The lysosome, vacuole in yeast, is a hydrolytically active compartment that can digest proteins to their component amino acids. It plays critical roles in the cell by degrading damaged proteins, or proteins the cell no-longer wants. It also plays critical roles in nutrient homeostasis particularly during starvation by recycling proteins and lipids into their molecular components, which the cell can then use for new biosynthesis

or energy (Dunlop and Tee, 2014; Guo et al., 2011; Kim and Lee, 2014; White et al., 2015).

One well studied pathway for the lysosome in nutrient homeostasis is macro-autophagy. Macro-autophagy is a conserved pathway that delivers cytoplasmic components into the lumen of the lysosome (Figure 1.3). In macroautophagy (hereafter autophagy), a double-membrane compartment known as the autophagosome surrounds cytoplasmic components such as proteins and organelles. The fully-formed autophagosome fuses with the lysosomes, which leads to the degradation of the cell components contained within the autophagosome. The degradation of proteins releases amino acids and new essential molecules which are returned to the cytoplasm for reuse (Heider et al., 2016). This process occurs under steady state conditions where it removes damaged proteins such as large proteins aggregates (Gatica et al., 2018; Reggiori and Klionsky, 2013). However, in response to stresses, including starvation, the autophagy pathway is upregulated. The upregulation of autophagy helps with the degradation of proteins, lipids and damaged organelles (Dunlop and Tee, 2014; Guo et al., 2011; Kim and Lee, 2014; White et al., 2015). The autophagy-driven degradation produces precursor building blocks for new biosynthesis and energy generation in response required to survive stresses, like nutrient starvation.

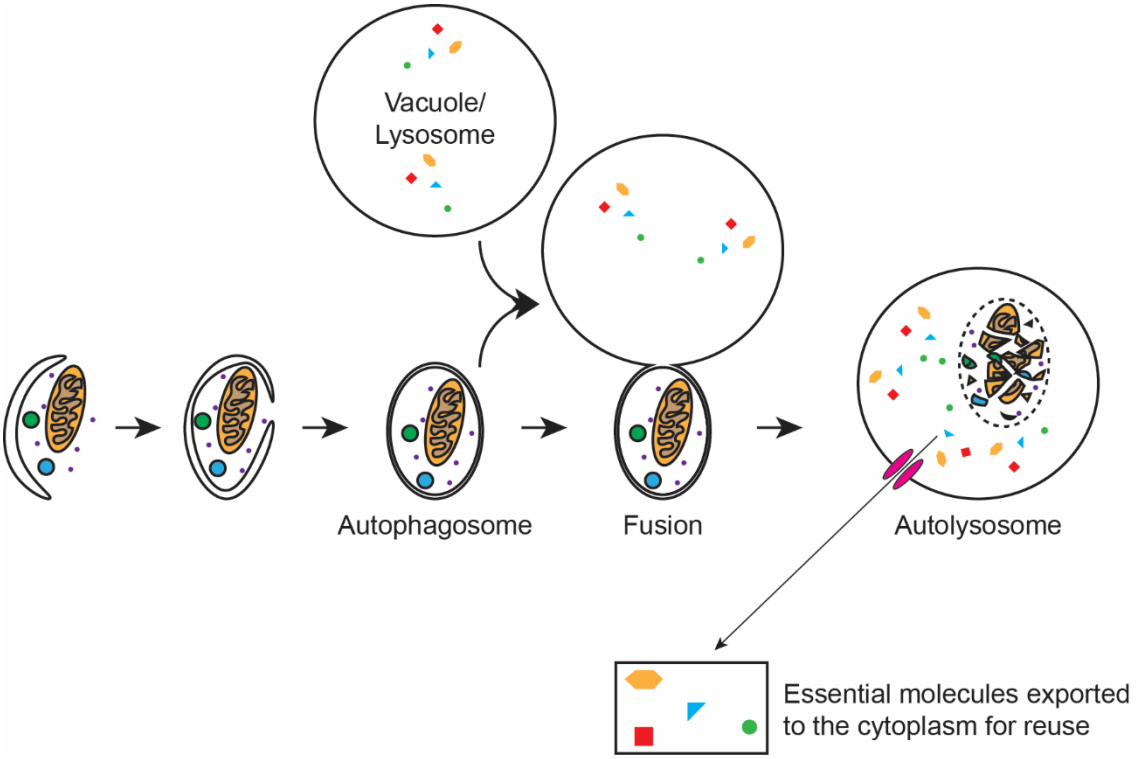

Figure 1.3. Autophagy overview
In the initial steps of autophagy, a single layer membrane structure starts to enlarge in the cytoplasm. As it enlarges, it engulfs material from the cytoplasm (proteins, organelles, etc). When the structure fully closes, it becomes a double membrane compartment called the autophagosome. The autophagosome then fuses to the vacuole/lysosomes, which leads to the degradation of the cell components delivered by the autophagosome. Degradation of these cell components produces new essential molecules that are returned to the cytoplasm for reuse

Although autophagy is known to be activated during many stress conditions, and was previously reported to be activated during glucose starvation, prior work indicated that it was not important for survival during glucose starvation. Autophagy genes are not required for survival in glucose starvation in yeast (Klosinska et al., 2011). In mammalian cells, several cancer types do not engage in pro-survival autophagy during glucose starvation (Ramirez-Peinado et al., 2013). In glucose starvation, the levels of adenosine triphosphate (ATP), the energy currency of the cell, drop acutely (Aoh et al., 2011; Aoh et al., 2013). Importantly, ATP is required for the induction of autophagy (Moruno-Manchon et al., 2013). Thus, the low levels of ATP in glucose-starved cells, coupled with survival in the absence of autophagy genes, suggest that the cell uses a different mechanism to survive glucose starvation.

In mammals, conditions of low ATP levels include starvation and hypoxia (Hardie, 2007; Hardie et al., 2012; Qi and Young, 2015). Conditions of low energy levels (i.e. high AMP/ATP ratio) activate adenosine monophosphate kinase (AMPK), a key metabolic regulator. The activation of AMPK induces a partially-selective internalization of many cell surface proteins (Ross et al., 2015). Activation of AMPK can, in turn, reduce cell surface levels of proteins involved in cell migration and adhesion (Ross et al., 2015). Lower levels of these proteins results in reduced migration, an energy-intensive process, as measured by *in vitro* wound healing experiments (Ross et al., 2015). These data suggest a mechanism for a membrane trafficking response to ensure cell survival in conditions of energy stress.

In addition to changes of the cargo landscape at the cell surface, clathrin adaptors at the TGN are also affected by glucose starvation stress. In the presence of

glucose, energy levels are high and the TGN clathrin adaptors largely distribute to membranes. If cells are starved for glucose, ATP levels plummet and the TGN clathrin adaptors redistribute to the cytosol (Aoh et al., 2011; Aoh et al., 2013). During prolonged starvation, the cells partially recover their ATP levels and the adaptors localize again to the TGN membranes (Aoh et al., 2011; Aoh et al., 2013). Together, these trafficking responses at the TGN and the cell surface highlight the responses of the cell to a constant changing environment.

Arrestin-dependent traffic in stress and nutrient starvation in yeast

As will be presented in chapter 2, glucose starvation induces large-scale cell surface clearance. At the time we discovered this glucose starvation-induced cell surface clearance, several other stress conditions were known to induce large-scale cell surface clearance of cargo proteins through endocytosis. These stresses include heat shock and cycloheximide (CHX) treatment (Lin et al., 2008; Nikko and Pelham, 2009; Zhao et al., 2013). For heat shock and CHX treatment, although globally the responses looked similar, there are key differences that suggest the pathways controlling the global response are distinct. During heat shock stress, the elevated temperature is thought to misfold plasma membrane proteins (Zhao et al., 2013). The accumulation of these misfolded proteins at the cell surface disrupt membrane integrity (Keener and Babst, 2013; Zhao et al., 2013). Therefore, the global endocytosis is thought to protect membrane integrity. The misfolded proteins are detected by a quality control mechanism that recognizes exposed cytosolic domains that would remain undetected

otherwise (Keener and Babst, 2013). In contrast, CHX treatment is not thought to damage cell surface proteins. Rather, it is thought to stimulate endocytosis by aberrantly activating a TORC1-dependent pathway (MacGurn et al., 2011). Treatment with CHX blocks synthesis of new proteins, leading to a high level of free intracellular amino acids. Importantly, increased levels of intracellular amino acids act as substrates to in induce permease internalization (Keener and Babst, 2013; Merhi and Andre, 2012). Interestingly, it is thought that substrate-binding by these amino acid permeases exposes the same cytosolic domain recognized when the proteins misfold during heat-shock (Keener and Babst, 2013). The increased levels of intracellular amino acids in CHX-treated cells activate TORC1, which leads to the downstream phosphorylation of the kinase Npr1 (Binda et al., 2009; MacGurn et al., 2011). Npr1 is a negative regulator of ubiquitin-dependent degradation of cell surface cargo (MacGurn et al., 2011). The TORC1-dependent phosphorylation of Npr1 inactivates it. The inactivation of Npr1, in turn, results in the activation of a cargo downregulation mechanism that regulates the proteins at the cell surface.

Although the regulatory mechanism for heat shock and CHX treatment differs, they share many features. Both use the canonical clathrin associated endocytic machinery. In addition, the internalization and degradation of target proteins in both processes depend on the ubiquitination of the target proteins. Ubiquitination is a post-translational modification that targets cell surface proteins, like the amino acid permeases, for degradation. The ubiquitination of many proteins at the plasma membrane depends on the E3 ligase Rsp5 (Hicke and Dunn, 2003; Keener and Babst, 2013; Nikko and Pelham, 2009; Soetens et al., 2001). Moreover, the cell responses to

heatshock and CHX treatment require the activity of proteins of the α-arrestin family (ARTs). The ARTs function as adaptors of Rsp5 to recruit it to target proteins for ubiquitination (Lin et al., 2008; Soetens et al., 2001). Accordingly, the ARTs are required for the internalization of cell surface proteins after heat shock (Keener and Babst, 2013; Zhao et al., 2013). Similarly, the ARTs were also required for the downregulation of cell surface proteins upon CHX treatment (MacGurn et al., 2011). Importantly, each ART is involved in the downregulation of specific cargo, with some redundancy between ARTs (MacGurn et al., 2011; Nikko and Pelham, 2009). Furthermore, the required ARTs for the downregulation of specific cargo also depends on the context of downregulation signal (Lin et al., 2008; Nikko and Pelham, 2009). For example, the lysine permease Lyp1 is internalized when cells are treated with CHX and when extracellular lysine is high. However, Lyp1 internalization requires Art1/Ldb19 when cells are treated with CHX but not during substrate-induced internalization (Lin et al., 2008). Instead, cells require Art2/Ecm21 to efficiently internalize Lyp1 when lysine levels are high. This complex regulation of cargo proteins by the arrestins provide the cell with a mechanism to respond to many stresses.

A brief history of arrestins

The arrestin superfamily was first identified in studies of how G-protein coupled receptor (GPCR) signaling was desensitized (reviewed in (Lefkowitz, 2013)). These arrestin proteins bind to phosphorylated GPCRs, “arresting” the function of the receptors. In mammals, the arrestins also function in endocytosis and endosomal

trafficking, and are known tumor suppressors (Arakaki et al., 2018; Dores et al., 2015; Lefkowitz, 2013; Patwari and Lee, 2012; Xiao et al., 2018). Importantly, arrestins are conserved from yeast to mammals. In humans, there are 10 known arrestin proteins: 2 visual arrestins, 2 beta-arrestins and 6 alpha-arrestins. The visual/beta-arrestins are known as the “true” arrestins, because they were the first described members of the arrestin family. The alpha-arrestins were grouped with the other proteins of the family after an arrestin-like domain fold was found in the alpha-arrestin TXNIP (Patwari and Lee, 2012; Polekhina et al., 2013; Puca and Brou, 2014). However, alpha-arrestins are thought to be the ancestral form of this family of proteins, because fungi contain alpha-, but no visual/beta-arrestins (Alvarez, 2008; Aubry et al., 2009). Furthermore, the structure of the alpha-arrestins differs slightly from the visual and beta-arrestins. Specifically, the alpha-arrestins are classified differently for the presence of a PY-motif (generally taking the (L/P)PXY form) in their C-termini, which enables them to interact and recruit E3 ubiquitin ligases (Andoh et al., 2002; Aubry et al., 2009; Lin et al., 2008; Yashiroda et al., 1998).

Arrestins in *Saccharomyces cerevisiae*

Arrestins in yeast, like their human counterparts, contain an arrestin-like fold in their N-terminus (Fig. 1.4). Yeast arrestins are classified as alpha-arrestins because they contain PY motifs in their C-termini (Fig1.5) (Becuwe et al., 2012a; Lin et al., 2008; Merhi and Andre, 2012). Also, like in human arrestins, PY motifs of yeast arrestins enable them to bind to the Nedd4-like E3 ubiquitin ligase in yeast, Rsp5 (Lin et al.,

2008). Their structural similarity to human arrestins suggests that yeast alpha-arrestins could perform similar functions.

Yeast arrestins are known effectors of membrane trafficking. Many studies show that arrestins in yeast are key regulators of cargo trafficking in diverse conditions (Becuwe et al., 2012b; Crapeau et al., 2014; Keener and Babst, 2013; Lin et al., 2008; Zhao et al., 2013). This includes the regulation of GPCRs, similar to mammalian arrestins (Alvaro et al., 2014). Additionally, arrestins in yeast can function in traffic at both the PM and the TGN. For example, the alpha-arrestin Rod1 is required for endocytosis and post-endocytic traffic of the monocarboxylate transporter, Jen1 (Becuwe and Leon, 2014). Recent data suggest that another arrestin, Ldb19/Art1, functions in traffic at the TGN. These data show that the arginine permease, Can1, is endocytosed but not delivered to the vacuole following endocytic induction of Can1 in *art1*Δ cells (Gournas et al., 2017). Instead, Can1 is recycled back to the PM. These

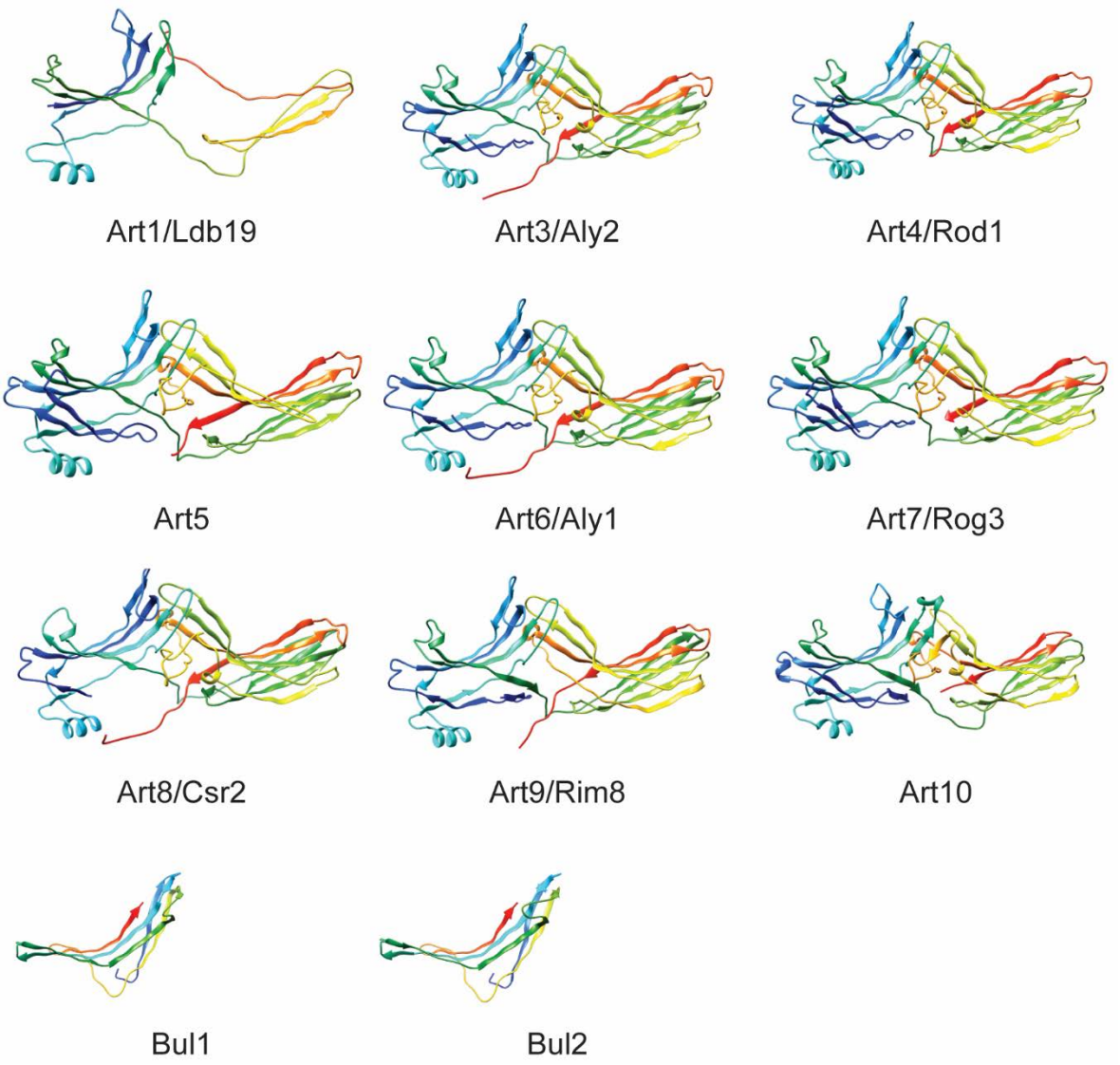

Figure 1.4. Modeling of Yeast ARTs.
The structure of the Saccharomyces cerevisiae ARTs was modeled using the Phyre2 web server in normal mode. The templates used for modeling were as follows: 1G4M for Art1/Lbd19 (23% coverage, 98% confidence) and Art10 (94% coverage, 91% confidence); 1SUJ for Art3/Aly2 (31% coverage, 99% confidence), Art4/Rod1 (38% coverage, 100% confidence), Art5 (51% coverage, 100% confidence), Art6/Aly1 (36% coverage, 99% confidence), Art7/Rog3 (44% coverage, 100% confidence), Art8/Csr2 (27% coverage, 99% confidence), Art9/Rim8 (54% coverage, 100% confidence); 4R7V for Bul1 (18% coverage, 96% confidence) and Bul2 (19% coverage, 96% confidence). Low coverage is the result of largely unstructured areas outside of the arrestin-folds. Art2/Ecm21 could not be modeled. Only one lobe of the arrestin-fold was able to be modeled for Bul1 and Bul2. UCSF Chimera was used to create the ribbon models. Coloring goes from blue N-terminus to red C-terminus.

Figure 1.5. Domain structure of yeast arrestins.
Shown are the diagrams of the full-length yeast α-arrestins (black). Except for Art10, the arrestin-fold domains sequences (white) were derived from pfam information described in the Saccharomyces Genome Database (SGD). The sequence for the Art10 arrestin-fold was derived from the modeling of Art10 with the 1G4M template using the Phyre2 modeling software. PY motifs (X-P-X-Y) are depicted in magenta.

results suggest that Art1 is required at the TGN/endosomes for efficient traffic of Can1 following endocytosis. In chapter 4, I show data that support possible non-endocytic roles of Art1.

Arrestin-dependent traffic in glucose starvation in yeast

Because alpha-arrestins were important for heatshock and CHX induced cell surface clearance, we investigated whether glucose starvation also required proteins of the arrestin family. To do so, we monitored the localization of GFP-tagged Tat1, a tryptophan permease, before and 2hr after glucose starvation in WT and *art1Δ* cells. In the presence of glucose, Tat1 was present at the PM in WT and *art1Δ* cells (Fig. 1.6). After 2hr of glucose starvation, Tat1 was fully internalized to the vacuole in WT cells. Conversely, Tat1 remained largely localized to the PM after glucose starvation in *art1Δ* cells. These results suggest that the arrestin Art1 is involved in the internalization of Tat1 in GS-CSC. Thus, together with previous studies, our results indicate that cargo downregulation in heatshock, CHX and GS-CSC depends in part on arrestins. These data stimulated our interest in the function of the yeast arrestin Art1 (See Chapter 3).

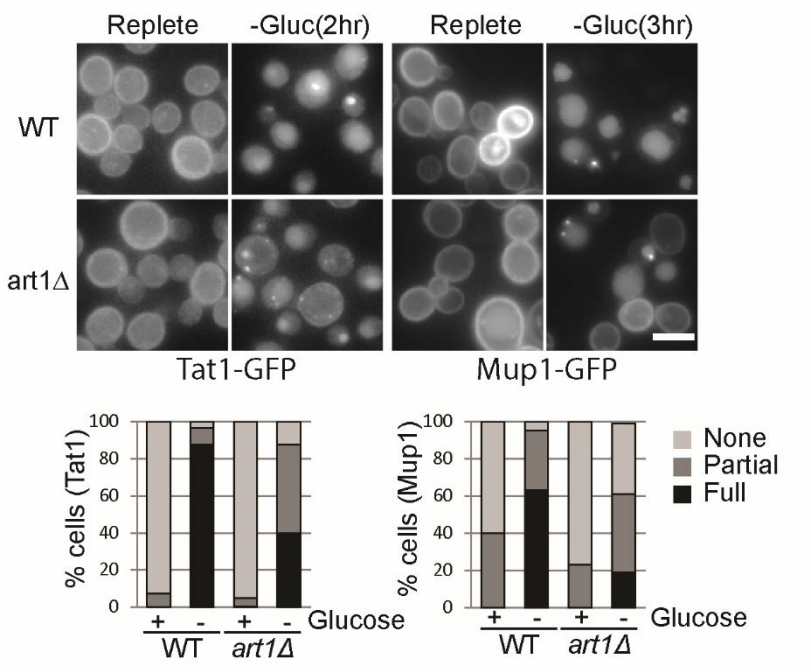

Figure 1.6. Deletion of *ART1* blocks GS-CSC of multiple cargo
WT and *art1*Δ cells expressing Tat1- or Mup1-GFP were imaged before and after 2hr of glucose starvation. Bottom, quantification of the percentage of cells with no (none), partial or full internalization of the imaged GFP-tagged cargo proteins.

Summary

In this thesis I will present research on two distinct studies of membrane trafficking. The first study is a novel mechanism for survival upon glucose starvation that induces large-scale cargo endocytosis and blocks recycling. This novel mechanism involves broad traffic from the PM to the vacuole for degradation of cellular components, but not autophagy. In the second study we show data that suggest that Art1/Ldb19, a protein with an established role in endocytosis, has a role in traffic at the TGN.

Chapter 2 provides evidence for a survival strategy in *S. cerevisiae* during glucose starvation, which was published in the *Journal of Biological Chemistry* in 2014 as “Glucose starvation inhibits autophagy via vacuolar hydrolysis and induces plasma membrane internalization by down-regulating recycling”. In Chapter 3, I will provide evidence that suggests the yeast arrestin Art1, a bonafide endocytic protein, has an additional role in TGN traffic.

References

Alvarez, C.E. 2008. On the origins of arrestin and rhodopsin. *BMC evolutionary biology*. 8:222.

Alvaro, C.G., A.F. O'Donnell, D.C. Prosser, A.A. Augustine, A. Goldman, J.L. Brodsky, M.S. Cyert, B. Wendland, and J. Thorner. 2014. Specific alpha-arrestins negatively regulate Saccharomyces cerevisiae pheromone response by down-modulating the G-protein-coupled receptor Ste2. *Molecular and cellular biology*. 34:2660-2681.

Andoh, T., Y. Hirata, and A. Kikuchi. 2002. PY motifs of Rod1 are required for binding to Rsp5 and for drug resistance. *FEBS Lett*. 525:131-134.

Aoh, Q.L., L.M. Graves, and M.C. Duncan. 2011. Glucose regulates clathrin adaptors at the trans-Golgi network and endosomes. *Molecular biology of the cell*. 22:3671-3683.

Aoh, Q.L., C.W. Hung, and M.C. Duncan. 2013. Energy metabolism regulates clathrin adaptors at the trans-Golgi network and endosomes. *Molecular biology of the cell*. 24:832-847.

Arakaki, A.K.S., W.A. Pan, H. Lin, and J. Trejo. 2018. The alpha-arrestin ARRDC3 suppresses breast carcinoma invasion by regulating G protein-coupled receptor lysosomal sorting and signaling. *The Journal of biological chemistry*. 293:3350-3362.

Aubry, L., D. Guetta, and G. Klein. 2009. The Arrestin Fold: Variations on a Theme. *Curr Genomics*. 10:133-142.

Becuwe, M., A. Herrador, R. Haguenauer-Tsapis, O. Vincent, and S. Leon. 2012a. Ubiquitin-mediated regulation of endocytosis by proteins of the arrestin family. *Biochemistry research international*. 2012:242764.

Becuwe, M., and S. Leon. 2014. Integrated control of transporter endocytosis and recycling by the arrestin-related protein Rod1 and the ubiquitin ligase Rsp5. *eLIFE*.

Becuwe, M., N. Vieira, D. Lara, J. Gomes-Rezende, C. Soares-Cunha, M. Casal, R. Haguenauer-Tsapis, O. Vincent, S. Paiva, and S. Leon. 2012b. A molecular switch on an arrestin-like protein relays glucose signaling to transporter endocytosis. *The Journal of cell biology*. 196:247-259.

Binda, M., M.P. Peli-Gulli, G. Bonfils, N. Panchaud, J. Urban, T.W. Sturgill, R. Loewith, and C. De Virgilio. 2009. The Vam6 GEF controls TORC1 by activating the EGO complex. *Molecular cell*. 35:563-573.

Crapeau, M., A. Merhi, and B. Andre. 2014. Stress conditions promote yeast Gap1 permease ubiquitylation and down-regulation via the arrestin-like Bul and Aly proteins. *The Journal of biological chemistry*. 289:22103-22116.

Daboussi, L., G. Costaguta, and G.S. Payne. 2012. Phosphoinositide-mediated clathrin adaptor progression at the trans-Golgi network. *Nature cell biology*. 14:239-248.

Dores, M.R., H. Lin, J.G. N, F. Mendez, and J. Trejo. 2015. The alpha-arrestin ARRDC3 mediates ALIX ubiquitination and G protein-coupled receptor lysosomal sorting. *Molecular biology of the cell*. 26:4660-4673.

Dunlop, E.A., and A.R. Tee. 2014. mTOR and autophagy: a dynamic relationship governed by nutrients and energy. *Seminars in cell & developmental biology*. 36:121-129.

Faini, M., R. Beck, F.T. Wieland, and J.A. Briggs. 2013. Vesicle coats: structure, function, and general principles of assembly. *Trends in cell biology*. 23:279-288.

Feyder, S., J.O. De Craene, S. Bar, D.L. Bertazzi, and S. Friant. 2015. Membrane trafficking in the yeast Saccharomyces cerevisiae model. *International journal of molecular sciences*. 16:1509-1525.

Foley, K., S. Boguslavsky, and A. Klip. 2011. Endocytosis, recycling, and regulated exocytosis of glucose transporter 4. *Biochemistry*. 50:3048-3061.

Gatica, D., V. Lahiri, and D.J. Klionsky. 2018. Cargo recognition and degradation by selective autophagy. *Nature cell biology*. 20:233-242.
Gournas, C., E. Saliba, E.M. Krammer, C. Barthelemy, M. Prevost, and B. Andre. 2017. Transition of yeast Can1 transporter to the inward-facing state unveils an alpha-arrestin target sequence promoting its ubiquitylation and endocytosis. *Molecular biology of the cell*. 28:2819-2832.
Guo, J.Y., H.Y. Chen, R. Mathew, J. Fan, A.M. Strohecker, G. Karsli-Uzunbas, J.J. Kamphorst, G. Chen, J.M. Lemons, V. Karantza, H.A. Coller, R.S. Dipaola, C. Gelinas, J.D. Rabinowitz, and E. White. 2011. Activated Ras requires autophagy to maintain oxidative metabolism and tumorigenesis. *Genes & development*. 25:460-470.
Guo, Y., D.W. Sirkis, and R. Schekman. 2014. Protein sorting at the trans-Golgi network. *Annual review of cell and developmental biology*. 30:169-206.
Hardie, D.G. 2007. AMP-activated/SNF1 protein kinases: conserved guardians of cellular energy. *Nature reviews. Molecular cell biology*. 8:774-785.
Hardie, D.G., F.A. Ross, and S.A. Hawley. 2012. AMPK: a nutrient and energy sensor that maintains energy homeostasis. *Nature reviews. Molecular cell biology*. 13:251-262.
Heider, M.R., M. Gu, C.M. Duffy, A.M. Mirza, L.L. Marcotte, A.C. Walls, N. Farrall, Z. Hakhverdyan, M.C. Field, M.P. Rout, A. Frost, and M. Munson. 2016. Subunit connectivity, assembly determinants and architecture of the yeast exocyst complex. *Nature structural & molecular biology*. 23:59-66.
Hicke, L., and R. Dunn. 2003. Regulation of membrane protein transport by ubiquitin and ubiquitin-binding proteins. *Annual review of cell and developmental biology*. 19:141-172.
Höning, S., M. Sosa, A. Hille-Rehfeld, and K. von Figura. 1997. The 46-kDa mannose 6-phosphate receptor contains multiple binding sites for clathrin adaptors. *The Journal of biological chemistry*. 272:19884-19890.
Hung, C.W., Q.L. Aoh, A.P. Joglekar, G.S. Payne, and M.C. Duncan. 2012. Adaptor autoregulation promotes coordinated binding within clathrin coats. *The Journal of biological chemistry*. 287:17398-17407.
Kaksonen, M., C.P. Toret, and D.G. Drubin. 2005. A modular design for the clathrin- and actin-mediated endocytosis machinery. *Cell*. 123:305-320.
Keener, J.M., and M. Babst. 2013. Quality control and substrate-dependent downregulation of the nutrient transporter Fur4. *Traffic*. 14:412-427.
Kim, J.J., Z. Lipatova, U. Majumdar, and N. Segev. 2016. Regulation of Golgi Cisternal Progression by Ypt/Rab GTPases. *Developmental cell*. 36:440-452.
Kim, K.H., and M.S. Lee. 2014. Autophagy--a key player in cellular and body metabolism. *Nature reviews. Endocrinology*. 10:322-337.
Klosinska, M.M., C.A. Crutchfield, P.H. Bradley, J.D. Rabinowitz, and J.R. Broach. 2011. Yeast cells can access distinct quiescent states. *Genes & development*. 25:336-349.
Lefkowitz, R.J. 2013. Arrestins come of age: a personal historical perspective. *Progress in molecular biology and translational science*. 118:3-18.
Lin, C.H., J.A. MacGurn, T. Chu, C.J. Stefan, and S.D. Emr. 2008. Arrestin-related ubiquitin-ligase adaptors regulate endocytosis and protein turnover at the cell surface. *Cell*. 135:714-725.
Losev, E., C.A. Reinke, J. Jellen, D.E. Strongin, B.J. Bevis, and B.S. Glick. 2006. Golgi maturation visualized in living yeast. *Nature*. 441:1002-1006.
MacGurn, J.A., P.C. Hsu, M.B. Smolka, and S.D. Emr. 2011. TORC1 regulates endocytosis via Npr1-mediated phosphoinhibition of a ubiquitin ligase adaptor. *Cell*. 147:1104-1117.
McDonold, C.M., and J.C. Fromme. 2014. Four GTPases differentially regulate the Sec7 Arf-GEF to direct traffic at the trans-golgi network. *Developmental cell*. 30:759-767.

Merhi, A., and B. Andre. 2012. Internal amino acids promote Gap1 permease ubiquitylation via TORC1/Npr1/14-3-3-dependent control of the Bul arrestin-like adaptors. *Molecular and cellular biology*. 32:4510-4522.
Moruno-Manchon, J.F., E. Perez-Jimenez, and E. Knecht. 2013. Glucose induces autophagy under starvation conditions by a p38 MAPK-dependent pathway. *The Biochemical journal*. 449:497-506.
Nielsen, M.S., P. Madsen, E.I. Christensen, A. Nykjaer, J. Gliemann, D. Kasper, R. Pohlmann, and C.M. Petersen. 2001. The sortilin cytoplasmic tail conveys Golgi-endosome transport and binds the VHS domain of the GGA2 sorting protein. *EMBO J*. 20:2183-2190.
Nikko, E., and H.R. Pelham. 2009. Arrestin-mediated endocytosis of yeast plasma membrane transporters. *Traffic*. 10:1856-1867.
O'Donnell, A.F., A. Apffel, R.G. Gardner, and M.S. Cyert. 2010. Alpha-arrestins Aly1 and Aly2 regulate intracellular trafficking in response to nutrient signaling. *Molecular biology of the cell*. 21:3552-3566.
Patwari, P., and R.T. Lee. 2012. An expanded family of arrestins regulate metabolism. *Trends in endocrinology and metabolism: TEM*. 23:216-222.
Polekhina, G., D.B. Ascher, S.F. Kok, S. Beckham, M. Wilce, and M. Waltham. 2013. Structure of the N-terminal domain of human thioredoxin-interacting protein. *Acta crystallographica. Section D, Biological crystallography*. 69:333-344.
Puca, L., and C. Brou. 2014. Alpha-arrestins - new players in Notch and GPCR signaling pathways in mammals. *Journal of cell science*. 127:1359-1367.
Puertollano, R., R.C. Aguilar, I. Gorshkova, R.J. Crouch, and J.S. Bonifacino. 2001. Sorting of mannose 6-phosphate receptors mediated by the GGAs. *Science*. 292:1712-1716.
Qi, D., and L.H. Young. 2015. AMPK: energy sensor and survival mechanism in the ischemic heart. *Trends in endocrinology and metabolism: TEM*. 26:422-429.
Ramirez-Peinado, S., C.L. Leon-Annicchiarico, J. Galindo-Moreno, R. Iurlaro, A. Caro-Maldonado, J.H. Prehn, K.M. Ryan, and C. Munoz-Pinedo. 2013. Glucose-starved cells do not engage in prosurvival autophagy. *The Journal of biological chemistry*. 288:30387-30398.
Reggiori, F., and D.J. Klionsky. 2013. Autophagic processes in yeast: mechanism, machinery and regulation. *Genetics*. 194:341-361.
Robinson, M.S. 2015. Forty Years of Clathrin-coated Vesicles. *Traffic*. 16:1210-1238.
Ross, E., R. Ata, T. Thavarajah, S. Medvedev, P. Bowden, J.G. Marshall, and C.N. Antonescu. 2015. AMP-Activated Protein Kinase Regulates the Cell Surface Proteome and Integrin Membrane Traffic. *PloS one*. 10:e0128013.
Sigismund, S., D. Avanzato, and L. Lanzetti. 2018. Emerging functions of the EGFR in cancer. *Molecular oncology*. 12:3-20.
Soetens, O., J.O. De Craene, and B. Andre. 2001. Ubiquitin is required for sorting to the vacuole of the yeast general amino acid permease, Gap1. *The Journal of biological chemistry*. 276:43949-43957.
White, E., J.M. Mehnert, and C.S. Chan. 2015. Autophagy, Metabolism, and Cancer. *Clinical cancer research : an official journal of the American Association for Cancer Research*. 21:5037-5046.
Whitfield, S.T., H.E. Burston, B.D. Bean, N. Raghuram, L. Maldonado-Baez, M. Davey, B. Wendland, and E. Conibear. 2016. The alternate AP-1 adaptor subunit Apm2 interacts with the Mil1 regulatory protein and confers differential cargo sorting. *Molecular biology of the cell*. 27:588-598.

Xiao, J., Q. Shi, W. Li, X. Mu, J. Peng, M. Li, M. Chen, H. Huang, C. Wang, K. Gao, and J. Fan. 2018. ARRDC1 and ARRDC3 act as tumor suppressors in renal cell carcinoma by facilitating YAP1 degradation. *Am J Cancer Res*. 8:132-143.

Yashiroda, H., D. Kaida, A. Toh-e, and Y. Kikuchi. 1998. The PY-motif Bul1 protein is essential for growth of *Saccharomyces cerevisiae* under various stress conditions. *Gene*. 225:39-46.

Zhao, Y., J.A. MacGurn, and S.D. Emr. 2013. The ART-Rsp5 ubiquitin ligase network comprises a plasma membrane quality control system that protects yeast cells from proteotoxic stress. *eLIFE*.

Zhu, Y., B. Doray, A. Poussu, V.P. Lehto, and S. Kornfeld. 2001. Binding of GGA2 to the lysosomal enzyme sorting motif of the mannose 6-phosphate receptor. *Science*. 292:1716-1718.

Chapter 2: Glucose starvation inhibits autophagy via vacuolar hydrolysis and induces plasma membrane internalization by down-regulating recycling

The work presented in this chapter has been previously published as follows: Lang, M. J., Martinez-Marquez, J. Y., Prosser, D. C., Ganser, L. R., Buelto, D., Wendland, B., Duncan, M. C. (2014) Glucose starvation inhibits autophagy via vacuolar hydrolysis and induces plasma membrane internalization by down-regulating recycling. J Biol Chem 289 (24) 16736-47. doi: 10.1074/jbc.M113.525782. I contributed experimentally in strain generation, performing viability assays and fluorescence microscopy. Specifically, I contributed in the following: Figure 3.1 and 3.2 (Figures 3.1A and 3.2B in original paper). Additionally, I contributed in writing part of the experimental procedures section and minor revisions.

Abstract

Cellular energy influences all aspects of cellular function. Although cells can adapt to a gradual reduction in energy, acute energy depletion poses a unique challenge. Because acute depletion hampers the transport of new energy sources into the cell, the cell must use endogenous substrates to replenish energy after acute depletion. In the yeast *Saccharomyces cerevisiae*, glucose starvation causes an acute depletion of intracellular energy that recovers during continued glucose starvation. However, how the cell replenishes energy during the early phase of glucose starvation is unknown. In this study, we investigate the role of pathways that deliver proteins and lipids to the vacuole during glucose starvation. We report that in response to glucose starvation, plasma membrane proteins are directed to the vacuole through reduced recycling at the endosomes. Furthermore, we find that vacuolar hydrolysis inhibits macroautophagy in a target of rapamycin complex 1 (TORC1) dependent manner. Accordingly, we find that endocytosis and hydrolysis are required for survival in glucose starvation, whereas macroautophagy is dispensable. Together these results suggest that hydrolysis of components delivered to the vacuole independent of autophagy is the cell survival mechanism used by *Saccharomyces cerevisiae* in response to glucose starvation.

Introduction

Glucose is the preferred energy source for many proliferating cells, including the yeast *Saccharomyces cerevisiae.* To utilize glucose, yeast adopts a specific metabolic program, which is similar to the Warburg metabolism seen in cancer and stem cells (Vander Heiden et al., 2009). In this program, the cell shuts down systems that allow utilization of energy sources other than glucose. It forgoes storage of carbohydrates or amino acids, and instead utilizes these nutrients directly for growth. Furthermore, this program inhibits ATP generation by the mitochondria; ATP is derived primarily from glycolysis. Consequently, a precipitous drop in ATP levels follows glucose starvation (Aoh et al., 2013; Ashe et al., 2000). With no reserves and little ATP to facilitate import of new catabolic substrates from extracellular sources, the cell likely hydrolyzes endogenous cellular components to overcome the ATP deficit during the initial phases of glucose starvation.

Macroautophagy (hereafter autophagy) is an important catabolic process activated by various types of starvation. In autophagy, cellular cytoplasm and organelles are engulfed in a double membraned structure called the autophagosome (reviewed in (Singh and Cuervo, 2011)). Fusion of the autophagosome with the lysosome (vacuole in yeast) leads to hydrolysis of the enclosed cellular components. This mechanism allows the cell to recycle amino acids, lipids, and nucleotides for use as energy sources and for new biosynthesis. Three conserved metabolic kinases regulate autophagy. The AMP-activated kinases (AMPK) activates autophagy whereas protein kinase A (PKA) and the target of rapamycin complex 1 (TORC1) inhibit autophagy (reviewed in (Stephan and

Herman, 2006)). During glucose starvation, AMPK is activated whereas PKA is inhibited (Aoh et al., 2013; Thevelein and de Winde, 1999). These effects suggest that autophagy may occur during glucose starvation. However, autophagy genes are dispensable for glucose survival (Klosinska et al., 2011). This indicates that the cell must use additional mechanisms to replenish nutrient stores during glucose starvation. The process that cells use to survive in the absence of autophagy is unknown.

One possible alternative to autophagy is the degradation of proteins that are delivered to the vacuole from the endosomes. This pathway promotes cell survival during amino acid starvation (Jones et al., 2012). Furthermore, in response to acute glucose starvation, proteins involved in endosomal sorting become cytosolic. However, proteins involved in endocytosis remain membrane associated (Aoh et al., 2011; Uesono et al., 2004). This could cause proteins endocytosed from the plasma membrane to be directed to intracellular compartments rather than getting recycled back to the membrane. Indeed, glucose starvation directs internalization of plasma membrane proteins that seem unrelated to glucose metabolism, such as the uracil permease, Fur4, and the hydrophobic amino acid permease, Tat2 (Beck et al., 1999; Volland et al., 1994). This suggests that glucose starvation may alter traffic within the endosomal system. In this study, we investigate the roles of endocytosis, endosomal membrane traffic, and autophagy in ensuring survival during glucose starvation.

Experimental Procedures

Chemicals:

Phenylmethanesulfonylfluoride (PMSF) and rapamycin were from Sigma. FM4-64 was from GE Life Sciences.

Strains and plasmids:

Strains are listed in Table 1 (Kamada et al., 2000; Maldonado-Baez et al., 2008; Prosser et al., 2010; Winston et al., 1995). Deletion strains from systematic collections were verified by PCR utilizing primers outside of the deletion cassette. GFP-strains from systematic collections were verified by microscopy. Strains generated in this study were generated using a PCR-based strategy with pFA6a-S65TGFP-KanMX, pFA6a-S65T-GFP-His3Mx, pFA6a-mcherry-His3Mx, pFA6a-KanMx, pRS303 or pRS305 as described previously (Longtine et al., 1998). Plasmids pRS316 GFP-Aut7 (Atg8), pADHU-GFP-cSNC1, pBW0768 (pEnt1 [CEN TRP1] and pBW0778 (pENTH1 [CEN TRP1]) were described previously (Kama et al., 2007; Prosser et al., 2011; Suzuki et al., 2001).

Growth conditions:

Media compositions used are listed in Table 2. Except where noted, add back mix contains 0.54mM adenine (adenine sulfate), 0.76mM L-leucine, 0.55mM L-lysine, 0.49mM L-tryptophan, 0.32 mM L-histidine, 0.45mM uracil, 0.13mM L-methionine. Nucleotide only add-back mix contains only 0.54mM adenine (adenine sulfate) and 0.45mM uracil. For cells expressing *GFP-ATG8,* uracil was omitted from add back mix.

For cells expressing *MUP1-GFP*, methionine was omitted from add back mix to induce expression.

With the exception of media for FET3-GFP, yeast nitrogen base was the Wickerham formula, without amino acids and ammonium sulfate, used at the manufacturer recommended concentrations (Becton Dickinson, Sparks MD). For FET3-GFP, yeast nitrogen base lacking iron was used (Formedium, Hunstanton, England). Unless otherwise indicated, cells were grown in replete medium for 72 h, maintaining the culture at a low density. For starvation, cells at mid-logarithmic (log) phase (A_{600}~0.2-0.5) were pelleted and washed three times with the appropriate starvation media indicated in Table 2 then incubated at 30°C for the indicated times.

FM4-64 Assays:

To assess initial rates of endocytosis, cells grown to log-phase or starved at different time points were pelleted and resuspended in appropriate media supplemented with 0.4µg/ml FM4-64. After 2.5 min, a stop mix was added to a final concentration of 10mM sodium fluoride and sodium azide and cells were placed on ice. Unbound FM4-64 was removed with three washes in ice-cold media containing 10mM sodium fluoride and sodium azide. Cells were kept on ice until imaged. To assess FM4-64 accumulation and delivery to the vacuole, cells grown to log-phase or starved at different time points were pelleted and resuspended in appropriate media supplemented with 0.4µg/ml FM4-64 at room temperature. After 15 min, FM4-64 was removed by three washes in appropriate media at room temperature and cells were incubated an additional 30 min at 30°C. Sodium fluoride and sodium azide were added to 10mM and cells were kept on ice until

imaged. To assess FM4-64 recycling, cells grown to log-phase or starved at different time points were pelleted and resuspended in appropriate media supplemented with 0.4µg/ml FM4-64. After 15 min (for BY4741 background) or 8 min (for W303 background), cells were resuspended in ice-cold media and washed three times in ice-cold media. For cells labeled in replete media and then starved, the cells were washed with ice-cold media lacking glucose. Cells were kept on ice until assayed. For recycling monitored by loss of fluorescence intensity in Fig. 2.3C cells were monitored every six seconds at room temperature in a fluorimeter as described (Wiederkehr et al., 2000). For recycling monitored by loss of fluorescence intensity in Fig 2.3D, 30µL of labeled cells were diluted to 1.5 OD with 100µL of room temperature media in a room temperature opaque 96 well plate. Fluorescence emission at 680nm was collected every 6 seconds from cells excited with 515nm in a Spectramax M5e plate reader (Molecular Devices) at room temperature. For recycling monitored by increase of FM4-64 in the media in Fig 2.3E, 0.3 ODs of labeled cells in 50µL were transferred to a pre-warmed microfuge tube and incubated at 30°C for 8 minutes. The supernatant was harvested by pelleting two times to remove any cells. CHAPs was added to 1% from a 20% stock solution in PBS and fluorescence was monitored at 680nm after excitation at 515 nm in a Spectramax M5e plate reader. To control for differences in FM4-64 accumulation between samples, background fluorescent signal from media without FM4-64 was first subtracted from all samples. The resultant background subtracted values were then normalized to the initial FM4-64 intensity of the cells assayed as in Fig 2.3D.

Microscopy:

For figures 2.1, 2.2B, 2.4 and 2.5, fluorescence microscopy was performed on an Eclipse TE2000-U (Nikon, Melville, NY) microscope with a 1.4 NA, 100x DIC oil immersion lens and the standard yEGFP and CFP/YFP/DsRed sets from Chroma (Rockingham, VT). Images were acquired with an ORCA ER cooled CCD camera (Hamamatsu Photonics, Bridgewater, NY) with no binning, using MetaMorph (Molecular Devices, Downingtown, PA) as the image acquisition software. For each cell, a 5 plane Z-stack was acquired with separation between adjacent planes set at 500nm. For figures 2.3 and 2.5, images were acquired on a Nikon Ti-E inverted microscope equipped with a 100x, 1.4 NA oil immersion objective as previously described(Aravamudhan et al., 2013). Fluorescent samples were excited with the Lumencor light engine equipped with individual LEDs for GFP/YFP/mCherry excitation (Lumencor, Inc., Beaverton, OR). All the filters were obtained from Chroma (Chroma Technology Corp., Bellows Falls, VT). Images were acquired with an Andor iXon camera (Andor Technology, South Windsor, CT) with a pixel size of 160 nm. For each cell, a 10 plane Z-stack was acquired with separation between adjacent planes set at 200 nm. The same integration time was used for all images of a labeled protein or fluorophore.

Intensity analysis of cell surface proteins was performed in ImageJ v1.43m (National Institutes of Health, http://rsb.info.nih.gov/ij/). For plasma membrane proteins with uniform plasma membrane localization, highest intensity measurements were collected from a 3 pixel wide line drawn through a region of the plasma membrane away from the neck region from a central plane image. For proteins with non-uniform or punctate

plasma membrane localization, highest intensity measurements were from a region with high intensity. Intensity measurements were collected for at least 20 different cells per sample. For intensity analysis of FM4-64 uptake, integrated cell intensity is reported from individual cells manually traced in Image J v1.43m.

For Fig 2.3A, images were acquired using an Axiovert 200 inverted microscope (Carl Zeiss) equipped with a Cooke Sensicam (Cooke), an X-Cite 120 PC fluorescence illumination system, and a 100X, 1.4 numerical aperture (NA) Plan-Apochromat objective. All imaging was performed at room temperature in SD or SM lacking methionine, and identical acquisition parameters were used for all samples within an experiment. Image analysis was performed using ImageJ v1.41n. For all Mup1-GFP images, identical maximum and minimum intensity values were applied to each sample within a set of WT, 4Δ+Ent1 and 4Δ+ENTH1 cells.

Statistical analysis:

Except where noted, statistical significance was determined using a two-tailed Mann-Whitney U test for the null hypothesis that the medians were equal.

Preparation of cell lysates and immunoblotting:

For analysis of GFP-Atg8, whole cell extracts were performed as previously described (Aoh et al., 2011). Following extractions, immunoblotting was performed as previously described. Monoclonal GFP antibody (B-2) was from Santa Cruz Biotechnology (Santa Cruz, CA). Polyclonal antibody Adh1 antibody and fluorescent secondary antibodies were from Ab-cam (Cambridge, MA) and Invitrogen (Carlsbad, CA) respectively.

Amino acid analysis:

Amino acid analysis was performed on cells grown to log-phase or on cells grown to log-phase, then washed three times into appropriate starvation media and grown for an additional 24 h. Amino acid extraction and analysis was performed as previously described (Jones et al., 2012).

Viability:

Cell viability assays were performed on cells grown to log-phase, then washed three times into appropriate starvation media. Cells were serially diluted and plated on YPD (1% yeast extract, 2% peptone, 2% glucose, 2% agar) plates or incubated with aeration for seven days, serially diluted and plated. Plated cells were counted after 48 h.

Results

Plasma membrane to vacuole traffic is required for cell survival

Previous whole genome studies of glucose starved cells suggested that autophagy is dispensable for survival during glucose starvation. However, several genes important for traffic to the vacuole are required for survival (Klosinska et al., 2011). We hypothesized that during glucose starvation, protein and lipid traffic to the vacuole may provide catabolic substrates necessary for cell viability. We assessed the contributions of endocytosis, endosomal membrane traffic, and autophagy to cell survival during glucose starvation by measuring the viability of strains lacking genes from each pathway. We measured the viability of wild-type cells, cells defective in endocytosis (*sla1Δ* and *rvs161Δ),* cells defective in vacuolar protein sorting (*vps4Δ*), cells defective in autophagy (*atg5Δ*) and cells defective in vacuolar proteolysis (*pep4Δ*) after seven days of starvation (Ammerer et al., 1986; Babst et al., 1997; Kametaka et al., 1996; Woolford et al., 1986). Wild-type and *atg5Δ* cells exhibited high viability after seven days of starvation (Fig. 2.1A). In contrast, *sla1Δ* or *vps4Δ* cells were approximately 50% viable *pep4Δ* cells were 30% viable and *rvs161Δ* cells were 15% viable. (Fig. 2.1A). Together these results indicate that endocytosis, vacuolar protein sorting, and vacuolar proteolytic function are important for cell survival during glucose starvation, whereas autophagy does not play an essential role.

We next monitored the fate of plasma membrane proteins during glucose starvation. We imaged cells expressing fluorescently tagged versions of several plasma membrane-localized proteins grown in the presence of 2% glucose and then starved for

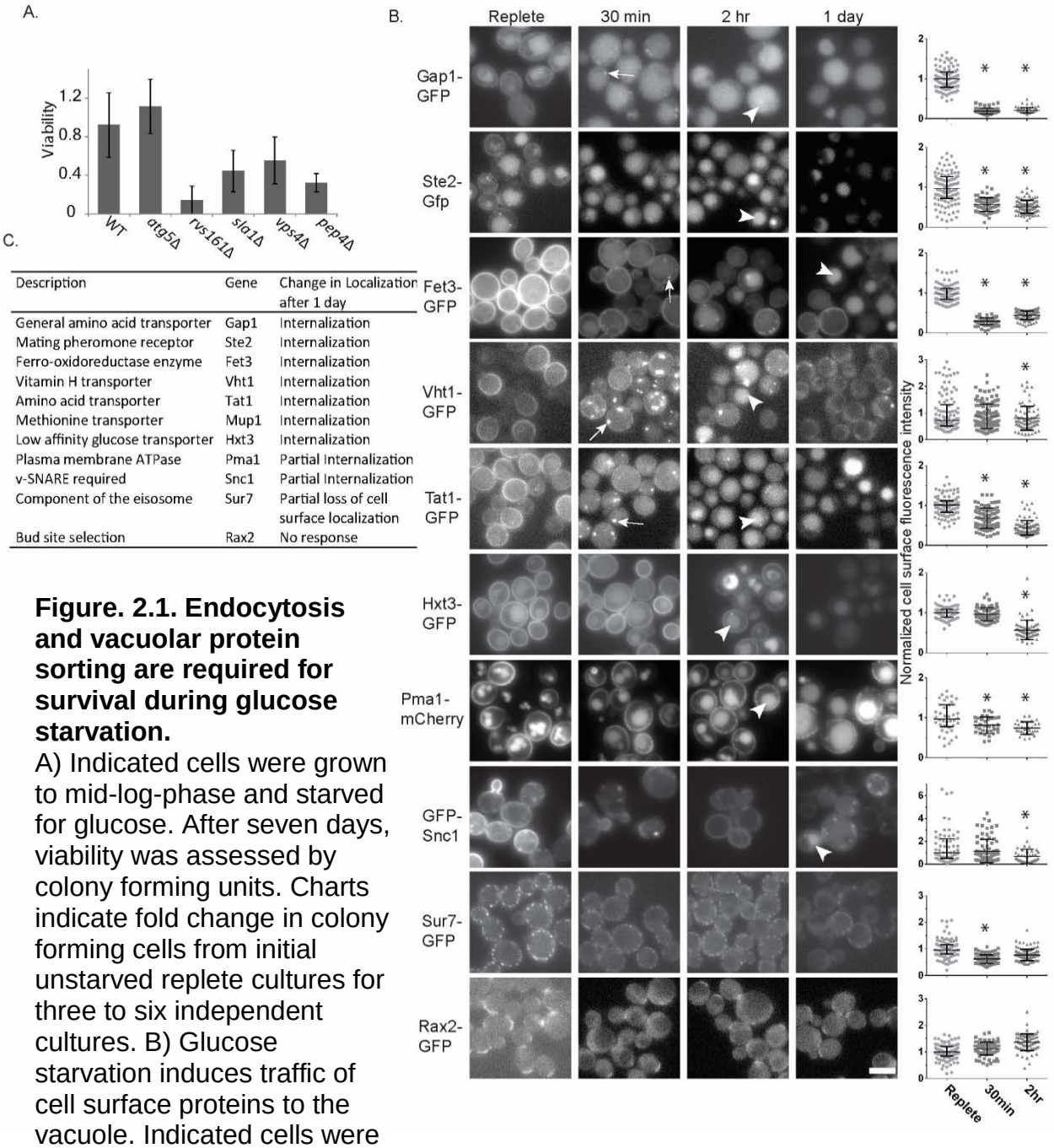

C.

Description	Gene	Change in Localization after 1 day
General amino acid transporter	Gap1	Internalization
Mating pheromone receptor	Ste2	Internalization
Ferro-oxidoreductase enzyme	Fet3	Internalization
Vitamin H transporter	Vht1	Internalization
Amino acid transporter	Tat1	Internalization
Methionine transporter	Mup1	Internalization
Low affinity glucose transporter	Hxt3	Internalization
Plasma membrane ATPase	Pma1	Partial Internalization
v-SNARE required	Snc1	Partial Internalization
Component of the eisosome	Sur7	Partial loss of cell surface localization
Bud site selection	Rax2	No response

Figure. 2.1. Endocytosis and vacuolar protein sorting are required for survival during glucose starvation.

A) Indicated cells were grown to mid-log-phase and starved for glucose. After seven days, viability was assessed by colony forming units. Charts indicate fold change in colony forming cells from initial unstarved replete cultures for three to six independent cultures. B) Glucose starvation induces traffic of cell surface proteins to the vacuole. Indicated cells were imaged during log-phase growth in replete media. Cells were washed into glucose starvation media and imaged at 30 min, 2 h or after 1 d. Arrows indicate intracellular structures. Arrowheads indicate a vacuole as identified by transmitted light microscopy (not shown). Scale bar is 5 µm. Charts show scatter dot plots of the cell surface intensity data normalized to median value for replete cells. The horizontal lines indicate the median and quartiles of the data. *indicates a P value <0.005 for a difference between replete and starved sample. C) Summary of cell surface proteins investigated and response to 1 day of glucose starvation.

glucose for 30 min, 2 h, or one day (Fig. 2.1B). Of the eleven proteins tested, the cell surface levels of nine proteins were significantly reduced within 2 hours of starvation (Fig. 2.1B&C). For these proteins, the cell surface levels decreased and, for many, punctate internal structures appeared within 30 min (Fig. 2.1B, arrows). Furthermore, after 2 h, the number or intensity of punctate internal structures were reduced whereas vacuolar fluorescence appeared or increased for many proteins (Fig. 2.1B arrowheads). Notably, endocytosis seemed to occur for proteins unrelated to metabolism such as the pheromone receptor, Ste2, and the v-SNARE, Snc1. Thus, glucose starvation leads to the flux of numerous and diverse plasma membrane proteins to the vacuole.

We next tested if clathrin mediated endocytosis (CME) is required for the observed plasma membrane protein internalization. To do this, we used a previously established assay of clathrin dependent endocytosis based on the clathrin adaptor mediated internalization of Mup1-GFP, a methionine permease (Prosser et al., 2011; Prosser et al., 2010). In control cells (wt and 4-pENT1), within 30 min of glucose starvation Mup1-GFP cell surface levels decreased and Mup1-GFP appeared in internal structures (Fig 2.2A). In contrast, in cells lacking CME due to deletion of multiple adaptors complemented by a plasmid encoding only a fragment of the adaptor Ent1 (Δ4-pENTH), Mup1-GFP remained at the cell surface for 2 h of glucose starvation and did not accumulate in internal structures. Similarly, in cells lacking *RVS161* more Tat2-GFP remained at the cell surface after 2 hours of starvation than in wild-type cells (Fig. 2.2B). Together these results demonstrate that the internalization of proteins in response to glucose starvation depends on CME.

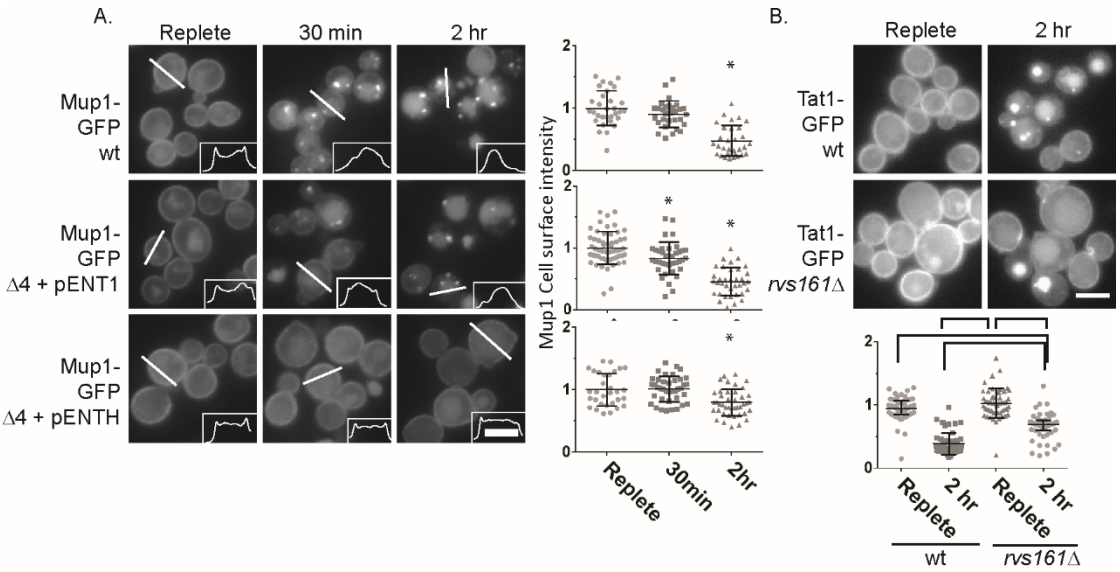

Figure 2.2. Clathrin mediated endocytosis is required for glucose starvation induced endocytosis.

A) CME is important for redistribution of Mup1-GFP. Left: Mup1-GFP localization in wild-type cells or cells lacking the four clathrin adaptors Ent1, Ent2, YAP1801 and Yap1802 (Δ4) and carrying either a plasmid encoding full length Ent1 (pENT1), which complements the CME defect caused by loss of clathrin adaptors, or the ENTH domain of Ent1 (pENTH), which does not complement the CME defect. Cells were imaged after growth in replete media lacking methionine (to induce *MUP1* expression) or after starvation for glucose for 30 min or 2hr. Insets show line scans of regions indicated. Right: Charts scatter dot plots of the data as in Fig. 3.1. * indicates a P value <0.005 for a difference between replete and starved samples. B) CME is important for redistribution of Tat1-GFP. Top: indicated cells were imaged after growth in replete media or after glucose starvation for two hours. Bottom: Charts show scatter box plots of the data as in Fig. 1 normalized to median intensity of wt cells in replete media. Brackets indicate pairs of samples for which P value <0.005.

Glucose starvation reduces recycling from the endosomes

The rerouting of plasma membrane proteins into the vacuole could result from increased rates of endocytosis, increased rates of traffic to the vacuole or reduced recycling of endocytosed proteins. We dissected the contribution of each of these mechanisms to the observed internalization of plasma membrane proteins upon glucose starvation using the dye FM4-64.

We first assessed changes in the rate of FM4-64 internalization. To monitor internalization, we incubated cells with FM4-64 for 2.5 min to allow internalization and then inhibited further traffic by placing the cells on ice and adding sodium azide and sodium fluoride to inhibit metabolic processes. Cells grown in replete media showed many small and medium sized foci of internalized FM4-64 consistent with many endocytic events and limited traffic to the early endosome (Fig. 2.3A). When cells were starved for glucose for 30 min prior to FM4-64 incubation, the internalization was less than half of that in the presence of glucose as monitored by total cell fluorescence and similar to the amount internalized by cells lacking *RVS161* (Fig. 2.3A, chart). This reduction in endocytosis rates in starved cells is consistent with the dependence of endocytosis on actin polymerization which requires ATP (Belmont and Drubin, 1998). These results show that the bulk internalization of plasma membrane proteins upon glucose starvation cannot be due to increased rates of endocytosis.

Next, we determined the rate of transport of internalized FM4-64 to the vacuole using a pulse-chase assay. We monitored FM4-64 traffic to the vacuole by labeling cells for a 15 min pulse followed by a 30 min chase. In the presence of glucose, FM4-64 was internalized and transported completely to the vacuole within 30 min (Fig. 2.3B, arrows).

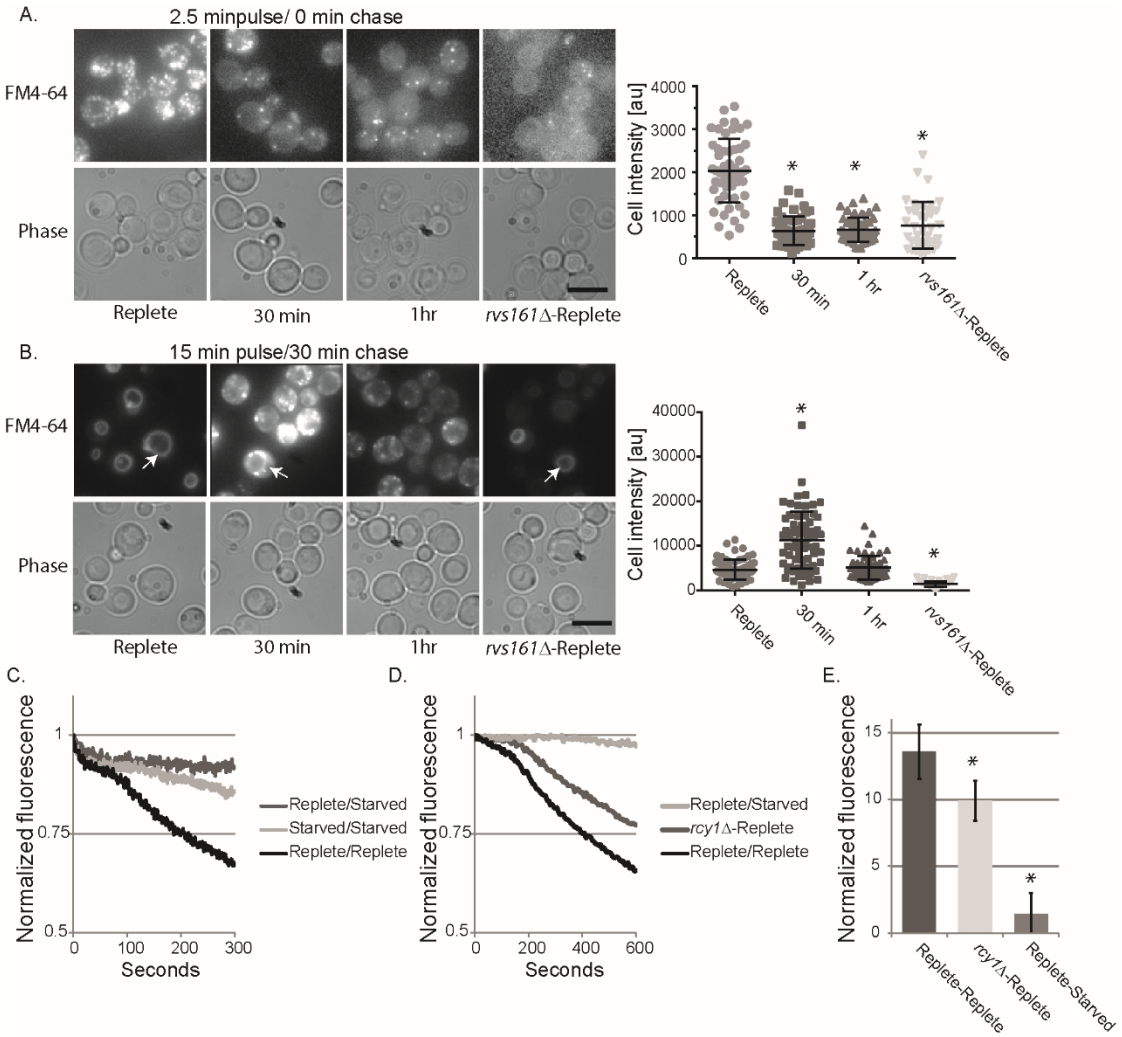

Figure 2.3. Glucose starvation alters FM4-64 traffic.

A. Internalization of FM4-64 was monitored in wild-type cells treated with FM4-64 for 2.5 minutes in replete media or in glucose starvation media after starvation for indicated time points or in *rvs161Δ* cells in replete media (far right). Lower panels show transmitted light images (Trans). Charts show scatter box plots of whole cell intensity data in arbitrary units. *indicates a P value <0.005 for a difference from wild- replete. B. FM4-64 delivery to the vacuole and whole cell accumulation was monitored by pulse-chase analysis in cells grown in replete media or glucose starved for indicated time points or in *rvs161Δ* cells in replete media (far right). Arrow indicates vacuolar labeling. Charts show scatter box plots of whole cell intensity in arbitrary units. *indicates a P value <0.005 for a difference from wild-type replete. C. FM4-64 recycling was monitored in cells that were labeled in replete media and then washed into replete media (Replete/Replete) or glucose starvation media (Replete/Starved) or in cells that were starved for glucose for thirty min prior to labeling and then washed into glucose starvation media. (Starved/Starved). Chart shows data normalized to initial sample fluorescence averages of three independent experiments. Standard deviations were <6% of the averaged value at each time-point; for clarity standard deviations are not shown. D. FM4-64 recycling was monitored in wild-type or *rcy1Δ* W303 cells as in C. Charts show representative data. E. FM4-64 recycling was monitored as FM4-64 present in culture media from cells in D after 8 minutes of recycling at 30°C. Chart shows average fluorescence for four samples. *indicates a P value <0.05 determined by a 2-tailed student T-test for a difference from wild-type replete.

In contrast, when cells were starved for glucose for 30 min or 1 h prior to incubation with FM4-64, FM4-64 delivery to the vacuole was reduced as monitored by accumulation of FM4-64 in puncta and reduced numbers of cells with vacuolar staining (Fig. 2.3B, arrows). In contrast, cells lacking *RVS161* completed traffic to the vacuole. Thus, traffic to the vacuole is reduced in glucose starved cells.

We noticed that cells starved for glucose for 30 min prior to FM4-64 labeling appeared to accumulate a high level of FM4-64 (Fig. 2.3B, chart). This suggests that at early time points after starvation, reduced endocytosis rates are counter-balanced with reduced recycling rates. Similarly, substantial FM4-64 accumulated in cells starved for 1 h prior to FM4-64 labeling despite the strong reduction in internalization rates at this time-point. When combined with the lower rates of internalization, the substantial accumulation of FM4-64 indicates that glucose starved cells have reduced rates of recycling.

Because the differences in whole cell intensity measurements in the pulse-chase experiment could be affected by the dramatically different morphology of the FM4-64 staining between starved and unstarved cells, we directly monitored changes in FM4-64 recycling from endosomes to the plasma membrane. We first incubated cells with FM4-64 for 15 min in the presence of glucose with no chase. When these cells were diluted into fresh media containing glucose, FM4-64 fluorescence rapidly decreased (Fig. 2.3C Replete/Replete). This decrease reflects recycling of internalized FM4-64 to the cell surface (Wiederkehr et al., 2000). In contrast, when cells were diluted into media lacking glucose, FM4-64 was retained in the cell (Fig. 2.3C Replete/Starved). Similar results were observed for cells starved for glucose for 30 min prior to labeling in the absence of

glucose (Fig. 2.3C Starved/Starved). We next tested how this decrease in recycling compared to cells with known defects in recycling. We used a previously characterized *rcy1*Δ and an isogenic wild-type strain (Chen et al., 2005). Starvation inhibited FM4-64 recycling more strongly than loss of *RCY1* (Fig. 2.3D, E). Taken together these results suggest that glucose starvation induces net flux from the cell surface to vacuole by inhibiting recycling of internalized cell surface proteins from the endosomes back to the plasma membrane.

Vacuolar hydrolysis inhibits autophagy during glucose starvation

The net flux of proteins from the plasma membrane to the vacuole, when combined with the reduced viability of endocytic mutants during glucose starvation, suggests that endocytosis performs an essential role in adaption to starvation. In contrast, we found that autophagy is dispensable for survival (Fig. 2.1A). Although our finding is in accordance with previous reports that autophagy is not essential during glucose starvation, this dispensability is surprising because autophagy was reported to occur in glucose starved yeast (Klosinska et al., 2011; Takeshige et al., 1992). Therefore, we investigated whether autophagy was induced under our glucose starvation conditions. We monitored autophagy using GFP-Atg8 expressed from its endogenous promoter from a centromeric (low-copy) plasmid. Atg8 covalently conjugates to the autophagosome membrane. Thus, autophagosome formation appears as GFP-Atg8 punctate localization. Upon autophagosome fusion with the vacuole, GFP-Atg8 is delivered into the vacuole where it is cleaved. Therefore, fusion of the autophagosome with the vacuole causes vacuolar localization of GFP and appearance

of free GFP, as detected by immunoblot analysis (Klionsky, 2012). Furthermore, this system allows us to investigate the normal transcriptional response of *ATG8* during starvation. In response to 16 h of glucose starvation, punctate GFP-Atg8 structures accumulated (Fig. 2.4 A). However, little Atg8 was delivered to the vacuole as monitored by fluorescence microscopy or by immunoblot analysis (Fig. 2.4. A, B). We found similar results with a quantitative assay of autophagy that measures delivery of a cytosolic form of the phosphatase Pho8 (Pho8Δ60) to the vacuole (Fig. 2.4C) (Noda and Klionsky, 2008). These results suggest that glucose starvation does not induce high levels of autophagy, contrary to previous reports.

The disagreement between our results and previous reports can be explained by a specific experimental design feature used previously (Takeshige et al., 1992). The prior study used cells lacking vacuolar hydrolysis to accumulate autophagic bodies in the vacuole. During glucose starvation, vacuolar hydrolysis should release amino acids and lipids, which could regulate autophagy (Stephan et al., 2009; Yorimitsu et al., 2007). Amino acids inhibit autophagy through activating TORC1 (Loewith, 2011). Similarly, energy derived from lipids can inhibit autophagy by converting ADP to ATP thereby inhibiting AMPK, a potent activator of autophagy (Mayer et al., 2011; Stephan and Herman, 2006). Therefore, we hypothesized that, in the prior study, autophagy was induced inadvertently upon glucose starvation because the normal regulation of pathways like TORC1 and AMPK by protein and lipid hydrolysis in the vacuole was disrupted.

To test this possibility, we monitored autophagy in cells lacking the primary vacuolar hydrolase Pep4. In *pep4Δ* cells, GFP-Atg8 puncta accumulated after 16 h of

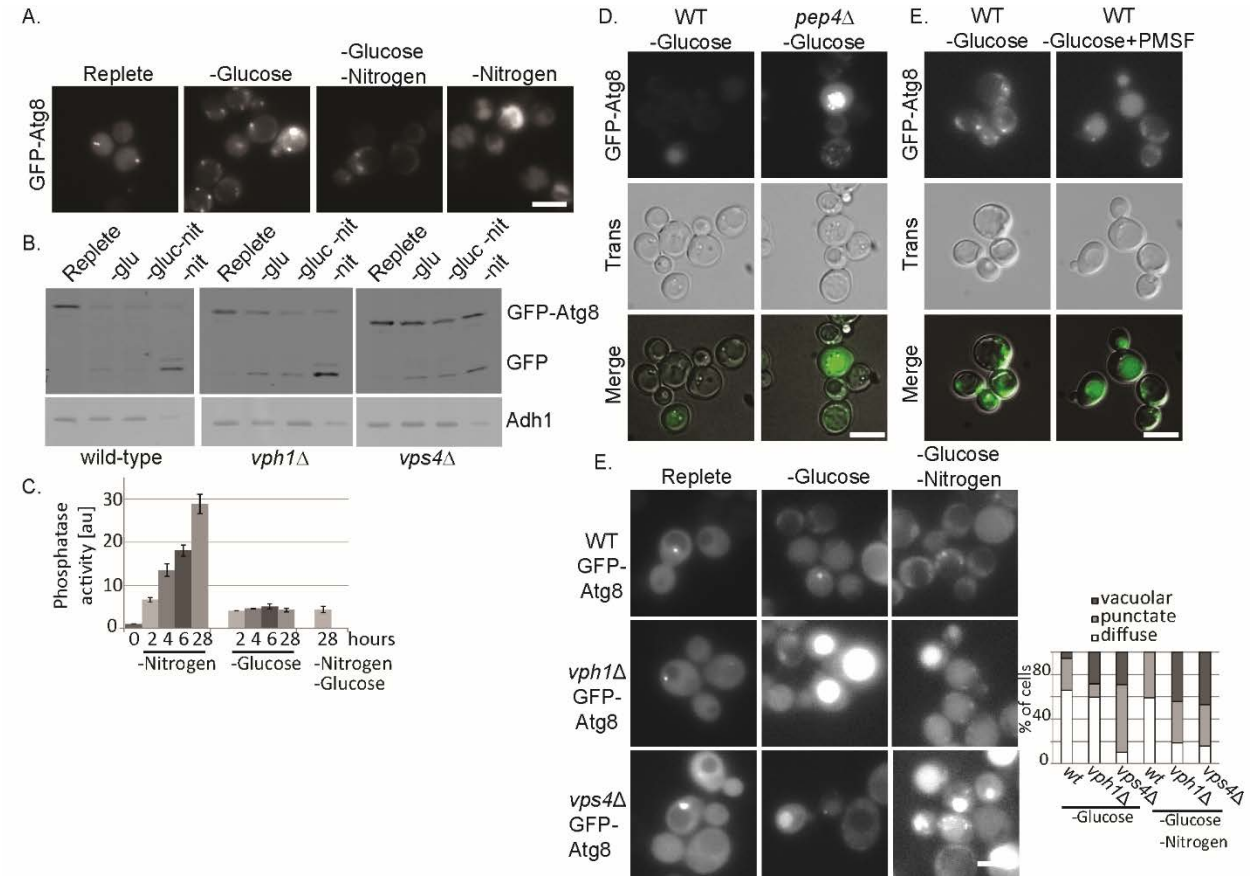

Figure 2.4. Vacuolar proteolysis inhibits autophagy in glucose starved cells.

A) Wild-type cells transformed with a plasmid expressing *GFP-ATG8* were grown in replete media lacking uracil and imaged. Portions of the remaining sample were washed into indicated starvation media. Starved cells were imaged after 16 h of treatment. B) Cell lysates were taken from samples described in A and F and subjected to immunoblot analysis for GFP or the load control Adh1. C) Autophagy was monitored by Pho8-Δ60 assay in cells grown in replete media and starved for indicated nutrients and time points. D&E) Indicated cells were treated as in A. For cells treated with PMSF, PMSF was added after final wash with glucose starvation media. Middle panel shows transmitted (Trans) light image of cells. F) Wild-type, *vph1Δ* or *vps4Δ* cells treated and imaged as in A. Chart shows percentage of cells categorized as containing diffuse cytosolic, punctate cytosolic or vacuolar GFP-Atg8 localization

glucose starvation, indicating autophagy onset (Fig. 2.4 D). Importantly, unlike puncta in wild-type cells, many puncta in the *pep4Δ* cells were in the vacuole as assessed by transmitted light microscopy (Fig. 2.4D). This suggests that in *pep4Δ* cells, autophagosomes fuse with the vacuole, however the autophagic bodies do not break down because Pep4 is required to activate vacuolar lipases that hydrolyze the membrane components of the autophagic bodies (Teter et al., 2001). As a further test, we treated wild-type cells with the cell permeant protease inhibitor PMSF during the course of glucose starvation. Cells treated with PMSF induced autophagy as monitored by GFP fluorescence in the vacuole (Fig. 2.4E). Together these results suggest that the products of vacuolar hydrolysis prevent autophagy upon glucose starvation.

To further test the hypothesis that vacuolar hydrolysis inhibits autophagy, we examined autophagy in cells lacking *VPH1* and *VPS4*. *VPH1* encodes a vacuolar specific component of the V-ATPase required for acidification of the vacuole and maximal hydrolytic activity (Kawasaki-Nishi et al., 2001; Manolson et al., 1992; Manolson et al., 1994). *VPS4* is involved in sorting of proteins into the lumen of the vacuole and through this role may be required for maximal proteolytic activity (Rothman and Stevens, 1986). In cells lacking *VPH1* or *VPS4*, autophagy was higher as monitored by fluorescence microscopy (Fig 2.4F). In immunoblot analysis, the levels of both full-length GFP-Atg8 and free GFP were higher in glucose starved *vph1*Δ and *vps4Δ* cells than in wild-type cells (Fig 2.4B). The elevation of both full-length and cleaved GFP-Atg8 is likely due to the combined effects of elevated transcription from the *ATG8* promoter due to transcriptional activation of autophagy, and enhanced delivery of GFP-Atg8 to the vacuole but decreased proteolysis in the vacuole (Kirisako

et al., 1999). These results further suggest that hydrolytic activity in the vacuole prevents autophagy during glucose starvation. They also explain the discrepancy between our observations and previous reports based in cells with protease deficient vacuoles.

Although glucose starvation did not induce high levels of autophagy as detected by delivery of GFP-Atg8 or Pho8Δ60 to the vacuole, glucose starved cells frequently contained more GFP-Atg8 puncta than cells in replete media. This suggests that although autophagy is initiated during glucose starvation, glucose starvation does not provide all signals required to complete autophagy or that glucose starvation produces a signal that inhibits autophagy completion. To test these possibilities, we asked whether glucose starvation influenced autophagy initiated by nitrogen starvation. Nitrogen starvation is a potent activator of autophagy. We starved cells for nitrogen only or both glucose and nitrogen at the same time. In cells starved for nitrogen, autophagy completed as monitored by all three assays used (Fig. 2.4A-C). In contrast, when cells were starved for both glucose and nitrogen concurrently, few cells showed evidence of completed autophagy by all three assays used (Fig. 2.4A-C). However, in *vph1*Δ and *vps4Δ* cells autophagy completed as monitored by GFP fluorescence in the vacuole and the accumulation of free GFP (Fig. 2.4B&F). Together these results indicate that glucose starvation actively inhibits autophagy and that the mechanism of inhibition requires efficient vacuolar hydrolysis.

We tested if the requirement for vacuolar proteolysis was due to the use of auxotrophic strains. We found that in a prototrophic strain GFP-Atg8 was not delivered to the vacuole during starvation for glucose or glucose and nitrogen (Fig. 2.5A).

Furthermore, in a prototrophic strain lacking *PEP4* or treated with PMSF, GFP-Atg8 was delivered to the vacuole during glucose starvation (Fig 2.5. B). To determine when GFP accumulation initiated in the vacuole in the prototrophic proteolytic deficient strains, we monitored GFP-Atg8 accumulation after one, three or 23 hours of glucose starvation (Fig 2.5 B). Prior to glucose starvation cells lacking *PEP4* had more GFP detected in the vacuole than wild-type cells. The GFP detected was primarily in the form of highly motile puncta. After one hour of starvation, more than one half of the *pep4Δ* cells had GFP present in the vacuole. Starvation for longer periods did not increase the number of cells with GFP in the vacuole, but it did increase the number of puncta. In cells treated with PMSF, after one hour of starvation the number of cells with vacuolar staining was similar to that of cells not treated with PMSF. However, by three hours, nearly 40% of PMSF treated cells had GFP in the vacuole and by 23 hours more than 70% of cells had GFP in the vacuole. Thus, even in cells capable of making all amino acids, glucose starvation does not induce autophagy and vacuolar hydrolysis inhibits autophagy.

The vacuole is the hydrolytic endpoint for numerous pathways including multiple forms of autophagy, membrane traffic from the endosomes, and membrane traffic from the Golgi. We tested the contribution of endocytosis to the inhibition of autophagy. We found that in cells lacking *SLA1* or *RVS161,* GFP-Atg8 was not delivered to the vacuole after 16 hours of starvation for glucose or glucose and nitrogen (Fig. 2.5C). This suggests that endocytosis does not contribute to the inhibition of autophagy.

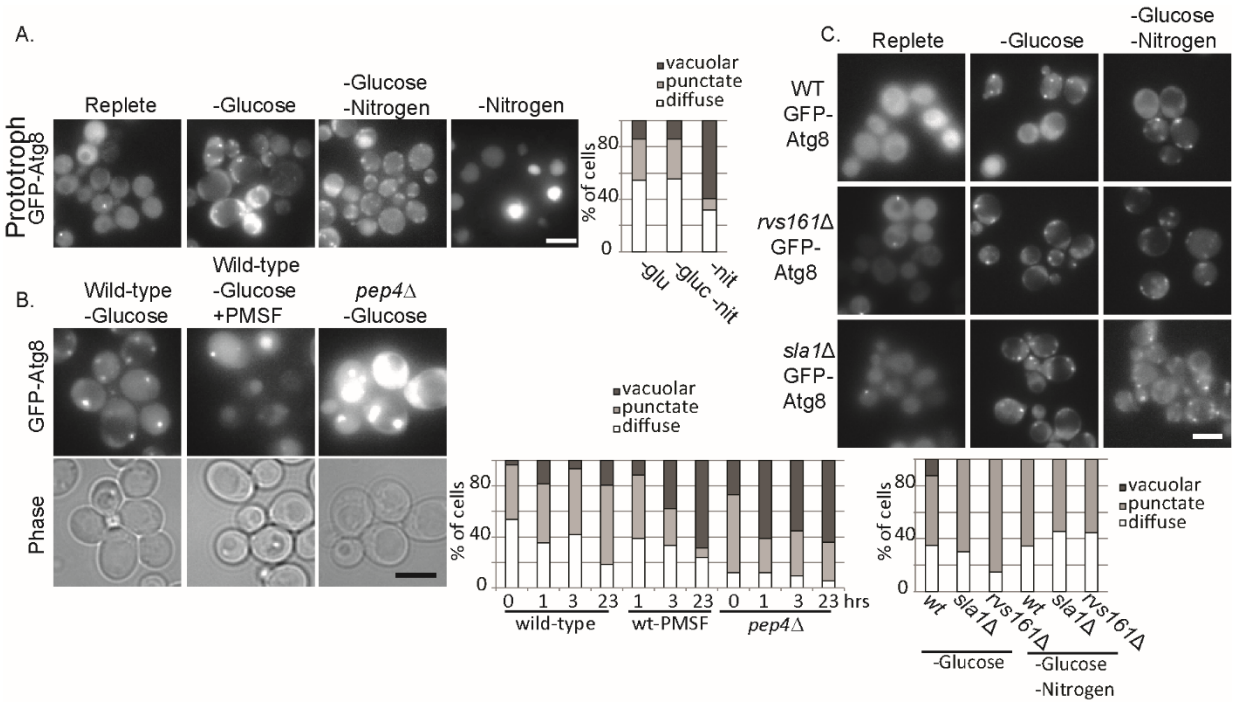

Figure 2.5. Vacuolar proteolysis inhibits autophagy in prototrophic glucose starved cells.

A) Wild-type cells auxotrophic for only *URA* (LWY 114) were transformed with a plasmid expressing *GFP-ATG8* and the uracil auxotrophic marker, grown in replete media without any add-back mix and starved as in Fig 4. B) Wild-type or *pep4Δ* cells auxotrophic for only *URA* (DLY434 & 432) were treated as in A and imaged at indicated time points after starvation for glucose. For cells treated with PMSF, PMSF was added after the final wash with glucose starvation media. C) Defects in endocytosis do not increase autophagy response to glucose starvation. Auxotrophic wild-type, *rvs161Δ* or *sla1Δ* cells transformed with a plasmid expressing *GFP-ATG8* were treated as in Figure 3.4 A. Starved cells were imaged after 16 h of treatment. Charts show the percentage of cells in the sample categorized as containing diffuse cytosolic, punctate cytosolic or vacuolar GFP-Atg8 localization. Scale bar is 5 µm.

Glucose starvation elevates free amino acid levels via vacuolar hydrolysis

Because amino acids are potent inhibitors of autophagy, we hypothesized that glucose starvation may inhibit autophagy through the production of amino acids via vacuolar hydrolysis. Accordingly, a previous metabolomics study demonstrated that free amino acids increase in glucose starved cells (Brauer et al., 2006). In order to test if vacuolar hydrolysis was important for this increase, we monitored a subset of free amino acid levels in wild-type, *pep4*Δ and *vps4*Δ cells. Of the 17 amino acids monitored, the levels of eight rose more than 2 fold in response to glucose starvation in wild-type cells (Fig. 2.6A, supplemental data). A notable exception is methionine, which decreased to less than half of the levels seen in replete conditions. In *pep4*Δ or *vps4*Δ cells, the increases of amino acids were strongly reduced for six of the eight amino acids: valine, isoleucine, tyrosine, phenylalanine, histidine and arginine, but not lysine or cysteic acid (Fig 2.6A). We also found that many free amino acids levels rose in cells starved for both glucose and nitrogen (Fig. 2.6A). Notably, many amino acids rose to higher levels in cells starved for both glucose and nitrogen than for cells starved for glucose alone. Furthermore, we found that in *pep4Δ* or *vps4Δ* cells starved for both glucose and nitrogen the amino acid levels were even lower than in glucose starvation alone (Fig. 2.6A). This observation suggests the mechanism by which glucose starvation inhibits autophagy in the presence of nitrogen starvation; when cells are starved for both glucose and nitrogen, amino acids released from vacuolar hydrolysis inhibits autophagy.

We next tested the contribution of endocytosis to the release of amino acids. We found that inhibiting endocytosis caused an intermediate effect on amino acid levels.

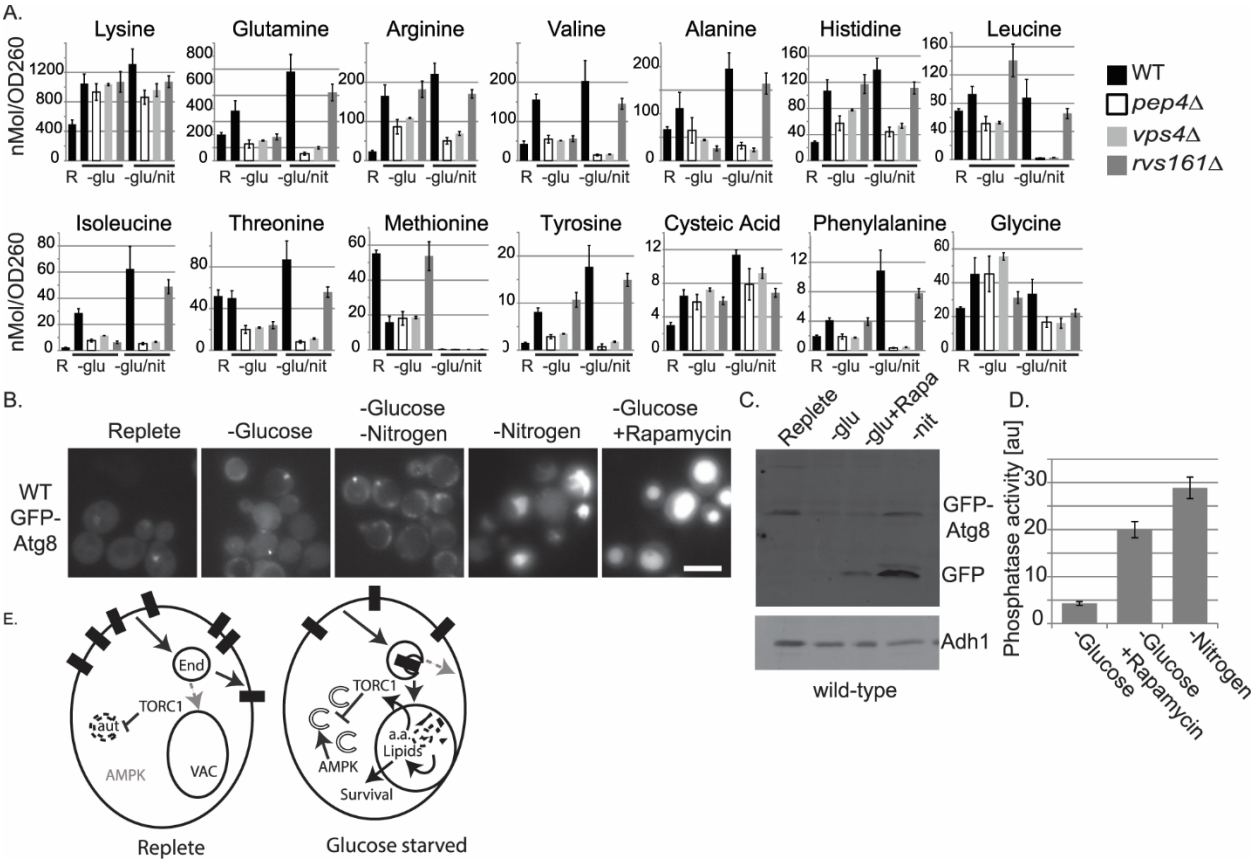

Figure 2.6. Vacuolar hydrolysis elevates amino acid levels and inhibits autophagy through TORC1.

A) Free amino acids were extracted from indicated cells grown to mid-log-phase (R) or starved for glucose (-glu) or for glucose and nitrogen (-glu/nit) for 24 h. Charts show a subset of the monitored amino acids. B) Autophagy was monitored as in Figure 3.4. For cells treated with rapamycin, cells were starved for 16 hours and then treated with 200 nM rapamycin. Rapamycin treated cells and untreated controls were imaged at 24 h. C) Cell lysates were taken from samples in B and subjected to immunoblot analysis for GFP or the load control Adh1. D) Autophagy was monitored with phosphatase activity as in Figure 3.4. For rapamycin treated cells, cells were starved for glucose for 10 hours then treated with rapamycin. Assay was performed at 28h. E) Model of cellular responses to glucose starvation. In replete cells, autophagy (aut) is inhibited by the activity of TORC1. Many cell surface proteins are endocytosed to the endosomes (end) but recycle back to the cell surface and do not traffic to the vacuole (vac). During glucose starvation, endocytosis continues at reduced rates whereas recycling stops. This leads to cell survival and, potentially, accumulation of amino acids as described the text. Increased amino acids activate TORC1, which counteracts the activity of AMPK leading to the initiation but not completion of autophagy.

Glucose starved *rvs161Δ* cells had lower levels of glutamine, valine, alanine, isoleucine, and threonine than glucose starved wild-type cells. However, in glucose and nitrogen starved cells most amino acids accumulated in *rvs161Δ* at levels similar to wild-type cells. Overall, these results show that endocytosis only contributes partially to release of amino acids in glucose starved cells.

Because TORC1 is a potent inhibitor of autophagy that is activated by amino acids, we tested if TORC1 was required to inhibit autophagy in glucose starved cells (Bonfils et al., 2012; Sancak et al., 2008; Zoncu et al., 2011). We first glucose starved cells for several hours then inhibited TORC1 with rapamycin for several hours and assessed autophagy. In contrast to untreated cells, rapamycin treated cells completed autophagy as assessed by three assays (Fig. 2.6B-D). These results indicate that TORC1 is normally active in glucose starved cells, and its activity inhibits autophagy during glucose starvation.

Discussion

Our results reveal a suite of cell behaviors induced by glucose starvation, which includes reduced recycling, increased free amino acids, and inhibited autophagy. We proposed that that these three behaviors are mechanistically linked (Fig 2.6 E). In this scenario, inhibited recycling is the crucial step. It is initiated by the acute drop in ATP levels caused by glucose starvation. Inhibited recycling drives the net flux of proteins to the vacuole, by preventing endocytosed proteins from trafficking back to the plasma membrane. Although low ATP also reduces bulk endocytosis rates, endocytosis rates

remain high enough to drive substantial internalization of proteins and FM4-64. The increase in free amino acids and subsequent inhibition of autophagy derive from the flux of proteins from the plasma membrane and elsewhere to the vacuole. Thus, these three cellular responses are likely a single mechanistic response to glucose starvation. However, several key questions remain.

It is unclear why recycling is strongly inhibited by glucose starvation while endocytosis seems less sensitive. Glucose starvation induces an acute drop in ATP. This reduces the levels of phosphatidyl-inositol 4-phosphate (PI4p) at the *trans*-Golgi network and endosomes (Aoh et al., 2013; Faulhammer et al., 2007; Hendricks et al., 1999). Furthermore, glucose starvation causes ADP-ribosylation factor (Arf) to delocalize from endosomes (Aoh et al., 2013). PI4p and Arf recruit many proteins implicated in endosomal recycling. Failure to recruit these endosomal proteins when ATP levels are low could cause reduced recycling (Crottet et al., 2002; Daboussi et al., 2012; Demmel et al., 2008; Puertollano et al., 2001; Zhdankina et al., 2001; Zhu et al., 1998). In addition to these known changes, unexplored mechanisms such as changes in ubiquitination/deubiquitination enzyme activities, alterations in endosomal or vacuolar pH, changes in activities of lipid flippases or any combination of these factors could be the mechanism(s) of inhibited recycling during glucose starvation (Dechant et al., 2010; Furuta et al., 2007; Liu et al., 2008; Perzov et al., 2002). Regardless of the mechanism, inhibited recycling seems to be a conserved response to ATP depletion. In metazoan cells, ATP depletion causes the internalization of proteins that seem unrelated to energy (Clarke and Weigel, 1985; Liao and Perkins, 1993; Podbilewicz and Mellman, 1990). Furthermore, similar to the behavior observed in glucose starved yeast cells, this

internalization is a result of reduced recycling (Podbilewicz and Mellman, 1990). Thus, the overall behavior likely reflects an ancient response to energy depletion.

How the cell selects proteins for endocytosis during glucose starvation is unclear. Diverse proteins undergo endocytosis upon glucose starvation. Because cells defective in endocytosis die during glucose starvation, endocytosis performs an essential function during glucose starvation. Endocytosis may be required to remove deleterious proteins from the cell surface. For example, ATP dependent transporters might deplete cellular ATP to lethal levels if left at the plasma membrane. An additional, but not mutually exclusive, model is that endocytosis acts as an alternative to autophagy and allows the cell to catabolize the lipids and amino acids from the plasma membrane as resources for survival. Understanding how proteins are selected for endocytosis may help explain the requirement for endocytosis.

The model that endocytosis provides catabolic substrates suggests a novel survival mechanism that is tailored to meet the specific cellular needs during acute energy starvation. By rerouting endocytic traffic to the vacuole, the cell can hydrolyze the lipid content of the plasma membrane. Since lipids are a rich source of energy, this mechanism will resupply the cell with energy. In contrast, autophagy is not known to access this pool of lipids. Furthermore, autophagy can promote the hydrolysis of peroxisomes and mitochondria (Suzuki, 2013). The degradation of these organelles is counter-productive in energy stress because these organelles are required to generate energy through β-oxidation and subsequent respiration. The risk of destroying these organelles may explain why, when faced with both amino acid and glucose starvation, the cell opts to inhibit autophagy.

Indeed, our results suggest that the downregulation of recycling and inhibition of autophagy could be linked. Our results demonstrate that vacuolar function inhibits autophagy. This inhibition depends at least in part on TORC1, suggesting that the accumulation of amino acids in glucose starved cells inhibits autophagy. An attractive model is that the accumulated amino acids derive from endocytosed proteins, however, cells lacking *RVS161* or *SLA1* inhibit autophagy as well as wild-type cells. Interestingly, deletion of *RVS161* reduces the accumulation of several amino acids, but not the key autophagy regulator leucine (Bonfils et al., 2012). Thus, endocytosis likely contributes to the accumulated amino acids but is not essential for the key autophagy regulating amino acids. Additional routes to the vacuole may thus contribute to accumulated amino acids during glucose starvation. Possible routes include microautophagy, clathrin independent endocytosis and reduced recycling to biosynthetic organelles leading to consumption of proteins and lipids from such organelles as the Golgi, ER and endosomes. Furthermore, amino acid accumulation will also be influenced by the release of free amino acids from proteasomal degradation, the import from extracellular supplies and the consumption of the free amino acids in the form of protein biosynthesis or other metabolic uses. Indeed, the accumulation of amino acids in cells starved for glucose could be caused by overall reduced protein synthesis due to low methionine in these cells (Fig 2.5A). Thus, the impact of mutations on amino acid accumulation is difficult to interpret. Regardless of the source of the free amino acids accumulating in wild-type cells, our results provide strong evidence that vacuolar hydrolysis of lipids or proteins activates TORC1 and inhibits autophagy in glucose starved cells.

The finding that vacuolar hydrolysis inhibits autophagy and activates TORC1 contributes to a growing literature about the importance of lysosomal function for correct regulation of these processes (Li et al., 2013; Zoncu et al., 2011). Indeed, there is growing concern about the use of lysosomal inhibitors in autophagy research (Barth et al., 2010; Juhasz, 2012). Such inhibitors are commonly used to accumulate intermediates of macroautophagy to facilitate their detection (Klionsky et al., 2012). However, such inhibitors will also prevent the normal release of many metabolites. In addition to lipids and amino acids, vacuolar hydrolysis in yeast is important for the mobilization of phosphate and storage carbohydrates (Indge, 1968; Wilson et al., 2002). By preventing the release of these resources, lysosomal inhibitors may increase the strength of a normal starvation response or may even activate a starvation response that would not normally occur. Thus, the finding reported here that inhibiting vacuolar hydrolysis in glucose starved cells promotes autophagy provides additional evidence about the possible confounding impact of lysosomal inhibitors on experimental outcomes.

Table 2.1: Strains used

Strain	genotype	Source
BY4741	MAT a *his3Δ1 leu2Δ0 ura3Δ0 met15Δ0*	Invitrogen
BY4742	MAT α *his3Δ1 leu2Δ0 ura3Δ0 lys2Δ0*	Invitrogen
DLY046	BY4742 *SUR7-GFP::KanMX*	This study
DLY050	BY4742 *HXT3-GFP::KanMX*	This study
DLY052	BY4742 *VHT1-GFP::KanMX*	This study
DLY055	BY4742 *RAX2-GFP::KanMX*	This study
MDY1113	BY4741 *FET3-GFP::His3Mx*	This study
QAY559	BY4742 *PMA1-mCherry::His3MX*	This study
QAY561	diploid *his3Δ1/his3Δ1 leu2Δ0/leu2Δ0 MET15+/met15Δ0 Lys2+/lys2Δ0 ura3Δ0/ura3Δ0 GAP1-GFP::His3MX*	This study
MDY543	BY4741 *TAT1-GFP::His3Mx*	Invitrogen
MDY902	BY4741 *STE2-GFP::HIS3Mx*	Invitrogen
DLY594	BY4742 *sla1Δ::HIS3Mx TAT1-GFP::KanMx*	This study
MDY1119	BY4742 *vps4Δ::KanMx*	Invitrogen
DLY269	BY4742 *pep4Δ::KanMx*	Invitrogen
MDY1117	BY4742 *atg5Δ::KanMx*	Invitrogen
DLY085	BY4742 *vph1Δ::KanMx*	Invitrogen
DLY118	BY4742 *sla1Δ::HIS3Mx*	This study
DLY120	BY4742 *rvs161Δ::HIS3Mx*	This study
DLY234	BY4742 pRS315-*GFP-SNC1*	This study
BWY2497	MATα *his3-Δ200 trp1-Δ901 leu2-3,112 ura3-52 lys2-801 suc2-Δ9 ent1Δ::LEU2 ent2Δ::HIS3 yap1801Δ::HIS3 yap1802Δ::LEU2 + pBW0768 (pEnt1 [CEN TRP1])*	Maldonado-Báez *et al* 2008
BWY3817	MATα *his3-Δ200 trp1-Δ901 leu2-3,112 ura3-52 lys2-801 suc2-Δ9 MUP1-GFP::KanMx*	Prosser *et al* 2010
BWY4892	BWY3817 MUP1-GFP::KanMx *ent1Δ::LEU2 ent2Δ::HIS3 yap1801Δ::HIS3 yap1802Δ::LEU2* + pBW0768 (pEnt1 [CEN *TRP1*])	This study derived from BWY2497 and BWY3817
BWY4893	BWY3817 MUP1-GFP::KanMx *ent1Δ::LEU2 ent2Δ::HIS3 yap1801Δ::HIS3 yap1802Δ::LEU2* + pBW0778 (pENTH1 [CEN *TRP1*])	This study derived from BWY2497 and BWY3817
TN215	MATa *ade2 his3 leu2 lys2 trp1 ura3 pho8::pho8Δ60*	Kamada *et al* 2000
LWY114	MAT α *ura3-52*	Lois Weisman lab strain
FY4	Mat a prototroph	Winston *et al* 1995

DLY432	Mat a pep4ΔkanMx ura3Δ0	This study derived from FY4 and DLY269
DLY434	Mat a ura3Δ0	This study derived from FY4 and DLY269
NSY125	Mat a his4-539am, lys2-801am, ura3-52	Chen *et al* 2005
NSY657	Mat a his4-539am, lys2-801am, ura3-52, rcy1Δ::KanMx	Chen et al 2005

Table 2.2: Formulations of media used.

Component	Replete	Glucose starvation	Glucose and Nitrogen starvation	Nitrogen starvation
Yeast Nitrogen Base	Added	Added	Added	Added
Nitrogen source	38mM Ammonium Sulfate**	38mM Ammonium Sulfate**	None	None
Carbon source	2% glucose (w/v)	None	None	2% glucose (w/v)
Add- back mix	Amino acids and nucleotides†	Amino acids and nucleotides†	Nucleotides only†	Nucleotides only†

**except for GAP1-GFP cultures, which used 87mM proline †except for protrophic strains, which omitted all add-back

References

Ammerer, G., C.P. Hunter, J.H. Rothman, G.C. Saari, L.A. Valls, and T.H. Stevens. 1986. PEP4 gene of Saccharomyces cerevisiae encodes proteinase A, a vacuolar enzyme required for processing of vacuolar precursors. *Mol Cell Biol*. 6:2490-2499.

Aoh, Q.L., L.M. Graves, and M.C. Duncan. 2011. Glucose Regulates Clathrin Adaptors at the TGN and Endosomes. *Mol Biol Cell*. 22:3671-3683.

Aoh, Q.L., C.W. Hung, and M.C. Duncan. 2013. Energy metabolism regulates clathrin adaptors at the trans-Golgi network and endosomes. *Molecular biology of the cell*. 24:832-847.

Aravamudhan, P., I. Felzer-Kim, and A.P. Joglekar. 2013. The budding yeast point centromere associates with two Cse4 molecules during mitosis. *Curr Biol*. 23:770-774.

Ashe, M.P., S.K. De Long, and A.B. Sachs. 2000. Glucose depletion rapidly inhibits translation initiation in yeast. *Mol Biol Cell*. 11:833-848.

Babst, M., T.K. Sato, L.M. Banta, and S.D. Emr. 1997. Endosomal transport function in yeast requires a novel AAA-type ATPase, Vps4p. *EMBO J*. 16:1820-1831.

Barth, S., D. Glick, and K.F. Macleod. 2010. Autophagy: assays and artifacts. *The Journal of pathology*. 221:117-124.

Beck, T., A. Schmidt, and M.N. Hall. 1999. Starvation induces vacuolar targeting and degradation of the tryptophan permease in yeast. *J Cell Biol*. 146:1227-1238.

Belmont, L.D., and D.G. Drubin. 1998. The yeast V159N actin mutant reveals roles for actin dynamics in vivo. *J Cell Biol*. 142:1289-1299.

Bonfils, G., M. Jaquenoud, S. Bontron, C. Ostrowicz, C. Ungermann, and C. De Virgilio. 2012. Leucyl-tRNA synthetase controls TORC1 via the EGO complex. *Mol Cell*. 46:105-110.

Brauer, M.J., J. Yuan, B.D. Bennett, W. Lu, E. Kimball, D. Botstein, and J.D. Rabinowitz. 2006. Conservation of the metabolomic response to starvation across two divergent microbes. *Proceedings of the National Academy of Sciences of the United States of America*. 103:19302-19307.

Chen, S.H., S. Chen, A.A. Tokarev, F. Liu, G. Jedd, and N. Segev. 2005. Ypt31/32 GTPases and their novel F-box effector protein Rcy1 regulate protein recycling. *Mol Biol Cell*. 16:178-192.

Clarke, B.L., and P.H. Weigel. 1985. Recycling of the asialoglycoprotein receptor in isolated rat hepatocytes. ATP depletion blocks receptor recycling but not a single round of endocytosis. *J Biol Chem*. 260:128-133.

Crottet, P., D.M. Meyer, J. Rohrer, and M. Spiess. 2002. ARF1.GTP, tyrosine-based signals, and phosphatidylinositol 4,5-bisphosphate constitute a minimal machinery to recruit the AP-1 clathrin adaptor to membranes. *Mol Biol Cell*. 13:3672-3682.

Daboussi, L., G. Costaguta, and G.S. Payne. 2012. Phosphoinositide-mediated clathrin adaptor progression at the trans-Golgi network. *Nat Cell Biol*. 19:239-248.

Dechant, R., M. Binda, S.S. Lee, S. Pelet, J. Winderickx, and M. Peter. 2010. Cytosolic pH is a second messenger for glucose and regulates the PKA pathway through V-ATPase. *EMBO J*. 29:2515-2526.

Demmel, L., M. Gravert, E. Ercan, B. Habermann, T. Muller-Reichert, V. Kukhtina, V. Haucke, T. Baust, M. Sohrmann, Y. Kalaidzidis, C. Klose, M. Beck, M. Peter, and C. Walch-Solimena. 2008. The clathrin adaptor Gga2p is a phosphatidylinositol 4-phosphate effector at the Golgi exit. *Mol Biol Cell*. 19:1991-2002.

Faulhammer, F., S. Kanjilal-Kolar, A. Knodler, J. Lo, Y. Lee, G. Konrad, and P. Mayinger. 2007. Growth control of Golgi phosphoinositides by reciprocal localization of sac1 lipid phosphatase and pik1 4-kinase. *Traffic*. 8:1554-1567.

Furuta, N., K. Fujimura-Kamada, K. Saito, T. Yamamoto, and K. Tanaka. 2007. Endocytic recycling in yeast is regulated by putative phospholipid translocases and the Ypt31p/32p-Rcy1p pathway. *Mol Biol Cell*. 18:295-312.

Hendricks, K.B., B.Q. Wang, E.A. Schnieders, and J. Thorner. 1999. Yeast homologue of neuronal frequenin is a regulator of phosphatidylinositol-4-OH kinase. *Nat Cell Biol*. 1:234-241.

Indge, K.J. 1968. Polyphosphates of the yeast cell vacuole. *J Gen Microbiol*. 51:447-455.

Jones, C.B., E.M. Ott, J.M. Keener, M. Curtiss, V. Sandrin, and M. Babst. 2012. Regulation of membrane protein degradation by starvation-response pathways. *Traffic*. 13:468-482.

Juhasz, G. 2012. Interpretation of bafilomycin, pH neutralizing or protease inhibitor treatments in autophagic flux experiments: novel considerations. *Autophagy*. 8:1875-1876.

Kama, R., M. Robinson, and J.E. Gerst. 2007. Btn2, a Hook1 ortholog and potential Batten disease-related protein, mediates late endosome-Golgi protein sorting in yeast. *Mol Cell Biol*. 27:605-621.

Kamada, Y., T. Funakoshi, T. Shintani, K. Nagano, M. Ohsumi, and Y. Ohsumi. 2000. Tor-mediated induction of autophagy via an Apg1 protein kinase complex. *J Cell Biol*. 150:1507-1513.

Kametaka, S., A. Matsuura, Y. Wada, and Y. Ohsumi. 1996. Structural and functional analyses of APG5, a gene involved in autophagy in yeast. *Gene*. 178:139-143.

Kawasaki-Nishi, S., K. Bowers, T. Nishi, M. Forgac, and T.H. Stevens. 2001. The amino-terminal domain of the vacuolar proton-translocating ATPase a subunit controls targeting and in vivo dissociation, and the carboxyl-terminal domain affects coupling of proton transport and ATP hydrolysis. *J Biol Chem*. 276:47411-47420.

Kirisako, T., M. Baba, N. Ishihara, K. Miyazawa, M. Ohsumi, T. Yoshimori, T. Noda, and Y. Ohsumi. 1999. Formation process of autophagosome is traced with Apg8/Aut7p in yeast. *J Cell Biol*. 147:435-446.

Klionsky, D.J. 2012. For the last time, it is GFP-Atg8, not Atg8-GFP (and the same goes for LC3). *Autophagy*. 7:1093-1094.

Klionsky, D.J., F.C. Abdalla, H. Abeliovich, R.T. Abraham, A. Acevedo-Arozena, K. Adeli, L. Agholme, M. Agnello, P. Agostinis, J.A. Aguirre-Ghiso, and H.J. Ahn. 2012. Guidelines for the use and interpretation of assays for monitoring autophagy. *Autophagy*. 8:445-544.

Klosinska, M.M., C.A. Crutchfield, P.H. Bradley, J.D. Rabinowitz, and J.R. Broach. 2011. Yeast cells can access distinct quiescent states. *Genes & development*. 25:336-349.

Li, M., B. Khambu, H. Zhang, J.H. Kang, X. Chen, D. Chen, L. Vollmer, P.Q. Liu, A. Vogt, and X.M. Yin. 2013. Suppression of lysosome function induces autophagy via a feedback down-regulation of MTOR complex 1 (MTORC1) activity. *J Biol Chem*. 288:35769-35780.

Liao, J.F., and J.P. Perkins. 1993. Differential effects of antimycin A on endocytosis and exocytosis of transferrin also are observed for internalization and externalization of beta-adrenergic receptors. *Molecular pharmacology*. 44:364-370.

Liu, K., K. Surendhran, S.F. Nothwehr, and T.R. Graham. 2008. P4-ATPase requirement for AP-1/clathrin function in protein transport from the trans-Golgi network and early endosomes. *Mol Biol Cell*. 19:3526-3535.

Loewith, R. 2011. A brief history of TOR. *Biochem Soc Trans*. 39:437-442.

Longtine, M.S., A. McKenzie, 3rd, D.J. Demarini, N.G. Shah, A. Wach, A. Brachat, P. Philippsen, and J.R. Pringle. 1998. Additional modules for versatile and economical PCR-based gene deletion and modification in Saccharomyces cerevisiae. *Yeast*. 14:953-961.

Maldonado-Baez, L., M.R. Dores, E.M. Perkins, T.G. Drivas, L. Hicke, and B. Wendland. 2008. Interaction between Epsin/Yap180 adaptors and the scaffolds Ede1/Pan1 is required for endocytosis. *Mol Biol Cell*. 19:2936-2948.

Manolson, M.F., D. Proteau, and E.W. Jones. 1992. Evidence for a conserved 95-120 kDa subunit associated with and essential for activity of V-ATPases. *J Exp Biol*. 172:105-112.

Manolson, M.F., B. Wu, D. Proteau, B.E. Taillon, B.T. Roberts, M.A. Hoyt, and E.W. Jones. 1994. STV1 gene encodes functional homologue of 95-kDa yeast vacuolar H(+)-ATPase subunit Vph1p. *J Biol Chem*. 269:14064-14074.

Mayer, F.V., R. Heath, E. Underwood, M.J. Sanders, D. Carmena, R.R. McCartney, F.C. Leiper, B. Xiao, C. Jing, P.A. Walker, L.F. Haire, R. Ogrodowicz, S.R. Martin, M.C. Schmidt, S.J. Gamblin, and D. Carling. 2011. ADP regulates SNF1, the Saccharomyces cerevisiae homolog of AMP-activated protein kinase. *Cell Metab*. 14:707-714.

Noda, T., and D.J. Klionsky. 2008. The quantitative Pho8Delta60 assay of nonspecific autophagy. *Methods Enzymol*. 451:33-42.

Perzov, N., V. Padler-Karavani, H. Nelson, and N. Nelson. 2002. Characterization of yeast V-ATPase mutants lacking Vph1p or Stv1p and the effect on endocytosis. *J Exp Biol*. 205:1209-1219.

Podbilewicz, B., and I. Mellman. 1990. ATP and cytosol requirements for transferrin recycling in intact and disrupted MDCK cells. *EMBO J*. 9:3477-3487.

Prosser, D.C., T.G. Drivas, L. Maldonado-Baez, and B. Wendland. 2011. Existence of a novel clathrin-independent endocytic pathway in yeast that depends on Rho1 and formin. *J Cell Biol*. 195:657-671.

Prosser, D.C., K. Whitworth, and B. Wendland. 2010. Quantitative analysis of endocytosis with cytoplasmic pHluorin chimeras. *Traffic*. 11:1141-1150.

Puertollano, R., P.A. Randazzo, J.F. Presley, L.M. Hartnell, and J.S. Bonifacino. 2001. The GGAs promote ARF-dependent recruitment of clathrin to the TGN. *Cell*. 105:93-102.

Rothman, J.H., and T.H. Stevens. 1986. Protein sorting in yeast: mutants defective in vacuole biogenesis mislocalize vacuolar proteins into the late secretory pathway. *Cell*. 47:1041-1051.

Sancak, Y., T.R. Peterson, Y.D. Shaul, R.A. Lindquist, C.C. Thoreen, L. Bar-Peled, and D.M. Sabatini. 2008. The Rag GTPases bind raptor and mediate amino acid signaling to mTORC1. *Science*. 320:1496-1501.

Singh, R., and A.M. Cuervo. 2011. Autophagy in the cellular energetic balance. *Cell metabolism*. 13:495-504.

Stephan, J.S., and P.K. Herman. 2006. The regulation of autophagy in eukaryotic cells: do all roads pass through Atg1? *Autophagy*. 2:146-148.

Stephan, J.S., Y.Y. Yeh, V. Ramachandran, S.J. Deminoff, and P.K. Herman. 2009. The Tor and PKA signaling pathways independently target the Atg1/Atg13 protein kinase complex to control autophagy. *Proc Natl Acad Sci U S A*. 106:17049-17054.

Suzuki, K. 2013. Selective autophagy in budding yeast. *Cell death and differentiation*. 20:43-48.

Suzuki, K., T. Kirisako, Y. Kamada, N. Mizushima, T. Noda, and Y. Ohsumi. 2001. The pre-autophagosomal structure organized by concerted functions of APG genes is essential for autophagosome formation. *EMBO J*. 20:5971-5981.

Takeshige, K., M. Baba, S. Tsuboi, T. Noda, and Y. Ohsumi. 1992. Autophagy in yeast demonstrated with proteinase-deficient mutants and conditions for its induction. *J Cell Biol*. 119:301-311.

Teter, S.A., K.P. Eggerton, S.V. Scott, J. Kim, A.M. Fischer, and D.J. Klionsky. 2001. Degradation of lipid vesicles in the yeast vacuole requires function of Cvt17, a putative lipase. *J Biol Chem*. 276:2083-2087.

Thevelein, J.M., and J.H. de Winde. 1999. Novel sensing mechanisms and targets for the cAMP-protein kinase A pathway in the yeast Saccharomyces cerevisiae. *Mol Microbiol*. 33:904-918.

Uesono, Y., M.P. Ashe, and E.A. Toh. 2004. Simultaneous yet independent regulation of actin cytoskeletal organization and translation initiation by glucose in Saccharomyces cerevisiae. *Mol Biol Cell*. 15:1544-1556.

Vander Heiden, M.G., L.C. Cantley, and C.B. Thompson. 2009. Understanding the Warburg effect: the metabolic requirements of cell proliferation. *Science*. 324:1029-1033.

Volland, C., D. Urban-Grimal, G. Geraud, and R. Haguenauer-Tsapis. 1994. Endocytosis and degradation of the yeast uracil permease under adverse conditions. *J Biol Chem*. 269:9833-9841.

Wiederkehr, A., S. Avaro, C. Prescianotto-Baschong, R. Haguenauer-Tsapis, and H. Riezman. 2000. The F-box protein Rcy1p is involved in endocytic membrane traffic and recycling out of an early endosome in Saccharomyces cerevisiae. *J Cell Biol*. 149:397-410.

Wilson, W.A., Z. Wang, and P.J. Roach. 2002. Systematic identification of the genes affecting glycogen storage in the yeast Saccharomyces cerevisiae: implication of the vacuole as a determinant of glycogen level. *Mol Cell Proteomics*. 1:232-242.

Winston, F., C. Dollard, and S.L. Ricupero-Hovasse. 1995. Construction of a set of convenient Saccharomyces cerevisiae strains that are isogenic to S288C. *Yeast*. 11:53-55.

Woolford, C.A., L.B. Daniels, F.J. Park, E.W. Jones, J.N. Van Arsdell, and M.A. Innis. 1986. The PEP4 gene encodes an aspartyl protease implicated in the posttranslational regulation of Saccharomyces cerevisiae vacuolar hydrolases. *Mol Cell Biol*. 6:2500-2510.

Yorimitsu, T., S. Zaman, J.R. Broach, and D.J. Klionsky. 2007. Protein kinase A and Sch9 cooperatively regulate induction of autophagy in Saccharomyces cerevisiae. *Mol Biol Cell*. 18:4180-4189.

Zhdankina, O., N.L. Strand, J.M. Redmond, and A.L. Boman. 2001. Yeast GGA proteins interact with GTP-bound Arf and facilitate transport through the Golgi. *Yeast*. 18:1-18.

Zhu, Y., L.M. Traub, and S. Kornfeld. 1998. ADP-ribosylation factor 1 transiently activates high-affinity adaptor protein complex AP-1 binding sites on Golgi membranes. *Mol Biol Cell*. 9:1323-1337.

Zoncu, R., L. Bar-Peled, A. Efeyan, S. Wang, Y. Sancak, and D.M. Sabatini. 2011. mTORC1 senses lysosomal amino acids through an inside-out mechanism that requires the vacuolar H(+)-ATPase. *Science*. 334:678-683.

Chapter 3: Investigation of Art1/Ldb19 localization and function at the late Golgi

Abstract

Proteins from the arrestin-related family of proteins (ARTs) are potent regulators of membrane traffic at multiple cellular locations in the yeast *Saccharomyces cerevisiae*. Several ARTs act at multiple locations, suggesting that ARTs with well-established functions at one location may have additional, and as of yet, uncharacterized roles at other locations in the cell. To more fully understand the spectrum of cellular functions regulated by ART proteins, we explored the localization and function of Art1/Ldb19, which has previously been shown to function at the plasma membrane, yet is reported to localize to the *trans*-Golgi network (TGN). We report that a GFP fusion of Art1 is functional and localizes to the TGN, as previously reported. We further establish that Art1 is preferentially associated with late stages of TGN maturation that are enriched in the clathrin adaptor protein complex-1 (AP-1). Additionally, we present genetic interaction assays that suggest Art1 acts at the late TGN in a mechanism related to that of AP-1. However, in assays of membrane traffic Art1 and AP-1 have dissimilar phenotypes, suggesting the specific function of Art1 at the TGN is distinct from that of AP-1. Together these results indicate Art1 functions at the TGN, in addition to its well-established role in endocytosis.

Introduction

Membrane traffic is a critical aspect of eukaryotic cell biology. It maintains cellular homeostasis by routing newly generated proteins to their correct locations, and by transporting damaged proteins to the lysosome where they are degraded. It is equally important in a changing environment because it allows rapid redistribution of proteins that regulate cellular functions including small molecule transport, secretion, and signaling.

Membrane traffic is carried out in large part by cytosolic proteins that form coats (Faini et al., 2013). Coat proteins coordinate with one another to sort the transmembrane protein cargo that will be trafficked away from resident proteins of the organelle, form a transport carrier, and then direct that carrier towards the correct target organelle. Different coats, which are composed of different sets or subsets of proteins, perform distinct functions by forming at different organelles, recognizing distinct cargo, and/or directing the carrier to different compartments.

Although some proteins work in a single trafficking pathway, other proteins are used in multiple pathways. A prime example of this second group of multi-use proteins is clathrin, a large hexameric protein complex that can self-assemble into a cage-like structure *in vitro* (Pearse, 1976). *In vivo*, clathrin comprises the major structural component of coats that form at the plasma membrane and of coats that form on internal compartments (Brodsky et al., 2001). At each of these different locations, specific clathrin adaptors play pivotal roles in recognizing cargo and initiating clathrin coat assembly. In most organisms, clathrin adaptors that act at the plasma membrane

and those that act at internal compartments are encoded by distinct but functionally orthologous genes (Owen et al., 2004). However, like clathrin, some of its associated proteins act in both endocytosis and at internal compartments. Such dual functioning proteins include amphiphysin, which is important for membrane fission, and, proteins of the arrestin family, which are important for cargo sorting (Huser et al., 2013; Lauwers et al., 2010; Mishra et al., 2001).

The budding yeast, *Saccharomyces cerevisiae*, contains at least 12 arrestin-related trafficking proteins (ARTs) (Lin et al., 2008; Nikko et al., 2008). ARTs are defined by the presence of an arrestin-like domain and one or more PY motifs that mediate direct interaction with the ubiquitin ligase Rsp5 (Lin et al., 2008). Different ARTs control the traffic of different cargo in response to specific environmental cues. For example, Art1/Ldb19 induces endocytosis of the methionine permease Mup1 in response to methionine, while Ecm21/Art2 induces endocytosis of the metal ion transporter Smf1 in response to extracellular heavy metals (Nikko and Pelham, 2009; Nikko et al., 2008). ARTs can act as adaptors for Rsp5 to direct ubiquitination, which allows the cargo to interact with clathrin adaptors. Alternatively, ARTs can direct cargo traffic independent of Rsp5; in this case they likely act as direct physical links between the cargo and the clathrin trafficking machinery (Alvaro et al., 2014; Lin et al., 2008; Prosser et al., 2015).

Although all ARTs appear to act in membrane traffic, our understanding of the specific function of individual ART proteins is still incomplete. In diverse yeasts, many ARTs act in endocytosis (Dong et al., 2016; Herranz et al., 2005; Karachaliou et al., 2013; Nikko et al., 2008; Tanaka et al., 2017). However, other ARTs have roles at

internal compartments. For example, Aly1/Art6 and Aly2/Art3 localize at the trans-Golgi network (TGN) or endosomes where they control the traffic of Gap1, a general amino acid transporter (O'Donnell et al., 2010). Furthermore, some ART proteins act at more than one cellular location. These multifunctional ARTs include Aly1 and Aly2 which, in addition to controlling Gap1 at the TGN, also control the endocytosis of the aspartic acid/glutamic acid transporter Dip5 (Hatakeyama et al., 2010). Similarly, the ARTs Bul1 and Bul2 act both at the TGN in biosynthetic sorting of the general amino acid permease, Gap1, and at the plasma membrane for substrate induced endocytosis of Gap1 (Soetens et al., 2001). More recently, the ART Rod1/Art4 was demonstrated to regulate sorting of the lactate permease Jen1, both at the plasma membrane and at the TGN (Becuwe and Leon, 2014b). These findings raise the possibility that ARTs with well-established roles in endocytosis may perform additional as of yet uncharacterized roles at other cellular locations.

One prime candidate for an ART that may act in both endocytosis and traffic at internal compartments is Art1/Ldb19 (hereafter referred to as Art1). Art1 has clearly defined functions in the endocytosis of Mup1 in response to methionine (Guiney et al., 2016; MacGurn et al., 2011). However, recent studies suggest that loss of Art1 impairs the traffic of the arginine transporter Can1 at the TGN, not the plasma membrane, suggesting that Art1 may have a functional role at internal compartments (Gournas et al., 2017). In support of the possibility that Art1 acts at internal compartments, a large pool of fluorescently labeled Art1 and its homolog in *Schizosaccharomyces pombe* localize to internal compartments also labeled with markers of the TGN, suggesting Art1 and its homolog localize to internal compartments (Huh et al., 2003; Lin et al., 2008;

MacGurn et al., 2011; Nakase et al., 2013). However, it is unclear whether this localization reflects that of native Art1, and, if so, whether this pool is functionally important. To explore potential roles of Art1 at internal compartments, we first established Art1 localization with a fully functional tag of Art1. We found that Art1 localized to internal compartments where it co-localized with markers of the TGN. Furthermore, Art1 co-localized strongly with and interacted with the non-endocytic clathrin adaptor AP-1, further supporting this localization. We found synthetic genetic interactions between *art1Δ* and a hypomorphic allele of the genes encoding clathrin heavy chain and deletion of the gene encoding the clathrin adaptor Gga2, but not deletions of genes encoding AP-1, consistent with a possible role of Art1 in AP-1 traffic. However, in contrast to deletion of AP-1, loss of Art1 did not increase defects in CPY secretion and alpha-factor maturation defects in cells carrying a hypomorphic allele of clathrin. Together these results suggest that Art1 functions at the late TGN in a mechanism related to but functionally distinct from AP-1. This establishes a role for Art1 at the TGN, in addition to its well-established function in endocytosis.

Results

Art1-GFP is functional and localizes to the late TGN

Although Art1 has strong effects on endocytosis, previous studies reported a significant pool of fluorescently tagged Art1 at internal compartments. In one high-throughput study, Art1 tagged at its endogenous locus co-localized with the clathrin heavy chain subunit Chc1, a marker commonly used to label the TGN (Huh et al.,

2003). Similarly, studies using Art1-GFP expressed from a plasmid, co-localized with the Arf-GEF Sec7, another marker commonly used to label the TGN (Lin et al., 2008; MacGurn et al., 2011). These localization results are surprising given the strong endocytic phenotype of cells lacking Art1 on endocytosis. However, to our knowledge, the functionality of the fluorescently tagged Art1 was not explored, raising the possibility that the fluorescently labeled Art1 was non-functional and potentially mislocalized. To determine whether Art1-GFP encodes a functional protein, we monitored methionine-induced endocytosis of Mup1-GFP in diploid cells that expressed a single copy of wild-type Art1 or Art1-GFP from its endogenous locus. In these cells, Mup1-GFP fluorescence is clearly distinguished from that of Art1 because Mup1 is expressed at 10-20 fold higher levels than Art1 (Chong et al., 2015; Newman et al., 2006).

In all strains tested Mup1 was found exclusively at the plasma membrane in the absence of methionine (Fig 3.1). After 1hr growth in the presence of methionine, in cells expressing wild-type Art1 Mup1 was found exclusively in the vacuole (Fig 3.1A). In contrast, in cells lacking Art1, Mup1 was only observed at the plasma membrane (Fig 3.1C). In cells expressing Art1-GFP, Mup1-GFP was found exclusively in the vacuole at levels nearly identical to wild-type cells (Fig 3.1B). These data indicate that the Art1-GFP fusion protein is fully functional, as measured by Mup1 for endocytosis.

We next explored the localization of Art1 in more detail. Previous studies suggested that Art1 localizes to internal compartments labeled by Sec7, which is commonly considered the TGN (Losev et al., 2006; Matsuura-Tokita et al., 2006). However, the emerging view is that the TGN is not a static organelle in yeast. It is produced from the maturation of a Golgi compartment (Kim et al., 2016). During this

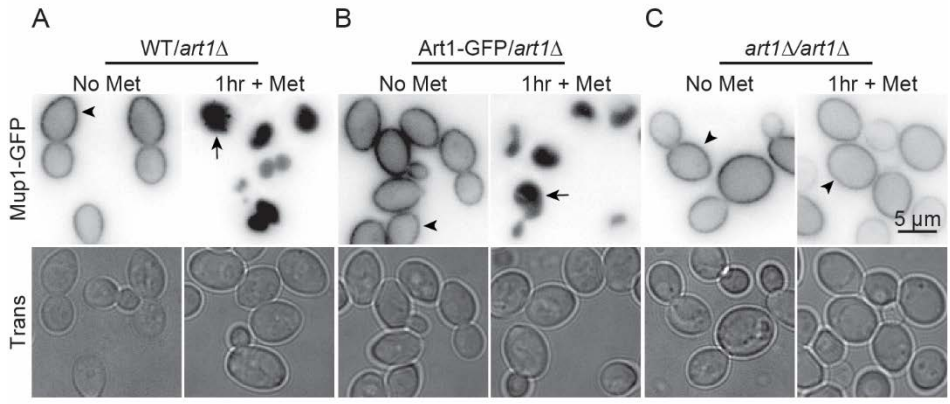

Figure 3.1. Art1-GFP is a functional protein.
(A) WT/*art1*Δ heterozygous diploid cells expressing Mup1-GFP were imaged in the absence or 1hr after the addition of methionine, which induces endocytosis of Mup1-GFP. (B), (C) Art1-GFP/*art1*Δ heterozygous diploid or *art1*Δ homozygous diploid cells imaged as in A. Arrowhead indicates plasma membrane localization, arrow indicates vacuolar localization. Top row, fluorescence microscopy images with black and white values inverted; bottom row, transmitted images.

maturation process, Sec7 is observed at transitional Golgi compartments and is retained as this transitional Golgi matures into the TGN which itself matures and eventually dissipates due to traffic to the plasma membrane, vacuole, and endosomes (McDonold and Fromme, 2014). To monitor the localization of Art1 with respect to Golgi maturation, we monitored the localization of Art1 with the clathrin adaptors Gga2, Ent5, and AP-1 that define late stages of TGN maturation (Daboussi et al., 2012; Hung et al., 2012). These proteins appear in a stereotypic order. Gga2 is the first adaptor apparent at the TGN and its appearance is coordinated with that of Sec7. Ent5 is recruited second, and AP-1 is recruited last.

Using these markers for TGN maturation, we asked whether Art1 was preferentially associated with any stage of TGN maturation. Consistent with its co-localization with Sec7, Art1 internal puncta frequently co-localized with Gga2, Ent5, and the gamma subunit of AP-1 (Apl4), but not with Vps35, a marker of endosomes (Fig 3.2). We also observed dim peripheral localization that was not associated with Gga2, Ent5, or AP-1, consistent with previous reports of a small pool of Art1 at the plasma membrane (Lin et al., 2008; MacGurn et al., 2011). To quantify the co-localization between Art1 and mCh-tagged adaptors, we measured how much of the GFP fluorescence (Art1) area also contained mCherry (mCh) fluorescence (adaptor) and vice versa. Art1 co-localized substantially with each of the adaptors. In each case nearly 60% of Art1 structures contained Gga2, Ent5, or AP-1. However, Art1 showed the least co-localization with Gga2 (58%+/- 13% SD, Fig 3.2A). Co-localization with Ent5 and AP-1 was slightly higher (66%+/- 6% SD and 64% +/- 3% SD, respectively; Figs 3.2B and 3.2C). These results suggest a slight enrichment of Art1 in the late stages. Consistent

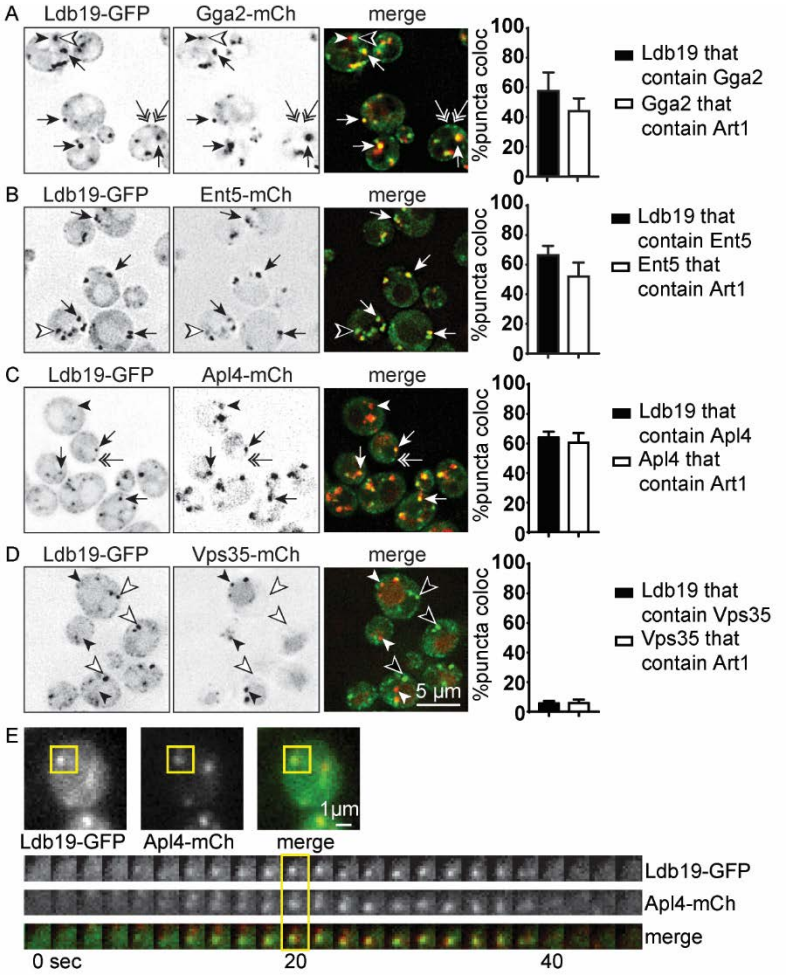

Figure 3.2. Art1 co-localizes with TGN clathrin adaptors.
(A-D) Cells expressing Art1-GFP were imaged in strains that also expressed mCh-tagged clathrin adaptors (Gga2, Ent5, Apl4) or a retromer subunit (Vps35). Arrows indicate co-localized fluorescence, filled and outlined arrowheads indicate structures with only mCh or GFP, respectively, and double arrows indicate cell surface-localized Art1-GFP structures. Right, quantification of the percentage of Art1-GFP fluorescence that contains mCh fluorescence (black bar) and the percentage of mCh-tagged marker fluorescence that contains GFP fluorescence (white bar). Error bars indicate standard deviation from the mean of three separate experiments (n = 3), each with at least 200 puncta and 70 cells. (E) Kymographs showing Art1-GFP recruitment overtime at compartments that contain Apl4-mCh. Top: Representative single cells showing the selected puncta for kymograph view in the boxed area. Bottom: kymographs of the boxed area in the top images is shown; the boxed area indicates the corresponding timepoint for the shown top images.

with this suggestion, more AP-1 structures than Gga2 structures contained Art1 (61% +/- 6% SD versus 44% +/- 9% SD, white bars).

Clathrin adaptors are dynamically recruited to the TGN. This dynamic recruitment can be monitored as transient punctate structures in time-lapse microscopy. To determine whether Art1 showed similar dynamic recruitment to the TGN, we performed time-lapse microscopy on cells expressing Art1-GFP and Apl4-mCh (Fig 3.2E). Like Apl4-mCh, Art1-GFP was transiently localized to punctate structures. Moreover, consistent with their co-localization in static images, Art1-GFP and Apl4-mCh often appeared and disappeared at approximately the same time. Together with the co-localization data, these results suggest that Art1 is recruited to the TGN at approximately the same time as AP-1.

Art1 closely localizes to AP-1

To further explore the relationship between Art1 and AP-1, we employed the bimolecular fluorescence complementation (BiFC) technique (Hu et al., 2002). BiFC monitors the proximity of two proteins, each tagged with half of a fluorescent protein (e.g. Venus). If the two proteins interact or localize close to one another, the two halves of the protein fold to form a fully fluorescent moiety. Thus, BiFC can show whether two proteins localize close to one another. Given the co-localization of Art1 with AP-1, we asked whether Art1 comes into close proximity with AP-1 (Fig 3.3B). We fused Art1 with the C-terminal fragment of Venus to generate Art1-VC. We tested for proximity to the AP-1 γ-subunit Apl4 and the β-subunit Apl2 fused the N-terminal fragment of Venus.

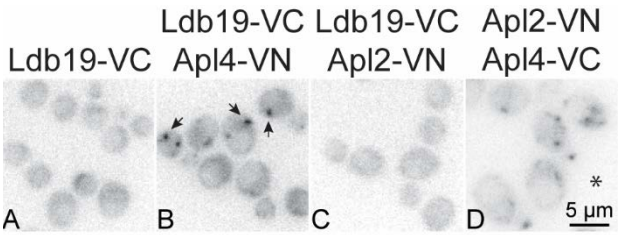

Figure 3.3. Bimolecular fluorescence complementation (BiFC) demonstrates close localization of Art1 with AP-1.
Cells expressing BiFC-tagged proteins as indicated were imaged for YFP fluorescence. Arrows point to positive BiFC punctate structures in the cells expressing Art1-VC and Apl4-VN; asterisk indicates use of diploid strain.

Cells expressing both Art1-VC and Apl4-VN exhibited one to three bright puncta within most cells. Curiously, cells expressing both Art1-VC and Apl2-VN did not exhibit fluorescence above background level (Fig 3.3C). This lack of fluorescence was not due to mislocalization or poor expression of Apl2-VN, because cells expressing Apl2-VN and Apl4-VC exhibit BiFC fluorescence (Fig 3.3D). This specificity may suggest a specific interaction between Art1 and the Apl4 subunit of AP-1, however we were unable to detect an interaction between Art1 and AP-1 using other methods (unpublished results). Together these results demonstrate that Art1 localizes to TGN/endosome regions rich in AP-1.

Art1 is not involved in clathrin adaptor localization

Given the close proximity of Art1 to AP-1, we next asked whether Art1 plays a role in the recruitment of AP-1 or other adaptors to the TGN. To do this, we performed quantitative fluorescent microscopy on cells lacking Art1 and expressing GFP-tagged AP-1 or the clathrin adaptor Gga2, which functions at the TGN before AP-1 (Daboussi et al., 2012; Day et al., 2018). In cells lacking Art1, both Gga2 and AP-1 localized to multiple puncta that appeared similar to the puncta in wild-type cells. Because cells lacking Art1 are morphologically abnormal, as previously reported, the distribution of Gga2 and AP-1 looked qualitatively different (Lin et al., 2008). This is because cells lacking Art1 are large with a large central vacuole. This central vacuole pushes Gga2 and AP-1 containing structures to the periphery (Fig 3.4). Therefore, to assess the effect of Art1 on Gga2 and AP-1 localization we monitored their intensity on puncta. In cells lacking Art1, the intensity of Gga2 structures was unchanged, whereas the fluorescence

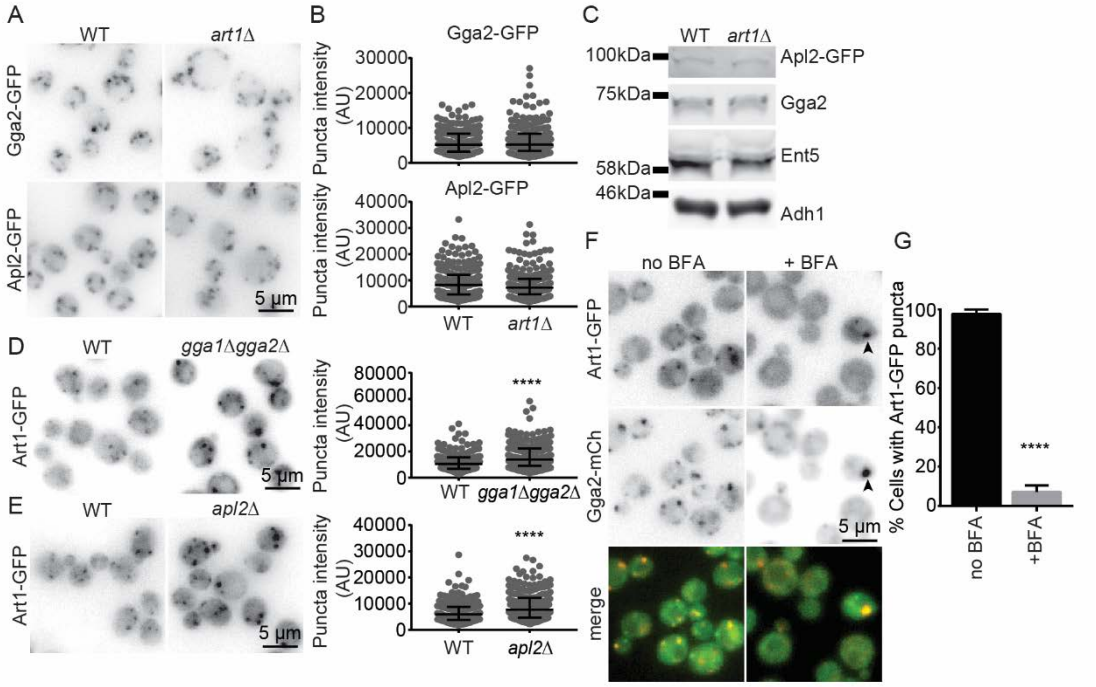

Figure 3.4. TGN clathrin adaptor localization is unaffected by deletion of *ART1*.

(A) Wild-type and *art1*Δ cells expressing Gga2-GFP or Apl2-GFP were imaged. (B) Quantification of the fluorescence intensities of the punctate structures from the images in A. Graphs are of data points measured from a representative experiment showing the median and interquartile ranges (25 and 75 percentile). Each data point corresponds to a single punctate structure. AU, arbitrary units. (C) Western blot showing the protein levels of clathrin adaptor proteins in WT and *art1*Δ cells. Adh1 was used as a lysis control. (D), (E) Wild-type and *gga1*Δ*gga2*Δ or *apl2*Δ cells expressing Art1-GFP were imaged. Right, quantification of Art1-GFP punctate structures as in B. Non parametric Mann Whitney test was performed (****p > 0.0001). (F) erg6Δ cells expressing Art1-GFP and Gga2-mCh were imaged following treatment with DMSO (no BFA) or 150µM Brefeldin A (+BFA). Arrowhead points to rare puncta in treated cells. (G) Quantification of the percentage cells from F that contain Art1-GFP puncta in the absence or presence of BFA. Non parametric t-test was performed (****p < 0.0001). Graphs from B, D and E were generated from at least 200 punctate structures and at least 70 cells.

intensity of Apl2 puncta showed a small but reproducible decrease (Fig 3.4B). Consistent with limited effect of Art1 on the localization and fluorescent intensity of the adaptors, loss of Art1 did not alter the protein levels Gga2 or Apl2 as monitored by western blot (Fig 3.4C). These results argue that Art1 does not play a major role in recruiting Gga2 or AP-1.

We next explored how Art1 is recruited to the TGN. We first asked whether Gga proteins or AP-1 were important for Art1 localization at the TGN. To do this, we performed quantitative fluorescence microscopy in cells lacking the two partially redundant Gga proteins, Gga1 and Gga2, or in cells lacking Apl2. In cells lacking Gga proteins or AP-1, Art1 retained its punctate localization (Fig 3.4D and 3.4E). Curiously, Art1 puncta were significantly brighter in cells lacking the adaptors (Fig 3.4D and 3.4E). The cause of the increased intensity is unclear, but could be due to stalled organelle maturation or stalled assembly of specific trafficking complexes leading to enrichment of Art1 at the TGN.

Because neither adaptor complex was required for Art1 localization, we next asked whether other major players at the TGN contribute to Art1 localization. Arf1 is a major regulator of traffic at the TGN (Jackson and Casanova, 2000). It is required for the association of AP-1 with the TGN, but not for the association of Gga2 or Ent5 (Aoh et al., 2013; Zhdankina et al., 2001). We asked whether Art1 localization is sensitive to Brefeldin A, a potent inhibitor of Arf1 function at the TGN. In cells treated with Brefeldin A for 5 minutes, Art1 largely redistributed to the cytosol (Fig 3.4F). In most cells, no Art1 puncta were visible; however, in a very small fraction of cells (7%) one large puncta was

visible (Fig 3.4G). In contrast, Gga2 was still clearly apparent in punctate structures in most cells, as previously reported (Zhdankina et al., 2001). These results suggest that Art1 localization largely depends on Arf1 function. This dependence on Arf1, together with the close proximity of Art1 to AP-1, strongly support the hypothesis that Art1 resides on the TGN in the late stages of its maturation, coincident with AP-1.

Examination of TGN-like phenotypes of Art1

We next asked whether Art1 plays functionally important roles at the TGN. To do this, we asked whether *art1Δ* cells show synthetic growth defects when combined with mutations in clathrin or clathrin adaptors at the TGN. Such synthetic growth defects can be potent read-outs of severe trafficking defects. For example, mutations in either AP-1 or Gga2 enhance the growth defect of cells expressing a hypomorphic allele of the clathrin heavy chain (*chc1-ts*) (Bensen et al., 2000; Phan et al., 1994; Rad et al., 1995). Alternatively, combined deletion of AP-1 and Gga functions causes lethality or poor growth depending on the subunit of AP-1 deleted (Costaguta et al., 2001). These slow growing genetic combinations are also associated with strong defects in membrane traffic at the TGN, including defects in traffic from the TGN to the endosome.

To test whether *ART1* has genetic interactions similar to AP-1 or *GGA2*, we first tested whether deletion of *ART1* enhances the *chc1-ts* growth defect. Loss of *ART1* strongly enhanced the growth defect caused by the *chct1-ts* allele. At 37°C, the double mutant cells did not grow at all whereas *chc1-ts* cells grow slowly (Fig 3.5A). At 32°C the double mutant grew much more poorly than cells carrying the *chc1-ts* allele alone. This growth defect was similar to the growth defect caused by loss of AP-1 in cells carrying

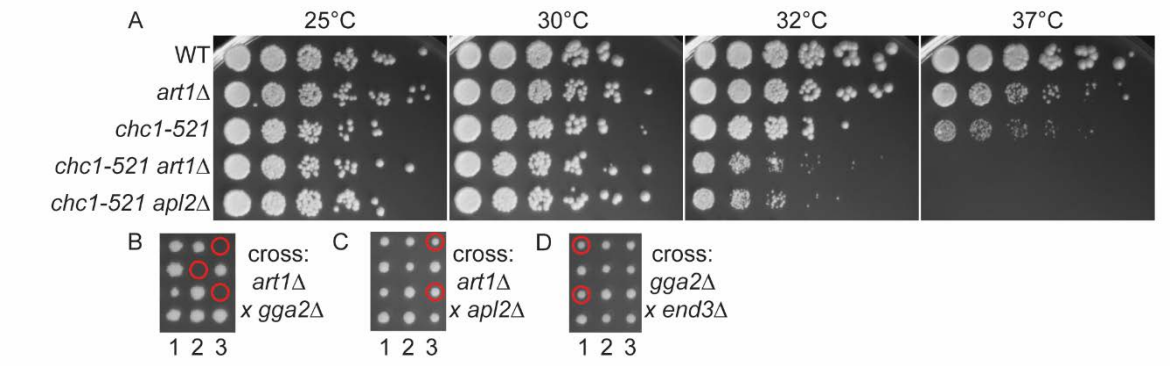

Figure 3.5. Deletion of *ART1* increases temperature sensitivity of *chc1-ts* and is synthetic lethal with *GGA2*.
(A) Serial dilutions of the indicated strains were spotted on YPD plates and grown for three days at the shown temperatures. (B) Tetrad dissection plates from a cross between art1Δ and *gga2*Δ strains. (C) Tetrad dissection from a cross between *art1*Δ and *apl2*Δ strains. (D) Tetrad dissection from a cross between *end3*Δ and *gga2*Δ strains. Red circles indicate colonies with double deletion genotypes deduced either by direct genotyping or by inference from viable siblings of inviable spores.

the *chc1-ts* allele. This genetic interaction is consistent with a role for Art1 at the TGN, however endocytic mutants also enhance the growth defect of *chc1-ts* cells. Therefore, we next asked whether *ART1* shows genetic interactions with AP-1 or *GGA2*. To do this, we generated diploid cells by crossing *art1Δ* cells with cells lacking either *GGA2* or *APL2.* We then induced sporulation, separated meiotic progeny of single diploid cells using a micromanipulator, and monitored the growth of the haploid spores. In crosses between cells carrying deletions of *ART1* and *GGA2,* approximately one quarter of the spores were inviable. Genotyping revealed that none of the viable spores contained deletion of both *ART1* and *GGA2*. Moreover, the genotype of the inviable spores could be deduced by the genotype of the viable siblings of inviable spores (Fig 3.5B, red circle). This analysis revealed that the inviable cells carried deletion of both *ART1* and *GGA2,* indicating the two deletions are synthetic lethal as previously reported (Fig 3.5B and (Zhao et al., 2013)). In contrast, *art1Δ* was not synthetic lethal with *apl2Δ* because double mutant spores were identified in the correct proportion from the cross between cells lacking *ART1* and *APL2* and the double mutant spores grew as well as their wild-type siblings. This indicates that the synthetic lethality between *art1Δ* and *gga2Δ* was highly specific. Because Art1 is known to function in endocytosis, we asked whether the synthetic lethality between *art1Δ* and *gga2Δ* could be explained by the endocytic functions of Art1. To do this we crossed cells carrying deletion *END3,* an endocytic gene, to cells lacking *GGA2. GGA2* was not synthetic lethal with *END3* (Fig 3.5D). These data suggest that the synthetic lethality between *ART1* and *GGA2* is not due to the role of Art1 in endocytosis and could suggest a role for Art1 in AP-1 dependent traffic at the TGN.

To further examine the role of Art1 at the TGN, we monitored the secretion of CPY, a vacuolar protease that normally is efficiently sorted at the TGN for traffic to the vacuole (Conibear and Stevens, 1998). In cells with strong defects in clathrin-dependent traffic at the TGN, CPY is mis-sorted to the plasma membrane and is secreted (Zhdankina et al., 2001). Cells carrying the *chc1-ts* allele secrete CPY. These effects are strongly enhanced by loss of AP-1. To monitor CPY secretion, we performed colony immunoblots using cells that express CPY-GFP (Fig 3.6). In WT cells and cells lacking only *ART1* or *APL2*, no CPY was detected by this method. In contrast, cells carrying the *chc1-ts* allele secreted CPY resulting in weakly detectable CPY signal. This defect was enhanced by deletion of *APL2*. Surprisingly, although the *art1Δ chc1-ts* double mutant grew as slowly as the *apl2Δ chc1-ts* double mutant, the *art1Δ chc1-ts* had less CPY signal than cells carrying the *chc1-ts* allele alone. This indicates that loss of *ART1* does not cause the same effect on CPY sorting as loss of AP-1.

Because *art1Δ* and *apl2Δ* showed opposites phenotype for CPY secretion when combined with the *chc1-ts* allele, we performed an alternative test of clathrin function at the TGN. To do this, we monitored the secretion of unprocessed α-factor using colony immunoblot. α-factor is a secreted hormone involved in yeast cell mating. At the TGN, α-factor is cleaved from its high-molecular weight pro-form to the mature peptide hormone (Conibear and Stevens, 1998). This cleavage is mediated by Kex2, a furin-like protease whose steady state localization at the TGN is disrupted in cells with strong defects in clathrin function at the TGN (Phan et al., 1994; Yeung and Payne, 2001).

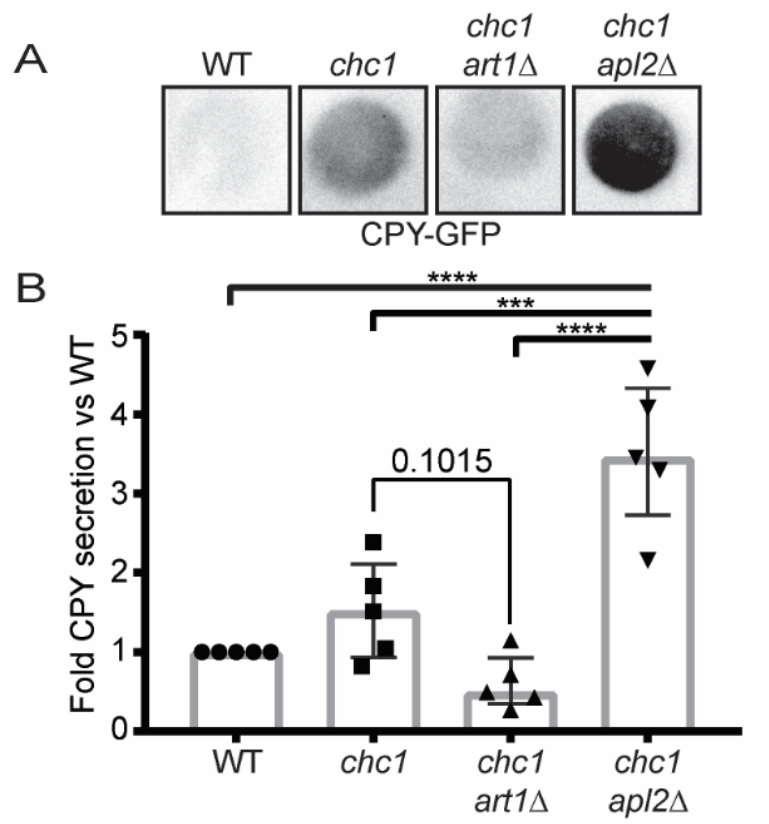

Figure 3.6. Deletion of ART1 supresses chc1-ts phenotypes.
(A) Colony immunoblot to monitor CPY secretion of the indicated strains. Shown are a representative immunoblots. (B) Corresponding quantification for the data in A by densitometry analysis. Bar graphs are of the median with interquartile range with data points shown (n = 5). Data were analyzed by one-way ANOVA. p-values: *** = <0.005, **** = <0.001.

When Kex2 localization is disrupted, unprocessed α-factor is secreted. This unprocessed α-factor, but not the mature form, adheres strongly to nitrocellulose allowing its detection by colony immunoblot (Conibear and Stevens, 2002). We found that cells carrying the *chc1-ts* secreted substantial levels of unprocessed α-factor and this effect was enhanced by deletion of *APL2* (Fig 3.7). Similar to the observations with CPY, the *art1Δ chc1-ts* double mutant had less α-factor signal than cells carrying the *chc1-ts* allele alone (Fig 3.7). These results suggest that despite their close proximity, similar requirements for localization, and similar genetic interactions, Art1 is not required for two known AP-1 functions at the TGN.

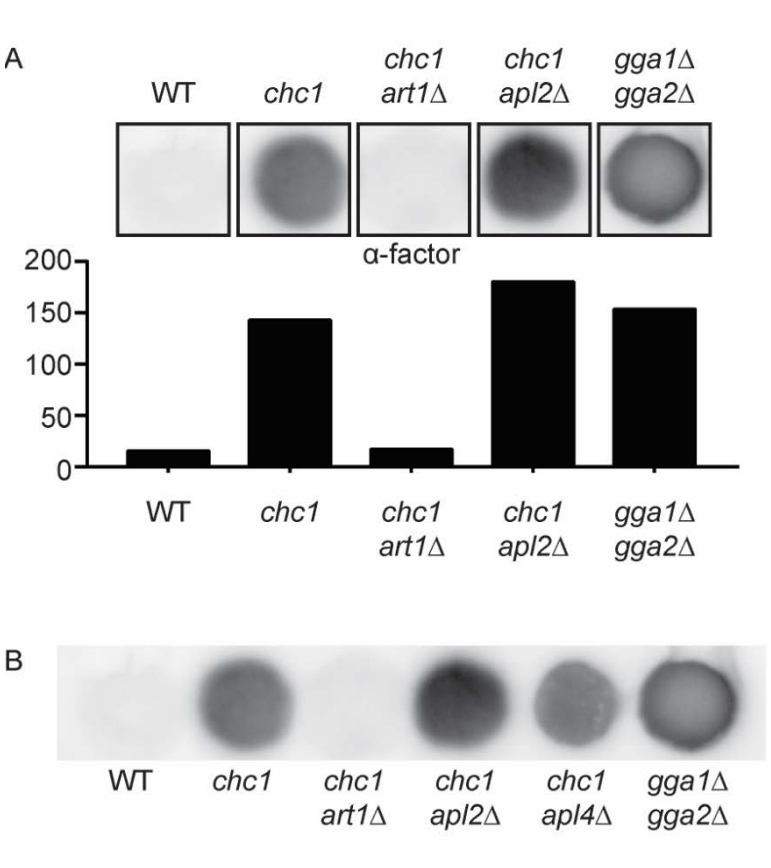

Figure 3.7. α-factor colony immunoblot.
(A) Colony immunolot to test α-factor secretion of the indicated strains. Shown are a representative immunoblot and the corresponding quantification by densitometry analysis. Colony spots come from the same immunoblot, but rearranged for clarity. (B) Original image of colony immunoblots shown in A.

Discussion

Our results firmly establish that Art1 localizes to the TGN, confirming prior reports (Huh et al., 2003; MacGurn et al., 2011). Although a small proportion of Art1 was visible at the plasma membrane, the majority of Art1-GFP strongly co-localized with markers of the TGN. Our results extend prior findings about Art1 localization by positioning Art1 within the dynamic lifespan of the TGN. The TGN is now thought to be a dynamic organelle that continually forms, matures, and dissipates due to repeated cycles of traffic (Losev et al., 2006; Matsuura-Tokita et al., 2006). In this maturation cycle, AP-1 labels a late stage (Daboussi et al., 2012; Day et al., 2018). Our results indicate that Art1 is preferentially associated with these late-stage, AP-1 positive TGN compartments. In fluorescence microscopy experiments, Art1 co-localized more strongly with AP-1 than Gga2, a marker of earlier stages. Furthermore, in BiFC experiments, Art1 came into close proximity to AP-1. This localization, together with genetic interactions with *chc1-ts* and *gga2Δ*, suggest Art1 plays a function at the TGN. However, the lack of effect of *art1Δ* on the secretion of CPY and maturation of α-factor in combination with *chc1-ts* argue that Art1 does not play a positive role in AP-1 mediated traffic. It therefore remains to be revealed what function Art1 has at the TGN.

Notably, recent published work supports a role for Art1 at the TGN. Overexpression of Art1 enhances the levels of mammalian potassium channel protein, Kir2.1, at the cell surface of yeast cells (Hager et al., 2018). This phenotype indicates that Art1 may play a role in recycling or the biosynethetic delivery of Kir2.1 to the plasma membrane. In addition, Art1 is required for post-endocytic traffic of the yeast

arginine permease, Can1 (Gournas et al., 2017). In this case, Can1 was readily endocytosed in cells lacking Art1. However, Can1 did not reach the vacuole, suggesting loss of Art1 promotes recycling of endocytosed Can1. Together with our experiments, these data strongly suggest that Art1, like other alpha-arrestins, is a multi-functional protein with roles both in endocytosis and at internal compartments.

These findings expand the list of ART proteins that function at multiple compartments and raise the possibility that this is a general feature of the ART family. To date, the ARTs Bul1, Bul2, Aly1, Aly2, and Rod1 have been implicated in functions at both the plasma membrane and internal compartments (Becuwe and Leon, 2014a; Crapeau et al., 2014; Hovsepian et al., 2018; O'Donnell et al., 2010; Soetens et al., 2001). Adding Art1 to this list expands the list of ARTs that function at multiple compartments to 6 out of 12. Notably, these six ART proteins occupy all branches of the ART family identified by sequence homology (Lin et al., 2008; Nikko and Pelham, 2009). Based on sequence homology, Bul1&2 form their own subfamily, Aly1&2 branch from one another within a larger subfamily that includes Art1 and a second pair of highly similar ARTs (Csr2/Art8, Ecm21/Art2), whereas Rod1 resides on a third branch that contains 3 additional ART proteins. It is therefore likely that the common progenitor gene of the family was capable of functioning at multiple compartments, and suggests that this multi-functionality may be a general feature of all ART proteins. Indeed multi-functionality appears to be a facet of ARTs in distantly related yeast, supporting this possibility (Dong et al., 2016).

Although Art1 strongly associates with the TGN, the direct molecular mechanism that recruits Art1 to the TGN is unclear. Despite close proximity to AP-1, as monitored

by BiFC, Art1 does not depend on AP-1 for localization to punctate structures. We found that Art1 localization was mostly disrupted by treatment with Brefeldin A, suggesting a dependence on Arf. It remains to be determined whether Art1 directly interacts with Arf or whether this is an indirect effect. Notably, Art1 has broad affinity for small GTPases (Prosser et al., 2015). In GST-pulldown experiments, Art1 bound to three unrelated GTPases Ypt1, Ras2, and Rho1, raising the possibility that Art1 may interact directly with Arf1. Alternatively, Art1 could interact with other GTPases that localize to the TGN including Ypt31, Ypt32, and Rho3 (Kita et al., 2011; Wu and Brennwald, 2010). Future work is necessary to understand whether these interactions control Art1 localization at the TGN, and whether similar interactions direct the intracellular localization of other ART proteins.

The function of the Art1 localized at the TGN remains elusive. The synthetic growth defects of *art1Δ* when combined with *chc1ts* and *gga2Δ* are highly similar to those caused by deletion of AP-1 subunit genes. However, the effect of *art1Δ* on the secretion of CPY and processing of α-factor are not consistent with Art1 playing a direct positive role in AP-1 dependent traffic. Instead, loss of Art1 partially does not increase sorting defects caused by *chc1-ts,* which are enhanced by deletion of AP-1 subunit genes*.* Indeed, it appears that *art1Δ chc1-ts* double mutant cells secrete less CPY and unprocessed α-factor. In light of the role of Art1 on Kir1.2 and Can1, this reduction could indicate that Art1 promotes the secretion of CPY and unprocessed α-factor and that Art1 has a general role promoting TGN to cell surface traffic.

Materials and Methods

Reagents, strains, growth conditions

Rabbit polyclonal antibodies against full-length Gga2, Ent5 and α-factor have been previously described (Aoh et al., 2011; Wilsbach and Payne, 1993). Rabbit polyclonal Adh1 and mouse monoclonal GFP antibodies were from Abcam (Cambridge, MA), goat anti-rabbit Alexa Fluor 647 secondary antibodies were from Invitrogen (Carlsbad, CA), goat anti-mouse HRP-conjugated secondary antibodies were from Jackson ImmunoResearch Laboratories (West Grove, PA).

Fluorescent tags, BiFC tags and gene deletions were introduced by standard PCR-based procedures (Longtine et al., 1998; Sung and Huh, 2007) in the *S. cerevisiae* BY4743 background and its progeny. Strains containing multiple genomic modifications were generated by standard yeast genetics.

Yeast cells were grown at 30°C and aerated by rotary shaking. For non-selective growth, cells were grown in Yeast peptone (YPD) media (1% bacto-yeast extract and 2% bacto-peptone (Difco, Detroit, MI) supplemented with 2% dextrose and 20 μg/ml adenine, uracil, and L-tryptophan. For selective conditions, cells were grown in Synthetic defined (SD) media (0.67% of yeast nitrogen base without amino acids (Difco) and 2% dextrose. Supplemented SD media contained 100μg/ml adenine, L-leucine, L-lysine, L-tryptophan; 50 μg/ml L-histidine, L-methionine, and 20 μg/ml uracil) or in media lacking L-methionine for the expression of Mup1-GFP. Sporulation of diploid cells was performed by incubation of saturated cultures for 4 days in sporulation media (10mg/mL potassium acetate, 1mg/mL yeast extract and 0.5mg/mL dextrose) supplemented with

10µg/ml adenine, L-leucine, L-lysine, L-tryptophan; 5 µg/ml L-histidine, L-methionine, and 2 µg/ml uracil.

For Mup1-GFP internalization experiments, cells were grown to mid-log phase in SD media lacking methionine. To induce internalization of Mup1, cells were resuspended in SD media containing methionine for 1hr prior to imaging. For Brefeldin A experiments, cells were treated with a final concentration of 150µM Brefeldin A (Acros Organics, New Jersey) for 5 minutes prior to imaging.

To determine changes in growth of *chc1-ts* expressing cells when combined with *art1Δ*, 200 µl of log phase cells (OD_{600}= 0.5) were transferred into wells of a 96-well plate. The cultures were serially diluted 5-fold in adjacent wells. The cells were replica pinned onto agar plates using a 48-well solid pin tool (Sigma, St. Louis, MO). The plates were incubated at room temperature until the liquid media was absorbed into the agar. The plates were incubated at indicated temperatures for 2-3 days before imaging the plates. Experiments were repeated 3 times using two different strains for each genotype.

To monitor synthetic lethal phenotypes, diploid cells were generated by standard methods and sporulation was induced by transferring into sporulation media and culturing at 25°C. When fully formed tetrad were visible (3-5 days), tetrads were dissected onto YPD plates using a microscope-mounted micromanipulator. Plates were incubated at 30°C until colonies were visible.

Immunoblotting

For immunoblots of cell extracts**,** cell extracts were prepared from 2 OD_{600} of cells. Extracts were generated by resuspending in Laemmli lysis buffer (Volland et al., 1994), boiling, and vortexing in the presence of glass disruption beads. The extracts were cleared by centrifugation. Proteins were separated by SDS–PAGE, transferred to nitrocellulose, blocked with 5% milk in Tris-buffered saline with Tween and then probed with primary (1:25,000 dilution for anti-Adh1, 1:3,000 dilution for all other antibodies) and fluorescent or HRP secondary antibodies (1:20,000 dilution). The Immobilon western chemiluminescent HRP substrate use for chemiluminescence was from Millipore (Millipore, Billerica, MA). Fluorescence or chemiluminescence signal was detected on an Azure c600 imaging system (Azure Biosystems, Dublin, CA).

For colony immunoblots, yeast cultures grown in YPD to mid-log phase (0.3-0.5 OD_{600}) were diluted to 0.1 OD_{600} and 5µL were transferred onto a YPD plate. Plates were incubated at 30°C overnight (16-18hr) to allow growth. To capture secreted proteins, a piece of nitrocellulose was first wetted with sterile water and placed on top of the YPD plate. The plate was incubated for a further 8-12hr at room temperature (25°C). The nitrocellulose membrane was removed and adhered cells were removed by rinsing with water. The nitrocellulose membrane was then immunoblotted with primary antibodies and secondary antibodies as described for cell extracts.

Microscopy

For microscopy, cells were grown to log phase in SD supplemented with appropriate amino acids mixes, and then briefly pelleted and resuspended to concentrate prior to imaging. Images for Fig. 3.2 were captured using a DeltaVision™

Elite system (GE Healthcare Life Sciences), equipped with an Olympus IX-71 inverted microscope, a sCMOS CAMERA, A 100x/1.4 Oil Super-Plan APO objective, and a DeltaVision Elite Standard Filter Set with the FITC filter (excitation:475/28, emission:525/48) for GFP and the TRITC filter (excitation: 542/27, emission: 594/45) for mCh. Image acquisition and deconvolution were performed with the program softWoRx. All other fluorescence imaging, was performed on a Nikon Ti-E inverted microscope with a 1.4 numerical aperture, 100× oil-immersion objective and an Andor iXon3 EMCCD camera. A Lumencor LED light engine was used for fluorophore excitation. Image acquisition was performed the MetaMorph acquisition software. For each field, 10-slice Z-stacks (0.25 µm apart) were captured. For image cropping and other figure preparation steps, the ImageJ version 1.50i (National Institutes of Health) software was used.

Image processing and imaging analysis

The intensity of fluorescence puncta in cells was quantified as follows: Z-stack images were first compressed to a single maximum-intensity image using ImageJ version 1.50i. The resulting image was denoised using the “Denoise image” menu from the SpatTrackV2 software (Lund et al., 2014). To define regions of GFP localization, the denoised image was thresholded using Otsu’s method with ImageJ with the stacked histogram option selected. GFP positive regions of interest were defined using the “Analyze Particles” menu from ImageJ on the binary thresholded image. The GFP positive regions of interest were then used to measure fluorescence intensity from the original, compressed non-denoised Z-stack. Fluorescence intensity was determined

from at least 100 cells and 200 total number of puncta. Experiments were repeated 3 times using at least two different strains for the same genotype.

For co-localization analysis, GFP and mCherry positive regions of interest were defined using the same process used for puncta intensity analysis. GFP structures that contain mCherry, were defined as structures for which at least 20% of the GFP positive area of the structure was also mCherry positive and vice versa for mCherry structures that contain GFP. Fluorescence intensity was determined from at least 100 cells and 200 total number of puncta. Experiments were repeated 3 times using two different strains for each genotype. Graphs were created using GraphPad Prism v7.00 (GraphPad Software, La Jolla, CA).

Data availability statement

The datasets generated during and/or analysed during the current study are available from the corresponding author on reasonable request.

Supporting information

Table 3.1. *Saccharomyces cerevisiae* strains used in this study.

Strain	Genotype	Source
BY4743	*Mat a his3Δ1/his3Δ1 leu2Δ0/leu2Δ0 ura3Δ0/ura3Δ0 met15Δ0/MET15 LYS2/lys2Δ0*	Brachmann et al., 1998
DLY1685	*Mat α his3Δ1 leu2Δ0 ura3Δ0 MET15 lys2Δ0 art1Δ::KanMx6 Mup1-GFP::HisMx6*	This study
DLY2020	*Mat a his3Δ1 leu2Δ0 ura3Δ0 MET15 LYS2*	This study
DLY1891	*Mat a his3Δ1 leu2Δ0 ura3Δ0 MET15 LYS2 art1Δ::KanMx6*	This study
DLY740	*Mat a his3Δ1 leu2Δ0 ura3Δ0 met15Δ0 LYS2 Art1-GFP::HisMx6*	This study

DLY1103	*Mat a his3Δ1 leu2Δ0 ura3Δ0 MET15 lys2Δ0 Art1-GFP::HisMx Gga2-mCh::KanMx*	This study
DLY1105	*Mat a his3Δ1 leu2Δ0 ura3Δ0 MET15 LYS2 Art1-GFP::HisMx Ent5-mCh::KanMx*	This study
DLY3028	*Mat a his3Δ1 leu2Δ0 ura3Δ0 met15Δ0 lys2Δ0 Art1-GFP::HisMx Apl4-mCh::HisMx*	This study
DLY1458	*Mat α his3Δ1 leu2Δ0 ura3Δ0 met15Δ0 LYS2 Art1-GFP::HisMx Vps35-mCh::HisMx*	This study
DLY1914	*Mat α his3Δ1 leu2Δ0 ura3Δ0 MET15 lys2Δ0 Art1-VC::HisMx*	This study
DLY3466	*Mat a his3Δ1 leu2Δ0 ura3Δ0 MET15 lys2Δ0 Art1-VC::HisMx Apl4-VN::HisMx*	This study
DLY3612	*Mat α his3Δ1 leu2Δ0 ura3Δ0 MET15 lys2Δ0 Art1-VC::HisMx Apl2-VN::HisMx*	This study
DLY3344	*Mat α his3Δ1 leu2Δ0 ura3Δ0 MET15 LYS2 Apl2-VN::HisMx*	This study
DLY3346	*Mat a his3Δ1 leu2Δ0 ura3Δ0 MET15 LYS2 Apl4-VC::HisMX*	This study
DLY929	*Mat a his3Δ1 leu2Δ0 ura3Δ0 MET15 lys2Δ0 Gga2-GFP::KanMX*	This study
DLY1710	*Mat a his3Δ1 leu2Δ0 ura3Δ0 MET15 lys2Δ0 art1Δ::KanMx Gga2-GFP::KanMx*	This study
DLY2669	*Mat a his3Δ1 leu2Δ0 ura3Δ0 MET15 LYS2 Apl2-GFP::HisMx*	This study
DLY3063	*Mat a his3Δ1 leu2Δ0 ura3Δ0 met15Δ LYS2 art1Δ::KanMx Apl2-GFP::HisMx*	This study
DLY3555	*Mat α his3Δ1 leu2Δ0 ura3Δ0 MET15 LYS2 erg6Δ::KanMx Art1-GFP::HisMx Gga2-mCh::HisMx*	This study
DLY3004	*Mat a his3Δ1 leu2Δ0 ura3Δ0 met15Δ0 LYS2 Art1-GFP::HisMx gga1Δ::HisMx gga2Δ::KanMx*	This study
DLY3764	*Mat a his3Δ1 leu2Δ0 ura3Δ0 MET15 LYS2 Art1-GFP::HisMx apl2Δ::KanMx*	This study
MDY650	*Mat α his3Δ1 leu2Δ0 ura3Δ0 MET15 lys2Δ0 chc1-ts::Ura3Mx*	This study
DLY2904	*Mat a his3Δ1 leu2Δ0 ura3Δ0 met15Δ0 LYS2 art1Δ::KanMx chc1-ts::Ura3Mx*	This study
DLY253	*Mat α his3Δ1 leu2Δ0 ura3Δ0 MET15 lys2Δ0 apl2Δ::KanMX chc1-ts::Ura3Mx*	This study
DLY254	*Mat α his3Δ1 leu2Δ0 ura3Δ0 met15Δ0 LYS2 gga2Δ::KanMX*	This study
DLY2857	*Mat a his3Δ1 leu2Δ0 ura3Δ0 MET15 lys2Δ0 apl2Δ::KanMX*	This study
DLY801	*Mat a his3Δ1 leu2Δ0 ura3Δ0 met15Δ0 LYS2 end3Δ::KanMx Tat1-GFP::HisMx*	This study
DLY2021	*Mat α his3Δ1 leu2Δ0 ura3Δ0 MET15 LYS2*	This study
DLY2906	*Mat α his3Δ1 leu2Δ0 ura3Δ0 met15Δ0 lys2Δ0 art1Δ::KanMx chc1-ts::Ura3Mx*	This study
DLY250	*Mat α his3Δ1 leu2Δ0 ura3Δ0 MET15 lys2Δ0 apl4Δ::KanMX chc1-ts::Ura3Mx*	This study

DLY2614	*Mat α his3Δ1 leu2Δ0 ura3Δ0 MET15 LYS2 gga1Δ::HisMx gga2Δ::KanMx*	This study
DLY3722	*Mat a his3Δ1 leu2Δ0 ura3Δ0 met15Δ0 LYS2 CPY-GFP::HisMx*	Huh et al., 2003
DLY3771	*Mat α his3Δ1 leu2Δ0 ura3Δ0 met15Δ0 LYS2 CPY-GFP::HisMx gga1Δ::HisMx gga2Δ::KanMx*	This study
DLY3774	*Mat a his3Δ1 leu2Δ0 ura3Δ0 met15Δ0 LYS2 CPY-GFP::HisMx apl2Δ::KanMx*	This study
DLY3779	*Mat α his3Δ1 leu2Δ0 ura3Δ0 met15Δ0 lys2Δ0 CPY-GFP::HisMx chc1-ts::Ura3Mx*	This study
DLY3781	*Mat a his3Δ1 leu2Δ0 ura3Δ0 MET15 LYS2 CPY-GFP::HisMx chc1-ts::Ura3Mx art1Δ::KanMx*	This study
DLY3777	*Mat α his3Δ1 leu2Δ0 ura3Δ0 MET15 lys2Δ0 CPY-GFP::HisMx chc1-ts::Ura3Mx apl2Δ::KanMx*	This study

References

Alvaro, C.G., A.F. O'Donnell, D.C. Prosser, A.A. Augustine, A. Goldman, J.L. Brodsky, M.S. Cyert, B. Wendland, and J. Thorner. 2014. Specific alpha-arrestins negatively regulate Saccharomyces cerevisiae pheromone response by down-modulating the G-protein-coupled receptor Ste2. *Molecular and cellular biology*. 34:2660-2681.

Aoh, Q.L., L.M. Graves, and M.C. Duncan. 2011. Glucose regulates clathrin adaptors at the trans-Golgi network and endosomes. *Molecular biology of the cell*. 22:3671-3683.

Aoh, Q.L., C.W. Hung, and M.C. Duncan. 2013. Energy metabolism regulates clathrin adaptors at the trans-Golgi network and endosomes. *Molecular biology of the cell*. 24:832-847.

Becuwe, M., and S. Leon. 2014a. Integrated control of transporter endocytosis and recycling by the arrestin-related protein Rod1 and the ubiquitin ligase Rsp5. *eLIFE*.

Becuwe, M., and S. Leon. 2014b. Integrated control of transporter endocytosis and recycling by the arrestin-related protein Rod1 and the ubiquitin ligase Rsp5. *eLife*. 3.

Bensen, E.S., G. Costaguta, and G.S. Payne. 2000. Synthetic genetic interactions with temperature-sensitive clathrin in Saccharomyces cerevisiae. Roles for synaptojanin-like Inp53p and dynamin-related Vps1p in clathrin-dependent protein sorting at the trans-Golgi network. *Genetics*. 154:83-97.

Brodsky, F.M., C.Y. Chen, C. Knuehl, M.C. Towler, and D.E. Wakeham. 2001. Biological basket weaving: formation and function of clathrin-coated vesicles. *Annu Rev Cell Dev Biol*. 17:517-568.

Chong, Y.T., J.L. Koh, H. Friesen, S.K. Duffy, M.J. Cox, A. Moses, J. Moffat, C. Boone, and B.J. Andrews. 2015. Yeast Proteome Dynamics from Single Cell Imaging and Automated Analysis. *Cell*. 161:1413-1424.

Conibear, E., and T.H. Stevens. 1998. Multiple sorting pathways between the late Golgi and the vacuole in yeast. *Biochim Biophys Acta*. 1404:211-230.

Conibear, E., and T.H. Stevens. 2002. Studying yeast vacuoles. *Methods Enzymol*. 351:408-432.

Costaguta, G., C.J. Stefan, E.S. Bensen, S.D. Emr, and G.S. Payne. 2001. Yeast Gga coat proteins function with clathrin in Golgi to endosome transport. *Mol Biol Cell*. 12:1885-1896.

Crapeau, M., A. Merhi, and B. Andre. 2014. Stress conditions promote yeast Gap1 permease ubiquitylation and down-regulation via the arrestin-like Bul and Aly proteins. *The Journal of biological chemistry*. 289:22103-22116.

Daboussi, L., G. Costaguta, and G.S. Payne. 2012. Phosphoinositide-mediated clathrin adaptor progression at the trans-Golgi network. *Nature cell biology*. 14:239-248.

Day, K.J., J.C. Casler, and B.S. Glick. 2018. Budding Yeast Has a Minimal Endomembrane System. *Developmental cell*. 44:56-72 e54.

Dong, B., X. Xu, G. Chen, D. Zhang, M. Tang, F. Xu, X. Liu, H. Wang, and B. Zhou. 2016. Autophagy-associated alpha-arrestin signaling is required for conidiogenous cell development in Magnaporthe oryzae. *Scientific reports*. 6:30963.

Faini, M., R. Beck, F.T. Wieland, and J.A. Briggs. 2013. Vesicle coats: structure, function, and general principles of assembly. *Trends in cell biology*. 23:279-288.

Gournas, C., E. Saliba, E.M. Krammer, C. Barthelemy, M. Prevost, and B. Andre. 2017. Transition of yeast Can1 transporter to the inward-facing state unveils an alpha-arrestin

target sequence promoting its ubiquitylation and endocytosis. *Molecular biology of the cell*. 28:2819-2832.
Guiney, E.L., T. Klecker, and S.D. Emr. 2016. Identification of the endocytic sorting signal recognized by the Art1-Rsp5 ubiquitin ligase complex. *Molecular biology of the cell*. 27:4043-4054.
Hager, N.A., C.J. Krasowski, T.D. Mackie, A.R. Kolb, P.G. Needham, A.A. Augustine, A. Dempsey, C. Szent-Gyorgyi, M.P. Bruchez, D.J. Bain, A.V. Kwiatkowski, A.F. O'Donnell, and J.L. Brodsky. 2018. Select alpha-arrestins control cell-surface abundance of the mammalian Kir2.1 potassium channel in a yeast model. *The Journal of biological chemistry*. 293:11006-11021.
Hatakeyama, R., M. Kamiya, T. Takahara, and T. Maeda. 2010. Endocytosis of the aspartic acid/glutamic acid transporter Dip5 is triggered by substrate-dependent recruitment of the Rsp5 ubiquitin ligase via the arrestin-like protein Aly2. *Mol Cell Biol*. 30:5598-5607.
Herranz, S., J.M. Rodriguez, H.J. Bussink, J.C. Sanchez-Ferrero, H.N. Arst, Jr., M.A. Penalva, and O. Vincent. 2005. Arrestin-related proteins mediate pH signaling in fungi. *Proc Natl Acad Sci U S A*. 102:12141-12146.
Hovsepian, J., V. Albanese, M. Becuwe, V. Ivashov, D. Teis, and S. Leon. 2018. The yeast arrestin-related protein Bul1 is a novel actor of glucose-induced endocytosis. *Molecular biology of the cell*. 29:1012-1020.
Hu, C.D., Y. Chinenov, and T.K. Kerppola. 2002. Visualization of interactions among bZIP and Rel family proteins in living cells using bimolecular fluorescence complementation. *Mol Cell*. 9:789-798.
Huh, W.K., J.V. Falvo, L.C. Gerke, A.S. Carroll, R.W. Howson, J.S. Weissman, and E.K. O'Shea. 2003. Global analysis of protein localization in budding yeast. *Nature*. 425:686-691.
Hung, C.W., Q.L. Aoh, A.P. Joglekar, G.S. Payne, and M.C. Duncan. 2012. Adaptor autoregulation promotes coordinated binding within clathrin coats. *The Journal of biological chemistry*. 287:17398-17407.
Huser, S., G. Suri, P. Crottet, and M. Spiess. 2013. Interaction of amphiphysins with AP-1 clathrin adaptors at the membrane. *Biochem J*. 450:73-83.
Jackson, C.L., and J.E. Casanova. 2000. Turning on ARF: the Sec7 family of guanine-nucleotide-exchange factors. *Trends Cell Biol*. 10:60-67.
Karachaliou, M., S. Amillis, M. Evangelinos, A.C. Kokotos, V. Yalelis, and G. Diallinas. 2013. The arrestin-like protein ArtA is essential for ubiquitination and endocytosis of the UapA transporter in response to both broad-range and specific signals. *Mol Microbiol*. 88:301-317.
Kim, J.J., Z. Lipatova, U. Majumdar, and N. Segev. 2016. Regulation of Golgi Cisternal Progression by Ypt/Rab GTPases. *Developmental cell*. 36:440-452.
Kita, A., C. Li, Y. Yu, N. Umeda, A. Doi, M. Yasuda, S. Ishiwata, A. Taga, Y. Horiuchi, and R. Sugiura. 2011. Role of the Small GTPase Rho3 in Golgi/Endosome trafficking through functional interaction with adaptin in Fission Yeast. *PLoS One*. 6:e16842.
Lauwers, E., Z. Erpapazoglou, R. Haguenauer-Tsapis, and B. Andre. 2010. The ubiquitin code of yeast permease trafficking. *Trends Cell Biol*. 20:196-204.
Lin, C.H., J.A. MacGurn, T. Chu, C.J. Stefan, and S.D. Emr. 2008. Arrestin-related ubiquitin-ligase adaptors regulate endocytosis and protein turnover at the cell surface. *Cell*. 135:714-725.
Longtine, M.S., A. McKenzie, 3rd, D.J. Demarini, N.G. Shah, A. Wach, A. Brachat, P. Philippsen, and J.R. Pringle. 1998. Additional modules for versatile and economical

PCR-based gene deletion and modification in Saccharomyces cerevisiae. *Yeast*. 14:953-961.
Losev, E., C.A. Reinke, J. Jellen, D.E. Strongin, B.J. Bevis, and B.S. Glick. 2006. Golgi maturation visualized in living yeast. *Nature*. 441:1002-1006.
Lund, F.W., M.L. Jensen, T. Christensen, G.K. Nielsen, C.W. Heegaard, and D. Wustner. 2014. SpatTrack: an imaging toolbox for analysis of vesicle motility and distribution in living cells. *Traffic*. 15:1406-1429.
MacGurn, J.A., P.C. Hsu, M.B. Smolka, and S.D. Emr. 2011. TORC1 regulates endocytosis via Npr1-mediated phosphoinhibition of a ubiquitin ligase adaptor. *Cell*. 147:1104-1117.
Matsuura-Tokita, K., M. Takeuchi, A. Ichihara, K. Mikuriya, and A. Nakano. 2006. Live imaging of yeast Golgi cisternal maturation. *Nature*. 441:1007-1010.
McDonold, C.M., and J.C. Fromme. 2014. Four GTPases differentially regulate the Sec7 Arf-GEF to direct traffic at the trans-golgi network. *Developmental cell*. 30:759-767.
Mishra, S.K., N.R. Agostinelli, T.J. Brett, I. Mizukami, T.S. Ross, and L.M. Traub. 2001. Clathrin- and AP-2-binding sites in HIP1 uncover a general assembly role for endocytic accessory proteins. *J Biol Chem*. 276:46230-46236.
Nakase, Y., M. Nakase, J. Kashiwazaki, T. Murai, Y. Otsubo, I. Mabuchi, M. Yamamoto, K. Takegawa, and T. Matsumoto. 2013. The fission yeast beta-arrestin-like protein Any1 is involved in TSC-Rheb signaling and the regulation of amino acid transporters. *J Cell Sci*. 126:3972-3981.
Newman, J.R., S. Ghaemmaghami, J. Ihmels, D.K. Breslow, M. Noble, J.L. DeRisi, and J.S. Weissman. 2006. Single-cell proteomic analysis of S. cerevisiae reveals the architecture of biological noise. *Nature*. 441:840-846.
Nikko, E., and H.R. Pelham. 2009. Arrestin-mediated endocytosis of yeast plasma membrane transporters. *Traffic*. 10:1856-1867.
Nikko, E., J.A. Sullivan, and H.R. Pelham. 2008. Arrestin-like proteins mediate ubiquitination and endocytosis of the yeast metal transporter Smf1. *EMBO reports*. 9:1216-1221.
O'Donnell, A.F., A. Apffel, R.G. Gardner, and M.S. Cyert. 2010. Alpha-arrestins Aly1 and Aly2 regulate intracellular trafficking in response to nutrient signaling. *Molecular biology of the cell*. 21:3552-3566.
Owen, D.J., B.M. Collins, and P.R. Evans. 2004. Adaptors for clathrin coats: structure and function. *Annu Rev Cell Dev Biol*. 20:153-191.
Pearse, B.M. 1976. Clathrin: a unique protein associated with intracellular transfer of membrane by coated vesicles. *Proc Natl Acad Sci U S A*. 73:1255-1259.
Phan, H.L., J.A. Finlay, D.S. Chu, P.K. Tan, T. Kirchhausen, and G.S. Payne. 1994. The Saccharomyces cerevisiae APS1 gene encodes a homolog of the small subunit of the mammalian clathrin AP-1 complex: evidence for functional interaction with clathrin at the Golgi complex. *Embo J*. 13:1706-1717.
Prosser, D.C., A.E. Pannunzio, J.L. Brodsky, J. Thorner, B. Wendland, and A.F. O'Donnell. 2015. Alpha-arrestins participate in cargo selection for both clathrin-independent and clathrin-mediated endocytosis. *J Cell Sci*.
Rad, M.R., H.L. Phan, L. Kirchrath, P.K. Tan, T. Kirchhausen, C.P. Hollenberg, and G.S. Payne. 1995. Saccharomyces cerevisiae Apl2p, a homologue of the mammalian clathrin AP beta subunit, plays a role in clathrin-dependent Golgi functions. *J Cell Sci*. 108 (Pt 4):1605-1615.
Soetens, O., J.O. De Craene, and B. Andre. 2001. Ubiquitin is required for sorting to the vacuole of the yeast general amino acid permease, Gap1. *The Journal of biological chemistry*. 276:43949-43957.

Sung, M.K., and W.K. Huh. 2007. Bimolecular fluorescence complementation analysis system for in vivo detection of protein-protein interaction in Saccharomyces cerevisiae. *Yeast*. 24:767-775.
Tanaka, M., T. Hiramoto, H. Tada, T. Shintani, and K. Gomi. 2017. Improved alpha-Amylase Production by Dephosphorylation Mutation of CreD, an Arrestin-Like Protein Required for Glucose-Induced Endocytosis of Maltose Permease and Carbon Catabolite Derepression in Aspergillus oryzae. *Appl Environ Microbiol*. 83.
Volland, C., D. Urban-Grimal, G. Geraud, and R. Haguenauer-Tsapis. 1994. Endocytosis and degradation of the yeast uracil permease under adverse conditions. *J Biol Chem*. 269:9833-9841.
Wilsbach, K., and G.S. Payne. 1993. Vps1p, a member of the dynamin GTPase family, is necessary for Golgi membrane protein retention in Saccharomyces cerevisiae. *EMBO J*. 12:3049-3059.
Wu, H., and P. Brennwald. 2010. The function of two Rho family GTPases is determined by distinct patterns of cell surface localization. *Mol Cell Biol*. 30:5207-5217.
Yeung, B.G., and G.S. Payne. 2001. Clathrin interactions with C-terminal regions of the yeast AP-1 beta and gamma subunits are important for AP-1 association with clathrin coats. *Traffic*. 2:565-576.
Zhao, Y., J.A. Macgurn, M. Liu, and S. Emr. 2013. The ART-Rsp5 ubiquitin ligase network comprises a plasma membrane quality control system that protects yeast cells from proteotoxic stress. *eLife*. 2:e00459.
Zhdankina, O., N.L. Strand, J.M. Redmond, and A.L. Boman. 2001. Yeast GGA proteins interact with GTP-bound Arf and facilitate transport through the Golgi. *Yeast*. 18:1-18.

Chapter 4: Conclusion

Autophagy inhibited in glucose starvation

We started the studies presented in this dissertation to understand how yeast cells survive long periods of time in glucose starvation. Several prior studies had suggested that autophagy was the main pathway for survival during starvation events. However, our data shows that autophagy is dispensable for survival during glucose starvation (Chapter 2 and (Lang et al., 2014)). Our data shows that during glucose starvation, the cell moves cargo proteins from the cell surface to the vacuole for degradation in an autophagy-independent manner. These results are in accordance with another study that shows autophagy as dispensable in glucose starvation (Klosinska et al., 2011). Additional data from our lab shows that glucose starvation results in the depletion of cellular energy, as measured by ATP levels (Aoh et al., 2013). In response, cells internalize many cell surface proteins for degradation at the vacuole (Lang et al., 2014), presumably to produce new products for biosynthesis and energy. Furthermore, our data suggest that, at the very least, yeast cells prioritize the activation of the pathway for glucose starvation survival (Lang et al., 2014). This position is supported by research in mammals that show that autophagy is not induced in glucose starvation (Moruno-Manchon et al., 2013; Ramirez-Peinado et al., 2013), although other research may suggest otherwise (Egan et al., 2011; Roberts et al., 2014). Importantly, a

recent report shows that, in yeast, carbon starvation-induced autophagy is activated in cells grown in glycerol, but not in cells grown in glucose (Adachi et al., 2017). The authors further show that this distinction is highly important from the perspective of the cellular energy levels (ATP). ATP levels rapidly drop when cells grown in glucose are carbon starved. In contrast, Adachi et al. show that carbon starved cells grown in glycerol, the ATP levels remain unaffected. Thus, carbon starved yeast grown in glycerol, but not those grown in glucose, have the energy required for the activation of autophagy. However, a similar resolution of whether glucose starvation induces or inhibits autophagy in mammals is currently unavailable.

Art1 as a multi-functional protein

Our follow-up studies identified arrestin proteins (and the E3 ligase Rsp5) as important for GS-CSC to occur. Specifically, we found the arrestin Art1 was required for efficient GS-CSC of cargo proteins in glucose starvation. In the course of these studies, we observed Art1, a known endocytic protein, localized to internal structures and not to the PM. The localization we observed for Art1 and its known function were at odds. Our studies resulted in data that showed Art1 genetic interactions and localization consistent with a role in TGN traffic.

Our studies suggest an unknown role of Art1 in TGN traffic. In accordance with our data, a recent study shows that Art1 functions in post-endocytic traffic of cell surface cargo proteins (Gournas et al., 2017). This study found that cells lacking *ART1* successfully endocytoses the arginine permease Can1 but are unable to traffic it further.

Instead, Can1 is recycled back to the PM. In addition to Art1, other yeast ARTs function in non-endocytic membrane traffic of cargo proteins (Becuwe and Leon, 2014; O'Donnell et al., 2010; Soetens et al., 2001). Together, these data suggest that ARTs are potentially important for the regulation of cargo protein traffic itinerary through the TGN and endosomes.

It is possible that ARTs perform the same role in endocytosis and at the TGN. Namely, to recruit the Rsp5 E3 ligase to proteins for ubiquitination. In this case, the location of arrestin function could depend on their recruitment by cargo or other proteins at specific compartments. However, our data that show synthetic defects of *ART1* with a clathrin hypomorph and lethality with *GGA2*, hint at the possibility of an as of yet unknown function of ARTs. For example, ARTs could function as scaffolds to help link cargo proteins with adaptors or other proteins at forming vesicles. Another hypothesis is the potential for heterocomplexes of ARTs. Although unexplored, interactions between different ARTs in yeast would echo the interactions observed between α- and β-arrestins in mammals (Puca and Brou, 2014; Puca et al., 2013; Shea et al., 2012).

Membrane traffic in development and disease

Similar to responses to stresses and nutrient availability, the developing embryo responds to changes in ligand gradients, in part, through membrane traffic (Furthauer and Gonzalez-Gaitan, 2009). Each ligand can activate a specific signaling pathway. Many signaling pathways during development depend on receptors at the cell surface to correctly initiate signaling. For example, hedgehog (HH) signaling involves the

trafficking of the patched (Ptc) receptor and the GPCR, smoothened (Smo). In the absence of HH ligand, Ptc localizes to the PM, where it prevents traffic to and activity of Smo at the primary cilia. In the presence of HH ligand, Ptc traffics to the lysosome for degradation. Removal of Ptc from the PM enables Smo to activate the downstream HH pathway. Importantly, traffic of Ptc to the lysosome depends on two ubiquitin ligases (Nedd4, Smurf) that bind to Ptc (Brigui et al., 2015; Yue et al., 2014). Furthermore, a mutant Ptc that lacks its Nedd4/Smurf interaction motif, shows increased levels of Ptc receptor at the cell surface. The increased levels of Ptc at the cell surface reduce the response to HH in *Drosophila* embryos (Brigui et al., 2015). Similar to the HH pathway, receptors from other developmental signaling pathways require faithful membrane traffic for the correct response to their ligands.

Defective membrane trafficking of proteins involved in developmental signaling pathways can induce diseases (Briscoe and Therond, 2013; Canterini et al., 2017). For example, mutations that affect the traffic of Ptc or Smo increase the risk for cancer development (Jiang and Hui, 2008). This risk increase is due to the loss of Smo inhibition by Ptc. The release of Smo inhibition enables downstream activation of the HH pathway, which leads to increased proliferation, a hallmark of cancer (Hanahan and Weinberg, 2011). Thus, defects in membrane traffic of developmental signaling pathway proteins can lead to diseases.

Defective membrane trafficking outside of developmental signaling pathways can also lead to diseases. Many mutations that affect membrane traffic are known to give rise to cancer and neurological disorders (Small and Petsko, 2015). For example, mutations that affect membrane traffic of signaling pathway receptors can reduce

desensitization of active signaling that may result in cancer (Jiang and Hui, 2008; Turner and Grose, 2010; Wu et al., 2017). Traffic defects can also result in failure to move proteases to endosomes. Under normal conditions, these proteases would prevent deleterious protein aggregation (e.g. Tau aggregation) in endosomal compartments. However, deficient protease delivery results in aggregation defects, a hallmark of some neurological disorders (Small and Petsko, 2015). Thus, correct membrane traffic is required for efficient organism development and to prevent disease formation.

Outstanding questions

Does glucose starvation induce cell surface protein clearance in mammals?

The correct responses to nutrient starvation are important for cell survival during such events. In Chapter 2, we show that yeast cells respond to glucose starvation by a mechanism that includes three components: internalization of cell surface proteins for degradation, inhibition of recycling and TORC1-dependent inhibition of autophagy. We believe the cells use this mechanism, in part, to produce the energy necessary to survive the acute reduction in ATP that follows glucose starvation (Aoh et al., 2013). Work in mammalian cells suggest a similar response. Ross and co-workers used a system in which they measured the levels of biotinylated cell surface proteins before and after activation of AMPK. AMPK is a metabolic regulator that is active in conditions of low energy. Using the aforementioned procedure, the researchers found a reduction

in protein levels of a large number of cell surface peptides (Ross et al., 2015). These results echo our own, in which low energy conditions in glucose starvation results in the internalization of many cell surface proteins. Furthermore, additional work showed that AMPK is activated during glucose starvation in mammals (Zhang et al., 2014). However, these studies do not resolve whether an endocytic response to glucose starvation is sufficient as a cell survival mechanism in mammals.

What is the role of Art1 at the TGN?

Although Art1 is established as an endocytic protein, it was previously observed at the TGN (Huh et al., 2003; Lin et al., 2008; MacGurn et al., 2011). Our investigation in Chapter 3 validates these prior findings and moreover suggests a role for it at the TGN. Although we were unable to identify the molecular mechanism of Art1 at the TGN, we found that deletion of *ART1* similarly increases temperature phenotypes when compared to mutations in TGN clathrin adaptors. However, we also show data that suggest that the mechanism underlying the temperature sensitivity phenotype is not the same, with the possibility of opposing traffic pathways being affected. Specifically, our data suggests that Art1 helps direct traffic at the TGN for anterograde traffic or recycling in the context of CPY trafficking.

A recent report by Hager et al., suggests a role for Art1 in cargo recycling or anterograde traffic. In their system, which expressed the mammalian potassium channel protein, Kir2.1, overexpression of Art1 resulted in higher levels of Kir2.1 at the cell surface (Hager et al., 2018). These results support our data that suggest that the expression of Art1 is required for the missorting of CPY in cells that express a clathrin

hypomorph. In contrast to these data that support a function of Art1 in recycling or anterograde traffic at the TGN, another report showed that cells that lack Art1 are unable to traffic cargo (i.e. Can1, an Arginine permease) from TGN/endosomes to the vacuole/lysosome following ligand-induced endocytosis (Gournas et al., 2017). Nevertheless, both of these reports support the idea of a role for Art1 at the TGN. Regardless of a role for Art1 at TGN, more data is firmly establishing it as a multi-functional protein.

What is the role of phosphoregulation on the function of Art1 at the TGN?

The endocytic function of Art1 is regulated by phosphorylation. Phosphorylation of Art1 inhibits its endocytosis function (MacGurn et al., 2011). A mutant of Art1 that lacks key phosphorylation sites enhances the localization of Art1 to the PM. Similarly, cells that lack Npr1, which phosphorylates Art1, also show enhanced localization of Art1 at the PM. Npr1 function depends on active TORC1. When TORC1 is inhibited with rapamycin, the PM localization of Art1 is decreased.

Just like it does in the endocytic function of Art1, it is likely that the phosphoregulation of Art1 plays a role in its function at the TGN. Potentially, the inverse results of what is observed in the endocytic function may hold true for the role of Art1 at the TGN. Namely, that the localization and function of Art1 at the TGN is increased when it is phosphorylated and viceversa. However, the Art1 mutant that lacked phosphorylation sites was still present at some internal structures (MacGurn et al., 2011), which could suggest further regulation of Art1 occurs.

Is TGN function a common function for all arrestins?

Research on yeast α-arrestins show that many of these proteins have functions at the TGN (Becuwe and Leon, 2014; O'Donnell et al., 2010; Soetens et al., 2001). Our research and that of other groups (Gournas et al., 2017; Hager et al., 2018) show that Art1 also exhibits functions at the TGN. Although the specific of the function for Art1 at the TGN is currently unknown, research on the mammalian α-arrestin ARRDC3 shows that it is involved in the regulation of GPCR traffic at endosomal compartments (Arakaki et al., 2018; Dores et al., 2015; Tian et al., 2016). ARRDC3 can directly bind to GPCRs to arrest their signaling (Tian et al., 2016). Interestingly, ARRDC3 was also shown to regulate the ubiquitination of non-cargo proteins at endosomal compartments to direct cargo traffic (Dores et al., 2015). These two behaviors of ARRDC3, cargo binding and non-cargo regulation, may help explain the current data available for Art1 function at the TGN. First, Art1 cargo binding at the TGN could result in an additional round of ubiquitination following cargo endocytosis. This is similar to the function of Art1 in Can1 degradative traffic from the cell surface (Gournas et al., 2017). Second, the regulation of non-cargo by Art1 could provide a mechanism for a possible role of Art1 in non-degradative trafficking processes like recycling or anterograde traffic. This scenario could provide an answer to our results from chapter 3, where incorrect secretion of CPY in cells expressing a hypomorph clathrin is reduced when ART1 is also deleted. In this case, Art1 would be directly or indirectly involved in the regulation of an unknown factor important for the correct traffic of cargo, like CPY.

References

Adachi, A., M. Koizumi, and Y. Ohsumi. 2017. Autophagy induction under carbon starvation conditions is negatively regulated by carbon catabolite repression. *The Journal of biological chemistry*. 292:19905-19918.

Aoh, Q.L., C.W. Hung, and M.C. Duncan. 2013. Energy metabolism regulates clathrin adaptors at the trans-Golgi network and endosomes. *Molecular biology of the cell*. 24:832-847.

Arakaki, A.K.S., W.A. Pan, H. Lin, and J. Trejo. 2018. The alpha-arrestin ARRDC3 suppresses breast carcinoma invasion by regulating G protein-coupled receptor lysosomal sorting and signaling. *The Journal of biological chemistry*. 293:3350-3362.

Becuwe, M., and S. Leon. 2014. Integrated control of transporter endocytosis and recycling by the arrestin-related protein Rod1 and the ubiquitin ligase Rsp5. *eLIFE*.

Brigui, A., L. Hofmann, C. Arguelles, M. Sanial, R.A. Holmgren, and A. Plessis. 2015. Control of the dynamics and homeostasis of the Drosophila Hedgehog receptor Patched by two C2-WW-HECT-E3 Ubiquitin ligases. *Open biology*. 5.

Briscoe, J., and P.P. Therond. 2013. The mechanisms of Hedgehog signalling and its roles in development and disease. *Nature reviews. Molecular cell biology*. 14:416-429.

Canterini, S., J. Dragotto, A. Dardis, S. Zampieri, M.E. De Stefano, F. Mangia, R.P. Erickson, and M.T. Fiorenza. 2017. Shortened primary cilium length and dysregulated Sonic hedgehog signaling in Niemann-Pick C1 disease. *Human molecular genetics*. 26:2277-2289.

Dores, M.R., H. Lin, J.G. N, F. Mendez, and J. Trejo. 2015. The alpha-arrestin ARRDC3 mediates ALIX ubiquitination and G protein-coupled receptor lysosomal sorting. *Molecular biology of the cell*. 26:4660-4673.

Egan, D., D. Shackelford, M. Mihaylova, S. Gelino, R. Kohnz, W. Mair, D. Vasquez, A. Joshi, D. Gwinn, R. Taylor, J. Asara, J. Fitzpatrick, A. Dillin, B. Viollet, M. Kundu, M. Hansen, and R. Shaw. 2011. Phosphorylation of ULK1 (hATG1) by AMP-activated protein kinase connects energy sensing to mitophagy. *Science*. 331:456-461.

Furthauer, M., and M. Gonzalez-Gaitan. 2009. Endocytic regulation of notch signalling during development. *Traffic*. 10:792-802.

Gournas, C., E. Saliba, E.M. Krammer, C. Barthelemy, M. Prevost, and B. Andre. 2017. Transition of yeast Can1 transporter to the inward-facing state unveils an alpha-arrestin target sequence promoting its ubiquitylation and endocytosis. *Molecular biology of the cell*. 28:2819-2832.

Hager, N.A., C.J. Krasowski, T.D. Mackie, A.R. Kolb, P.G. Needham, A.A. Augustine, A. Dempsey, C. Szent-Gyorgyi, M.P. Bruchez, D.J. Bain, A.V. Kwiatkowski, A.F. O'Donnell, and J.L. Brodsky. 2018. Select alpha-arrestins control cell-surface abundance of the mammalian Kir2.1 potassium channel in a yeast model. *The Journal of biological chemistry*. 293:11006-11021.

Hanahan, D., and R.A. Weinberg. 2011. Hallmarks of cancer: the next generation. *Cell*. 144:646-674.

Huh, W.K., J.V. Falvo, L.C. Gerke, A.S. Carroll, R.W. Howson, J.S. Weissman, and E.K. O'Shea. 2003. Global analysis of protein localization in budding yeast. *Nature*. 425:686-691.

Jiang, J., and C.C. Hui. 2008. Hedgehog signaling in development and cancer. *Developmental cell*. 15:801-812.

Klosinska, M.M., C.A. Crutchfield, P.H. Bradley, J.D. Rabinowitz, and J.R. Broach. 2011. Yeast cells can access distinct quiescent states. *Genes & development*. 25:336-349.
Lang, M.J., J.Y. Martinez-Marquez, D.C. Prosser, L.R. Ganser, D. Buelto, B. Wendland, and M.C. Duncan. 2014. Glucose starvation inhibits autophagy via vacuolar hydrolysis and induces plasma membrane internalization by down-regulating recycling. *The Journal of biological chemistry*. 289:16736-16747.
Lin, C.H., J.A. MacGurn, T. Chu, C.J. Stefan, and S.D. Emr. 2008. Arrestin-related ubiquitin-ligase adaptors regulate endocytosis and protein turnover at the cell surface. *Cell*. 135:714-725.
MacGurn, J.A., P.C. Hsu, M.B. Smolka, and S.D. Emr. 2011. TORC1 regulates endocytosis via Npr1-mediated phosphoinhibition of a ubiquitin ligase adaptor. *Cell*. 147:1104-1117.
Moruno-Manchon, J.F., E. Perez-Jimenez, and E. Knecht. 2013. Glucose induces autophagy under starvation conditions by a p38 MAPK-dependent pathway. *The Biochemical journal*. 449:497-506.
O'Donnell, A.F., A. Apffel, R.G. Gardner, and M.S. Cyert. 2010. Alpha-arrestins Aly1 and Aly2 regulate intracellular trafficking in response to nutrient signaling. *Molecular biology of the cell*. 21:3552-3566.
Puca, L., and C. Brou. 2014. Alpha-arrestins - new players in Notch and GPCR signaling pathways in mammals. *Journal of cell science*. 127:1359-1367.
Puca, L., P. Chastagner, V. Meas-Yedid, A. Israel, and C. Brou. 2013. Alpha-arrestin 1 (ARRDC1) and beta-arrestins cooperate to mediate Notch degradation in mammals. *Journal of cell science*. 126:4457-4468.
Ramirez-Peinado, S., C.L. Leon-Annicchiarico, J. Galindo-Moreno, R. Iurlaro, A. Caro-Maldonado, J.H. Prehn, K.M. Ryan, and C. Munoz-Pinedo. 2013. Glucose-starved cells do not engage in prosurvival autophagy. *The Journal of biological chemistry*. 288:30387-30398.
Roberts, D.J., V.P. Tan-Sah, E.Y. Ding, J.M. Smith, and S. Miyamoto. 2014. Hexokinase-II positively regulates glucose starvation-induced autophagy through TORC1 inhibition. *Molecular cell*. 53:521-533.
Ross, E., R. Ata, T. Thavarajah, S. Medvedev, P. Bowden, J.G. Marshall, and C.N. Antonescu. 2015. AMP-Activated Protein Kinase Regulates the Cell Surface Proteome and Integrin Membrane Traffic. *PloS one*. 10:e0128013.
Shea, F.F., J.L. Rowell, Y. Li, T.H. Chang, and C.E. Alvarez. 2012. Mammalian alpha arrestins link activated seven transmembrane receptors to Nedd4 family e3 ubiquitin ligases and interact with beta arrestins. *PloS one*. 7:e50557.
Small, S.A., and G.A. Petsko. 2015. Retromer in Alzheimer disease, Parkinson disease and other neurological disorders. *Nat Rev Neurosci*. 16:126-132.
Soetens, O., J.O. De Craene, and B. Andre. 2001. Ubiquitin is required for sorting to the vacuole of the yeast general amino acid permease, Gap1. *The Journal of biological chemistry*. 276:43949-43957.
Tian, X., R. Irannejad, S.L. Bowman, Y. Du, M.A. Puthenveedu, M. von Zastrow, and J.L. Benovic. 2016. The alpha-Arrestin ARRDC3 Regulates the Endosomal Residence Time and Intracellular Signaling of the beta2-Adrenergic Receptor. *The Journal of biological chemistry*. 291:14510-14525.
Turner, N., and R. Grose. 2010. Fibroblast growth factor signalling: from development to cancer. *Nature reviews. Cancer*. 10:116-129.
Wu, F., Y. Zhang, B. Sun, A.P. McMahon, and Y. Wang. 2017. Hedgehog Signaling: From Basic Biology to Cancer Therapy. *Cell chemical biology*. 24:252-280.

Yue, S., L.Y. Tang, Y. Tang, Y. Tang, Q.H. Shen, J. Ding, Y. Chaen, Z. Zhang, T.T. Yu, Y.E. Zhang, and S.Y. Cheng. 2014. Requirement of Smurf-mediated endocytosis of Patched1 in sonic hedgehog signal reception. *eLIFE*. 3.

Zhang, C.S., B. Jiang, M. Li, M. Zhu, Y. Peng, Y.L. Zhang, Y.Q. Wu, T.Y. Li, Y. Liang, Z. Lu, G. Lian, Q. Liu, H. Guo, Z. Yin, Z. Ye, J. Han, J.W. Wu, H. Yin, S.Y. Lin, and S.C. Lin. 2014. The lysosomal v-ATPase-Ragulator complex is a common activator for AMPK and mTORC1, acting as a switch between catabolism and anabolism. *Cell metabolism*. 20:526-540.

Appendices

Appendix A: Summary in Spanish

El tráfico membranal adecuado es importante para movilizar las proteínas membranales a su lugar previsto dentro de la célula y para mantener la homeostasis. El movimiento de las proteínas membranales carga es un proceso altamente regulado. El tráfico de proteínas membranales a través del sistema endomembranal depende, en parte, de las vesículas de clatrina. Estas vesículas de clatrina son usadas por las células en los procesos de endocitosis (la internalización de membrana plásmatica) y en tráfico posterior al Golgi (tráfico entre el aparato de Golgi y los endosomas, o entre endosomas). La formación de las vesículas de clatrina depende muchas proteínas con distintas labores. Entre estas proteínas podemos encontrar adaptadores de clatrina, proteínas que seleccionan las proteínas membranales a ser empacadas, proteínas que terminan la formación de las vesículas y otras proteínas que regulan cada paso de la formación de las vesículas de clatrina. El funcionamiento correcto de estas proteínas de tráfico membranal asegura la supervivencia de las células en condiciones de estrés. Entre estas condiciones de estrés, se encuentra las condiciones de hambre. Entiéndase como condiciones de hambre, aquellas en las que las células están faltas de nutrientes esenciales específicos como la glucosa o amino ácidos. Las células

pueden sobrevivir condiciones de hambre reciclando sus propios componentes. Un ejemplo de esto es el proceso de autofagia, con el cual las células pueden reciclar los sus componentes que se encuentran en el citoplasma. Para nuestra investigación acerca de la supervivencia célular en ausencia de glucosa, utilizamos la levadura de cerveza (*Saccharomyces cerevisiae*). Los resultados de esta investigación sugieren que la autofagia no es esencial para la supervivencia célular en la ausencia de glucosa. En cambio, nuestra investigación destaca que, para sobrevivir la ausencia de glucosa, las células internalizan muchas proteínas membranales que luego movilizan hacia la vacuola (el lisosoma de la levadura) para su degradación. Presuntamente, la degradación de estas proteínas membranales es necesario para sobrevivir la falta de glucosa (la fuente principal y predilecta de carbón). Más aún, nuestra investigación indica que en la ausencia de glucosa el proceso de autofagia es inhibida. El resultado novel en el que las células requieren degradar en masa muchas proteínas membranales, es parecido a otras condiciones en las que las células internalizan muchas proteínas de la membrana plasmática (por ejemplo, el aumento súbito de la temperatura o el tratamiento con cicloheximida). Estos eventos de internalización de proteínas membranales en masa dependen en la función de las α-arrestins, una familia de proteínas importantes en la degradación de proteínas. En nuestras investigaciones encontramos que la internalización eficiente de proteínas membranales durante la ausencia de glucosa requiere la proteína Art1 (también conocida como Ldb19, miembro de las arrestinas). Curiosamente, mientras estudiábamos esta proteína, observamos que se localizaba a estructuras internas. Esta localización se nos pareció mucho a la localización de adaptadores de clatrina. Esta observación es curiosa, ya que es

conocido que Art1 es importante para procesos de endocitosis en la membrana plamática. Sin embargo, esta nueva localización podría significar que Art1 tiene una labor adicional, esta vez en la red de la cara “trans” del aparato de Golgi (TGN, por sus siglas en inglés). Estas observaciones fueron confirmadas por nuestras investigaciones en las que visualizamos a Art1 en las mismas estructuras que contienen proteínas del TGN. Adicionalmente, encontramos interacciones genéticas entre *ART1* y un adaptador de clatrina (*GGA2*) y con una versión mutante de clatrina. Por último, también descubrimos que células que no expresan Art1 suprimen los defectos de secreción en células que expresan un alelo mutante de clatrina. En conjunto, esta investigación doctoral provée nuevos mecanismos de tráfico membranal, en especial a procesos importante para el tráfico del TGN.

Appendix B: Additional contributions

Monitoring possible mechanisms for GS-CSC

In chapter 2, we showed that large-scale endocytosis of PM cargo occurs in glucose starvation. To understand why this glucose starvation-induced cell surface clearance (GS-CSC) occurred, we monitored whether GS-CSC used a similar mechanism as other stress-inducing conditions (Lin et al., 2008; Nikko and Pelham, 2009; Zhao et al., 2013). To test whether glucose starvation resulted in protein misfolding, we stained cells with dye (propidium iodide) during glucose starvation. In heatshock treatment, all cells were stained with extracellular dye because misfolded proteins at the cell surface make the cell permeable to extracellular fluid (Figure B.1). However, in glucose starved cells showed no staining for different amounts of time no cells were stained with the extracellular dye (Figure B.1). These data suggest that GS-CSC is not induced by protein misfolding after the starvation event.

Cell surface clearance (CSC) of PM cargo proteins also occurs when cells are treated with cycloheximide (CHX). Treatment with CHX blocks protein synthesize, which results in an increase of free amino acids in the cytoplasm. This increase in cytosolic amino acid activates TORC1 signaling, which induces arrestin-dependent CSC of many cargo. To test whether GS-CSC depends on TORC1, we imaged GFP-tagged tryptophan permease, Tat1, before and after glucose starvation with or without TORC1

signaling. To inhibit TORC1 signaling we performed the experiment in cells lacking the TORC1 subunit, Tco89. In WT and *tco89*Δ cells, Tat1 localized to the cell surface in the presence of glucose. In WT cells, Tat1 was fully internalized after 2hr of glucose starvation (Figure B.1). Likewise, cells lacking Tco89 fully internalized Tat1 after 2hr of glucose starvation (Figure B.1). Together with the propidium iodide results, our studies suggest that GS-CSC does not induce PM cargo misfolding (e.g. heatshock pathway) and is independent of TORC1 (e.g. CHX pathway). However, like we explored in chapter 4, ARTs are involved in the GS-CSC pathway.

Interactions between Art1 and Gga2

Our initial studies hinted at a possible role for Art1 in Gga2 regulation. However, although these results did not pan out, we were able to detect an interaction between Art1 and Gga2. To test this interaction, I performed GST pulldowns using GST-tagged proteins purified from bacteria and yeast lysates. Using this system, we found that Gga2 binds Art1 through the VHS domain of Gga2 (Figure B.2). Nonetheless, we were unable to characterize this interaction in vivo (i.e. immunoprecipitation experiments).

Generation of an Art1-AID strain

Genomic deletion of genes can result in the spontaneous generation of suppressor mutations that can mask the real effect of a gene deletion. Because cells lacking Art1 have phenotypes characteristic of sick cells (i.e. temperature sensitive), we wanted to develop a strain in which we could quickly, and reversibly, remove Art1. To test the effect of acute removal of Art1, I developed a strain in which Art1 was tagged

with an auxin-inducible degradation (AID) tag (Heider et al., 2016). This new strain should provide me with a platform to test acute loss of Art1 with a very reduced possibility of suppressor mutation development.

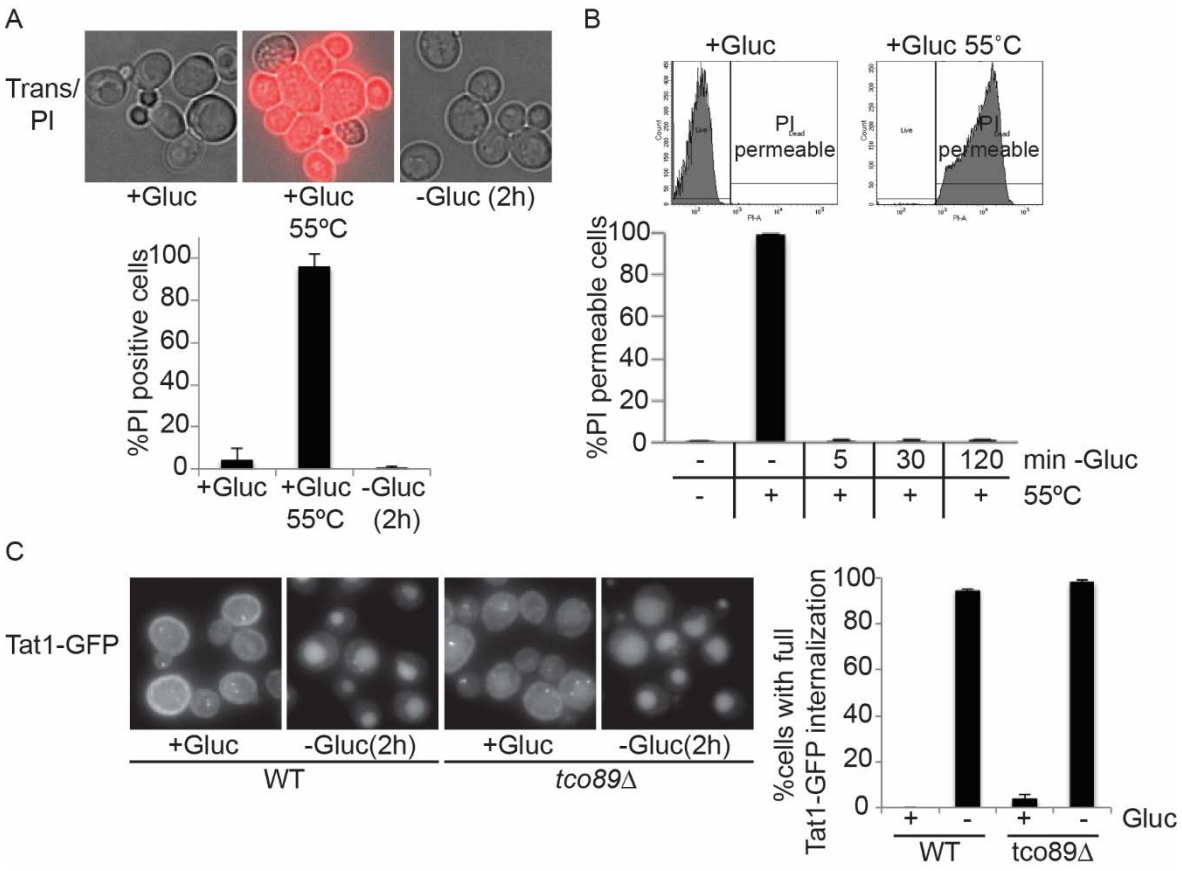

Figure B.1. Mechanism comparison between GS-CSC and other CSCs
A) WT cells grown in the presence of glucose were stained with propidium iodide (PI) before and after heatshock at 55°C or glucose starvation for 2hr. Top, representative merged images; bottom, quantification of cells positive for PI staining. B) Fluorescence activated cell sorting (FACS) of cells stained with PI before and after heatshock at 55°C, before and after glucose starvation for 5, 30 and 120 min. Top, example traces from FACS experiments showing gating used to distinguish between stained and unstained cells (PI permeable = positive staining). C) WT and tco89Δ cells expressing Tat1-GFP were imaged before and after glucose starvation for 2hr. Right, quantification of the percentage of cells with GFP exclusively localized to the vacuole.

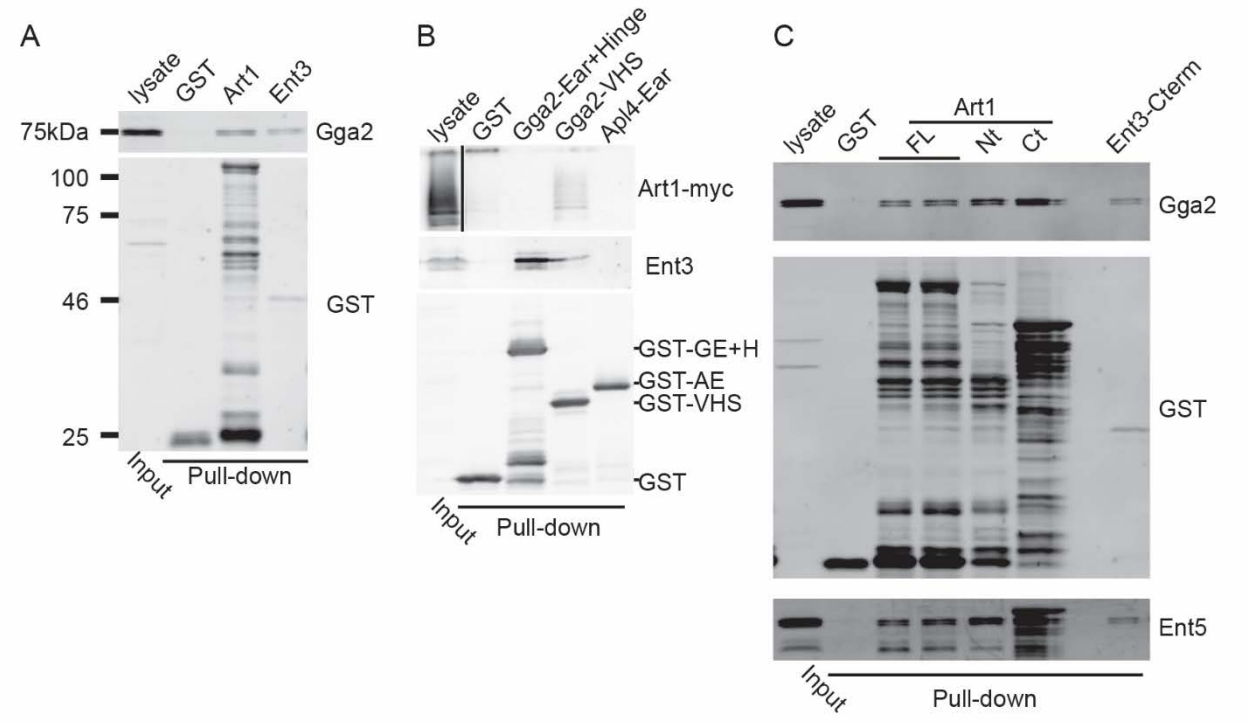

Figure B.2. Art1 interacts with the clathrin adaptor Gga2.
A) GST pulldowns were performed with the labeled GST constructs in the presence of yeast lysate. Blots were probed with antibodies against Gga2 and GST. B) The indicated GST proteins were incubated with lysates from cells expressing Art1-myc. Interacting proteins were detected by immunoblot analysis (myc, Ent3 or GST). For Art1-myc immunoblot, the pulldown panel minimun is enhanced to input. The grey value is 13% of the input panel. C) GST pulldowns were performed with the labeled GST constructs in the presence of yeast lysate. Blots were probed with antibodies against Gga2, GST and Ent5 (Ent5 antibody contains contaminating antibodies against GST).

Generation of an Art1-AID strain

Genomic deletion of genes can result in the spontaneous generation of suppressor mutations that can mask the real effect of a gene deletion. Because cells lacking Art1 have phenotypes characteristic of sick cells (i.e. temperature sensitive), we wanted to develop a strain in which we could quickly, and reversibly, remove Art1. To test the effect of acute removal of Art1, we developed a strain in which Art1 was tagged with an auxin-inducible degradation (AID) tag. This new strain should provide a platform to test acute loss of Art1 (Figure B.3A, B) with a very reduced possibility of suppressor mutation development.

We tested the new strain in cells that also expressed GFP-tagged Mup1 or clathrin adaptors (Gga2, Apl2) (Figure B.3C, D). To test the effect of acute removal of Art1 on Mup1 traffic, we performed ligand-induced internalization experiments. Mup1 localizes to the PM when cells are grown in the absence of methionine. In WT cells, adding methionine to the media induces the traffic of Mup1 to the vacuole for degradation. In contrast, cells that lack Art1 block the internalization of Mup1 in the presence of methionine. Cells in which Art1 was removed with the auxin-induced degradation system, we observed a partial block of Mup1 traffic to the vacuole. This partial block could be due to newly synthesized Art1, during auxin treatment (we have not tested this possibility). Moreover, in cells with acute removal of Art1 we observed no changes in the localization of clathrin adaptors, consistent with the results from Chapter 3. Together, these results suggest that, upon further optimization, the AID system can be a powerful tool to use in the studies performed at the Duncan lab.

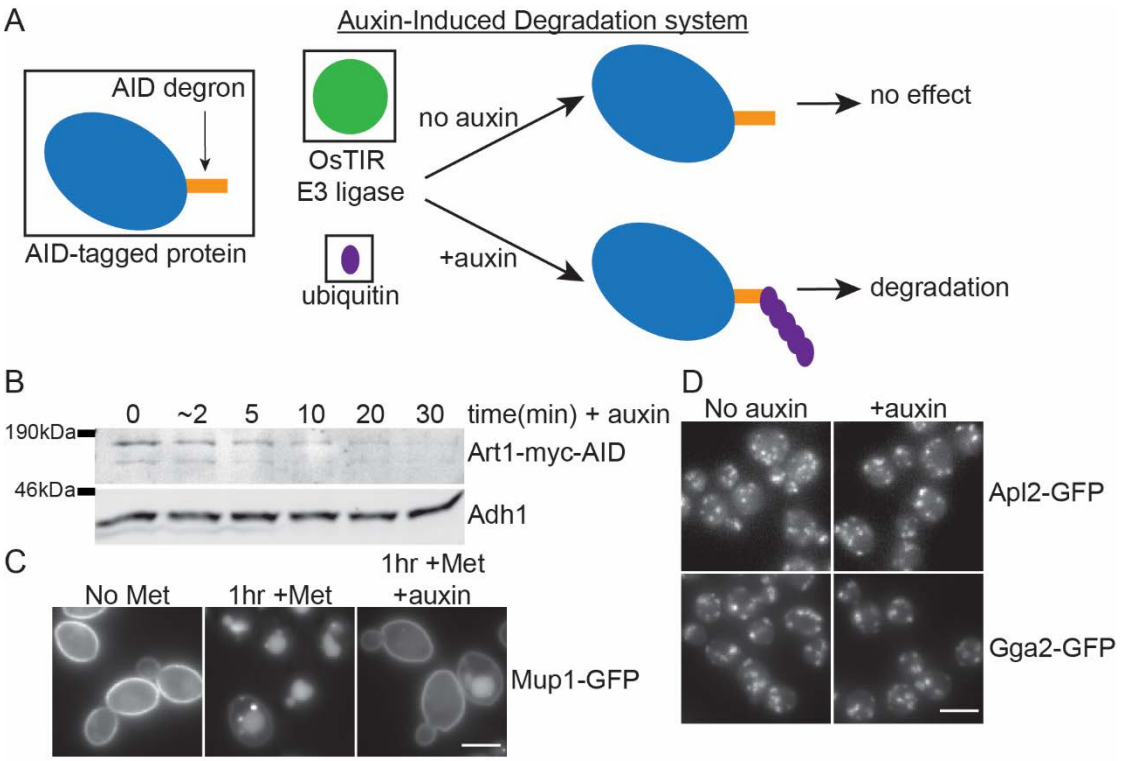

Figure B.3. Effects of acute removal of Art1 function.
A) Diagram of the auxin-induced degradation system. Cells that express a protein tagged with an AID degron are readily degrade the tagged protein when treated with auxin in cells that also express the OsTIR E3 ligase. B) Cell extracts of cells expressing an AID-tag Art1 before and after treatment with auxin at the mentioned times. Adh1 was used as a lysis control. C) Mup1-GFP was imaged in cells expressing Art1-AID in the absence and 1hr after addition of methionine, before and 1hr after treatment with auxin to degrade Art1. D) Cells expressing Art1-AID and Apl2- or Gga2-GFP were imaged before and after 1hr after treatment with auxin. Scale bar: 5µm.

References

Heider, M.R., M. Gu, C.M. Duffy, A.M. Mirza, L.L. Marcotte, A.C. Walls, N. Farrall, Z. Hakhverdyan, M.C. Field, M.P. Rout, A. Frost, and M. Munson. 2016. Subunit connectivity, assembly determinants and architecture of the yeast exocyst complex. *Nature structural & molecular biology*. 23:59-66.

Lin, C.H., J.A. MacGurn, T. Chu, C.J. Stefan, and S.D. Emr. 2008. Arrestin-related ubiquitin-ligase adaptors regulate endocytosis and protein turnover at the cell surface. *Cell*. 135:714-725.

Nikko, E., and H.R. Pelham. 2009. Arrestin-mediated endocytosis of yeast plasma membrane transporters. *Traffic*. 10:1856-1867.

Zhao, Y., J.A. Macgurn, M. Liu, and S. Emr. 2013. The ART-Rsp5 ubiquitin ligase network comprises a plasma membrane quality control system that protects yeast cells from proteotoxic stress. *Elife*. 2:e00459.